AD NUMBER
AD848763
LIMITATION CHANGES

TO:

Approved for public release; distribution is unlimited.

FROM:

Distribution authorized to U.S. Gov't. agencies and their contractors; Administrative/Operational Use; SEP 1968. Other requests shall be referred to Air Force Inst. of Technology, Weight-Patterson AFB, OH 45433.
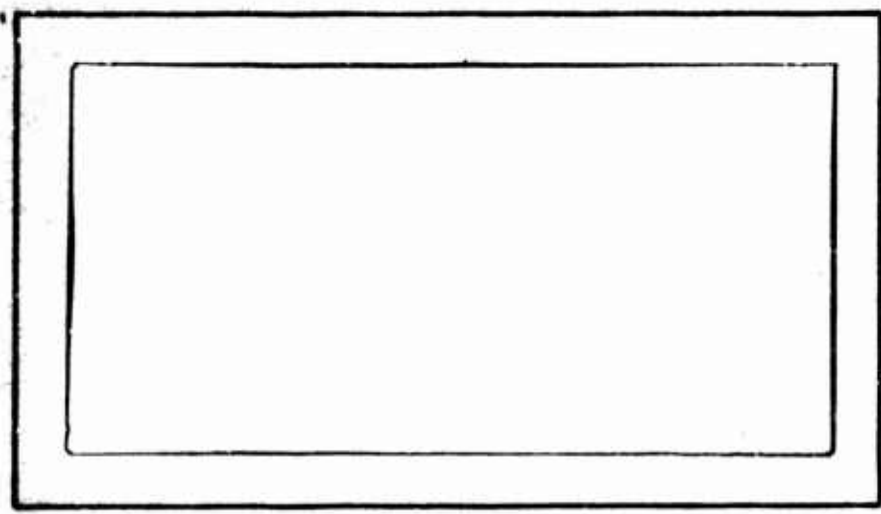
AUTHORITY

AFIT ltr 22 Jul 1971

AIR FORCE INSTITUTE OF TECHNOLOGY

AIR UNIVERSITY
UNITED STATES AIR FORCE

SCHOOL OF ENGINEERING

WRIGHT-PATTERSON AIR FORCE BASE, OHIO

DYNAMIC CHARACTERISTICS OF CASCADED,
BLOCKED, RECTANGULAR CROSS SECTION
PNEUMATIC LINES

THESIS

GE/ME/68-3   Charles V. Fada
                     Capt   USAF

DYNAMIC CHARACTERISTICS OF CASCADED, BLOCKED,

RECTANGULAR CROSS SECTION PNEUMATIC LINES

THESIS

Presented to the Faculty of the School of Engineering of

the Air Force Institute of Technology

Air University

in Partial Fulfillment of the

Requirements for the Degree of

Master of Science

By

Charles V. Fada, B.S.E.E.

Capt   USAF

Graduate Electrical Engineering

September 1968

Preface

This report is a continuation of the sequence of studies by Karam (Ref 11), Wilda (Ref 26), and Miller (Ref 14) on blocked and cascaded pneumatic transmission lines. The primary purpose of this thesis was the desire to determine the transfer gain characteristics for rectangular pneumatic lines since pneumatic lines that are rectangular in cross section predominate in the design of fluidic devices. When this study was begun, no analyses (such as are available for circular pneumatic transmission lines), either theoretical or empirical, were available which predicted transfer gain for rectangular pneumatic lines. However, it was my belief that rectangular pneumatic lines should exhibit a transfer gain characteristic similar to those discussed by Karam, Wilda, and Miller.

To this end, then, this study was directed. During the study I was fortunate in obtaining a paper by Schaedel (Ref 20) which develops the theoretical distributed impedance and admittance parameters for rectangular pneumatic transmission lines by using one dimensional flow analysis and is based on earlier work by Nichols (Ref 17).

Many people shared in providing valuable advice and assistance toward the realization of this study. It is here that I wish to take the opportunity to give special thanks to Dr. Milton Franke, my thesis advisor, who shared in this research by offering valuable comments and advice, to Mr. Earl Criswell in Zone Shop No. 5 who turned my sketches into a workable, precise test fixture, and to Mr. James Hall of the Air

Force Flight Dynamics Laboratory who long ago suggested to me that this is an area which requires experimental data and study.

Especially, I wish to thank Mr. John Houtz, also of the Air Force Flight Dynamics Laboratory, for translating the extremely complicated, theoretical transfer gain equation into a workable computer program which provided the outputs required. It goes without saying that my technical advisor, Squadron Leader Ken Hebborn, RAF, provided me with the technical background and encouragement which made this study a reality.

Finally, I wish to thank my wife, ███ for her patience, determination, encouragement, and typing ability. Without her help this study could not have been possible.

<div style="text-align: right">Charles V. Fada</div>

GE/ME/68-3

Contents

Contents

List of Figures

List of Tables

List of Symbols

A	line cross-sectional area	$in.^2$
a	aspect ratio, height/base	dimensionless
$b_{1,2,3}$	base of pneumatic line (subscripted)	in.
c	phase velocity	in./sec
c_a	adiabatic speed of sound	in./sec
C'_s	capacitance/unit length	$\frac{cis\text{-}sec}{psi}$/in.*
G	gain, pressure ratio	dimensionless or dB
G'_s	conductance/unit length	$\frac{cis}{psi}$/in.
Hz	signal frequency, Hertz	cycles/sec
h	height of transmission line	in.
$i, 1, m, n$	iteration sequence numbers	dimensionless
j	$\sqrt{-1}$	dimensionless
L'_s	inductance/unit length	$\frac{psi\text{-}sec}{cis}$/in.
P_L	DC pressure (mean)	psi
$P_{r,s}$	AC pressure (variation about P_L)	psi-rms
R'_s	resistance/unit length	$\frac{psi}{cis}$/in.
R	gas constant	$\frac{.^2}{sec^2\text{-}^oR}$
x, y, z	variable length	in.
$\bar{X}_{1,2,3}$	length of line (subscripted)	in.
Y'_s	admittance/unit length	$\frac{cis}{psi}$/in.
Z'_s	impedance/unit length	$\frac{psi}{cis}$/in.

*Units refer to pneumatic parameters when there is an electrical-pneumatic equivalent with respect to symbols.

$()'_{s,1}$	using Schaedel's solution	
$S()$	Schaedel's notation	
α_1	attenuation/unit length	$\dfrac{\text{nepers}}{\text{in.}}$
α_i	iteration parameter	dimensionless
β_1	phase shift/unit length	$\dfrac{\text{radians}}{\text{in.}}$
Γ'	propagation constant/unit length	units/in.
γ	ratio of specific heats	dimensionless
ϵ	isothermal compressibility	$\dfrac{1}{\text{psi}}$
θ	phase shift	radians
μ	viscosity	psi-sec
ν	kinematic viscosity	in.^{2}/sec
λ	wavelength	in.
σ^2	Prandtl number	dimensionless
ω	signal frequency	rad/sec

Abstract

The transfer gain (amplitude frequency response curve) of a rectangular volume-terminated pneumatic transmission line was experimentally determined. The cross-sectional dimensions of a 29.454-in.-long line were 0.254 in. by 0.126 in., and the cross-sectional dimensions of the volume termination were 2.396 in. by 1.205 in. Several lengths of the volume termination (7 in. and less) were studied at mean line pressures of 10, 25, and 40 psig. The sinusoidal driving signal was varied between 10 and 1220 Hz.

An IBM 7094 computer program was designed to provide solutions for theoretical transfer gain curves of the volume-terminated rectangular pneumatic line. The transfer gain equation, using an electrical-pneumatic analogy, was formulated using distributed impedance and admittance parameter equations for rectangular pneumatic lines based on the work of Schaedel. Correlation with experiment showed that the theory predicted the transfer gain usually within 3 dB and resonant frequencies within two per cent, as long as line measurements were accurate to within ± 0.001 in.

DYNAMIC CHARACTERISTICS OF CASCADED,

BLOCKED, RECTANGULAR CROSS SECTION PNEUMATIC LINES

I. Introduction

Background for the Rectangular Line Analogy

In recent years scientists and engineers have investigated several
methods that describe the small signal transfer characteristics or, in
other words, the response of pneumatic lines which have no mean flow to
time-varying pneumatic signals. Iberall (Ref 10) derived the transfer
characteristics for circular pneumatic lines; however, the rigorous
solutions are extremely complex. The circular line transfer character-
istic solutions derived by Iberall have formed the basis for simplified
solutions developed by Brown (Ref 2), Nichols (Ref 17), Rohman and
Grogan (Ref 19), and more recently Bergh and Tijdeman (Ref 1). Watts
(Ref 24) developed a computer program which computes solutions to the
equations derived by Iberall, and Watts verified the computer program
solutions experimentally. Notable among the simplified versions of the
circular line transfer characteristic solutions are those by Brown and
Nichols. The equations derived by them have been used as models for
further studies by other investigators in pneumatic transmission line
phenomena.

Papers have been published which agree very closely with the
analytical investigations of Nichols and others. Such papers include
those by Karam (Ref 11), Karam and Franke (Ref 12), Wilda (Ref 26), and

1

Miller (Ref 14). Miller simplified the electrical analog model developed by Nichols and showed that the electrical analog model could be used to calculate the overall transfer gain of cascaded circular pneumatic transmission lines having differing impedance transfer characteristics.

Krishnayer and Lechner (Ref 13) have applied curve fitting techniques to the equations developed by Nichols and have determined the approximate first-order error in Nichols' development. However, the first-order error is small and may be considered negligible for most engineering purposes.

Considerable work has been accomplished in the derivations of impedance transfer functions in the very high frequency range for pneumatic lines having rectangular cross sections. Included among these works are discussions and investigations by Lord Rayleigh (Ref 22), Hartig and Lambert (Ref 7), Moore (Ref 15), Morse and Ingard (Ref 16), and Stephens and Bates (Ref 21). During the nineteenth century, Lord Rayleigh developed the wave equation solutions for a pressure disturbance propagating through a rectangular tube. However, Lord Rayleigh's solutions are limited in the respect that only those frequencies above a cut-off frequency in the disturbance are considered to propagate through the rectangular duct. All frequencies in the disturbance below the cut-off frequency are assumed to decay exponentially. The cut-off frequency is defined as:

$$f_{co} = \frac{c}{2b} , \tag{1}$$

where c is the speed of sound in free air, and b is the width of base of the rectangular duct (Fig. 1). Therefore, the solutions derived by

Lord Rayleigh develop the very high frequency transfer impedance char-
acteristics for pneumatic rectangular lines.
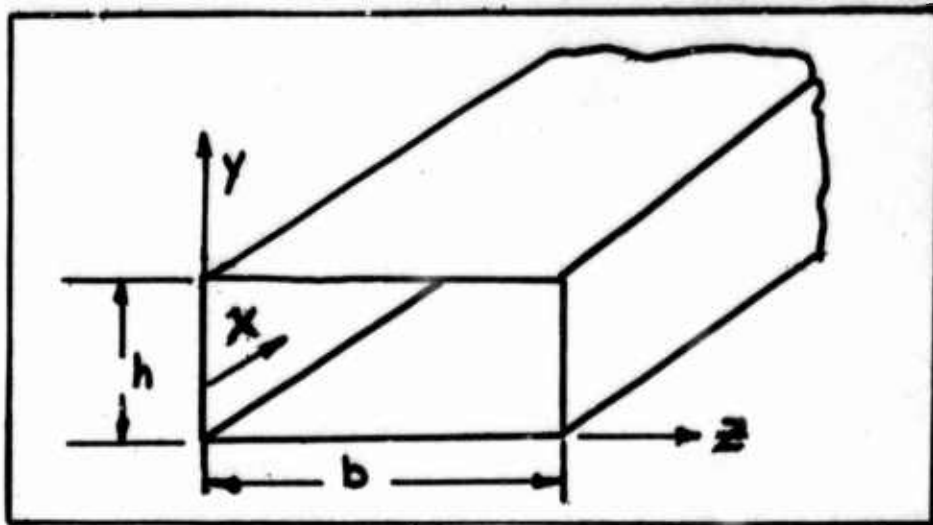
Fig. 1. Rectangular Line Dimensions

Schaedel (Ref 20) derived the low-frequency impedance and admit-
tance transfer characteristics of rectangular pneumatic lines having
no mean flow. He linearized the basic three-dimensional Navier-Stokes
equations by assuming time-varying, very low level pneumatic signals.
He based the velocity distribution in a rectangular duct on a paper by
Ebert and Sparrow (Ref 4). The equations derived by Schaedel are
similar to the transfer characteristic equations derived by Nichols for
circular pneumatic transmission lines.

Objectives

Integrated fluidic circuits are connected by ducts having rec-
tangular cross sections. To adequately describe the transfer functions
for individual fluidic elements, it is necessary to determine the
transfer function of the inter-connecting ducts. Schaedel (Ref 20)
has derived analytical solutions of the impedance transfer functions

3

for rectangular pneumatic lines. However, these solutions have not
been tested experimentally. Therefore, the following objectives were
selected:

(1) To program the transfer gain characteristics of cas-
caded rectangular pneumatic lines using the dis-
tributed impedance and admittance equations
developed by Schaedel as a model for the computer
program.

(2) To construct a cascaded rectangular line and experi-
mentally determine the transfer gain characteristics
of the cascaded lines terminated in a blocked line.

(3) To compare the experimental data with the analytical
parameters determined by the computer program solu-
tions, thus verifying the pneumatic transmission line
theory developed for rectangular lines.

II. Theory and Approach

Miller (Ref 4) treated the volume terminated line as a system of
lines comprising a series of lines in cascade ending with the volume
termination. Since Miller's approach proved valid for the lines he
studied, it appeared appropriate to base the theoretical approach in
this study using the same method as Miller. For the purposes of this
study, the volume terminated lines were treated as cascaded lines
having distributed impedance and admittance parameters with the volume
termination treated as a blocked line in the series.

Schaedel's Rectangular Transmission Line Theory

Schaedel (Ref 20:35-41) derived the rectangular pneumatic trans-
mission line equations using the electrical-pneumatic analog such that
voltage is analogous to pressure and current is analogous to volumetric
flow. The derivations parallel the circular transmission line equations
derived by Nichols (Ref 17).

According to Pai (Ref 18:80), no closed form solutions to the
Navier-Stokes equations are known to exist for the compressible flow
through a rectangular duct. However, Schaedel linearized the Navier-
Stokes axial velocity distribution equation using a series solution to
the velocity distribution equation for rectangular ducts developed by
Ebert and Sparrow (Ref 4:2). Thus Schaedel develops the distributed
series impedance parameter per unit length of rectangular pneumatic
line by integrating the velocity distribution function over the area
and solving for the pressure drop per unit length. In his derivation,

Schaedel specifies the distributed series impedance parameter Z_S' to be (Ref 20:38):

$$Z_S' = \frac{2\mu}{A^2 a} S(\omega_\nu)^{-1} \tag{2}$$

where

$$S(\omega_\nu) = \sum_{i=1}^{\infty} \frac{1}{\alpha_i^2 (\alpha_i^2 + ja\frac{\omega}{\omega_\nu})} \left[1 - \frac{\tanh\left\{ \frac{1}{a}\sqrt{\alpha_i^2 + ja\frac{\omega}{\omega_\nu}} \right\}}{\frac{1}{a}\sqrt{\alpha_i^2 + ja\frac{\omega}{\omega_\nu}}} \right] \tag{3}$$

$$\alpha_i = \frac{2i-1}{2}\pi, \quad i = 1, 2, 3, \ldots \tag{3a}$$

Thus Z_S' contains frequency dependent real and imaginary terms, i.e.,

$$Z_S' = R_S'(\omega) + jL_S'(\omega) \tag{4}$$

Schaedel used a similar method to solve the energy equation so that he could define the distributed shunt admittance parameters for rectangular lines. The shunt admittance is specified to be (Ref 20:41):

$$Y_S' = \frac{2a\omega^2 \epsilon A(\gamma - 1) S(\omega_T)}{\omega_T \gamma} + j\omega\epsilon A \tag{5}$$

where

$$S(\omega_T) = \sum_{i=1}^{\infty} \frac{1}{\alpha_i^2 (\alpha_i^2 + ja\frac{\omega}{\omega_T})} \left[1 - \frac{\tanh\left\{ \frac{1}{a}\sqrt{\alpha_i^2 + ja\frac{\omega}{\omega_T}} \right\}}{\frac{1}{a}\sqrt{\alpha_i^2 + ja\frac{\omega}{\omega_T}}} \right] \tag{6}$$

$$\alpha_i = \frac{2i-1}{2}\pi, \quad i = 1, 2, 3, \ldots \tag{6a}$$

Therefore, Y_S' contains frequency dependent real and imaginary terms:

$$Y_S' = G_S'(\omega) + jC_S'(\omega) \tag{7}$$

6

The characteristic frequencies ω_ν and ω_T defined by Schaedel are

$$\omega_\nu = \frac{4\nu}{A} \tag{8}$$

and

$$\omega_T = \frac{\omega_\nu}{\sigma^2} \tag{9}$$

These characteristic frequencies differ by 2π from those defined by Nichols (Ref 17:8), where:

$$\omega_{\nu(\text{Nichols})} = 2\pi\omega_{\nu(\text{Schaedel})} \tag{8a}$$

$$\omega_{T(\text{Nichols})} = 2\pi\omega_{T(\text{Schaedel})} \tag{9a}$$

Rectangular Line Transfer Gain Equations

Once the distributed impedance and admittance parameters are given per unit length of rectangular pneumatic line, the electrical transmission line analog may be used to solve for the transfer gain characteristics of a rectangular pneumatic line. From the telegrapher's equations as described in Ware and Reed (Ref 23:71-108), the characteristic impedance Z_0' is shown to be:

$$Z_0' = \sqrt{\frac{Z_S'}{Y_S'}} \tag{10}$$

and the propagation constant Γ', where

$$\Gamma' = \sqrt{Z_S' Y_S'} = \alpha_1 + j\beta_1 \tag{11}$$

For a blocked pneumatic line the transfer gain is given as:

$$G_{dB} = 20 \log_{10}\left|\frac{1}{\cosh\Gamma' x}\right| dB \tag{12}$$

where x is the distance between the receiving transducer at the point at which the line is blocked and any other point on the line. At any point in the line the input impedance is

$$Z_i = Z_0 \left[\frac{Z_L \cosh \Gamma \bar{X} + Z_0 \sinh \Gamma \bar{X}}{Z_0 \cosh \Gamma \bar{X} + Z_L \sinh \Gamma \bar{X}} \right] \tag{13}$$

For a line terminated in a load the transfer gain has been shown to be (Ref 14:74)

$$G = \frac{Z_L}{Z_i x} \cosh \Gamma x - \frac{Z_L}{Z_0} \sinh \Gamma x \tag{14}$$

Guillemin (Ref 6:374) and D'Azzo and Houpis (Ref 5:146) show that the transfer gain for a series of lines in cascade is the product of the individual gains, i.e.,

$$G_0 = G_1 \cdot G_2 \cdot G_3 \cdots G_N \tag{15}$$

Therefore, it can be shown that the gain between any two points in a cascaded line is (Ref 14:75)

$$G = \prod_{i=1}^{i=p} \left[\frac{Z_{I(i+1)} (\bar{X}_{i+1}) \cosh \Gamma_i x_i}{Z_{Ii} x_i} - \frac{Z_{I(i+1)} (\bar{X}_{i+1}) \sinh \Gamma_i x_i}{Z_{0i}} \right] \tag{16}$$

For the nth line, Eq (14) holds. The capability to calculate the transfer gain characteristic for a pneumatic line is perhaps the most useful analytical tool for an engineer to use because the transfer gain characteristic is the equation which is easiest to verify experimentally, by taking pressure measurements at various points in the line where

8

$$G_{dB} = 20 \log_{10} \frac{P_{(RMS)}\text{OUTPUT}}{P_{(RMS)}\text{INPUT}} \tag{17}$$

and comparing with the analytical solution:

where
$$G = |G| \, e^{j\theta} \tag{18}$$

and
$$G_{dB} = 20 \log_{10}|G| \tag{19}$$

and where θ is the phase shift in the line.

III. Experimental Apparatus

The test system was basically similar to the apparatus used by Karam (Ref 11), Wilda (Ref 26), and Miller (Ref 14). The apparatus consisted of an electro-pneumatic signal generator, sending and receiving dynamic pressure-measuring equipment, monitoring equipment, and the rectangular transmission line under test (Fig. 2). With the exception of the test line, the equipment is commercially available.
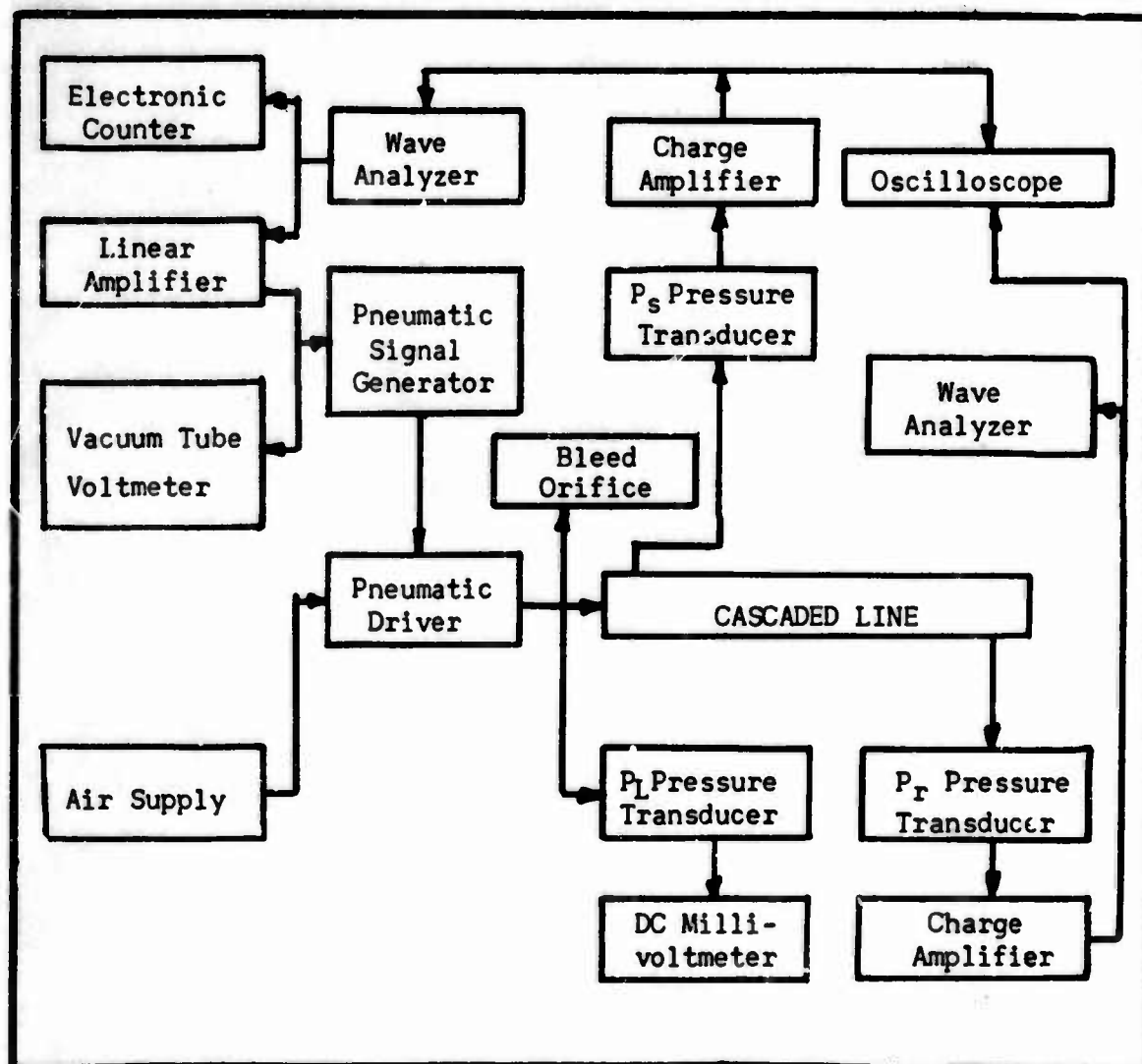
Fig. 2. Schematic Diagram of Experimental Test System

The Pneumatic Transmission Line

The pneumatic signal generator was connected to rectangular transmission lines in cascade by a sending fixture containing a bleed orifice (Ref 26), (Fig. 3). A short length of 0.170-in. ID Imperial Eastman Poly-Flow tubing connected the sending fixture with the rectangular line (Fig. 3). The transition from the circular line to the rectangular was made at the entrance to the rectangular line. The entrance transition was located about 1/2 in. ahead of the sending dynamic transducer port. For flowing lines, Eckert and Irvine (Ref 5:27) have shown that for a rectangular pneumatic line having a 0.17-in. hydraulic diameter and a rounded entrance transition, the pressure drop is nearly constant when the entrance transition length is greater than 1/2 in. The sending

A - Pneumatic Driver

B - Sending Fixture

C - Bleed Orifice

D - Static Pressure Transducer (P_L)

E - Connecting Line

F - Transition Region

G - Dynamic Pressure Transducer (P_s)
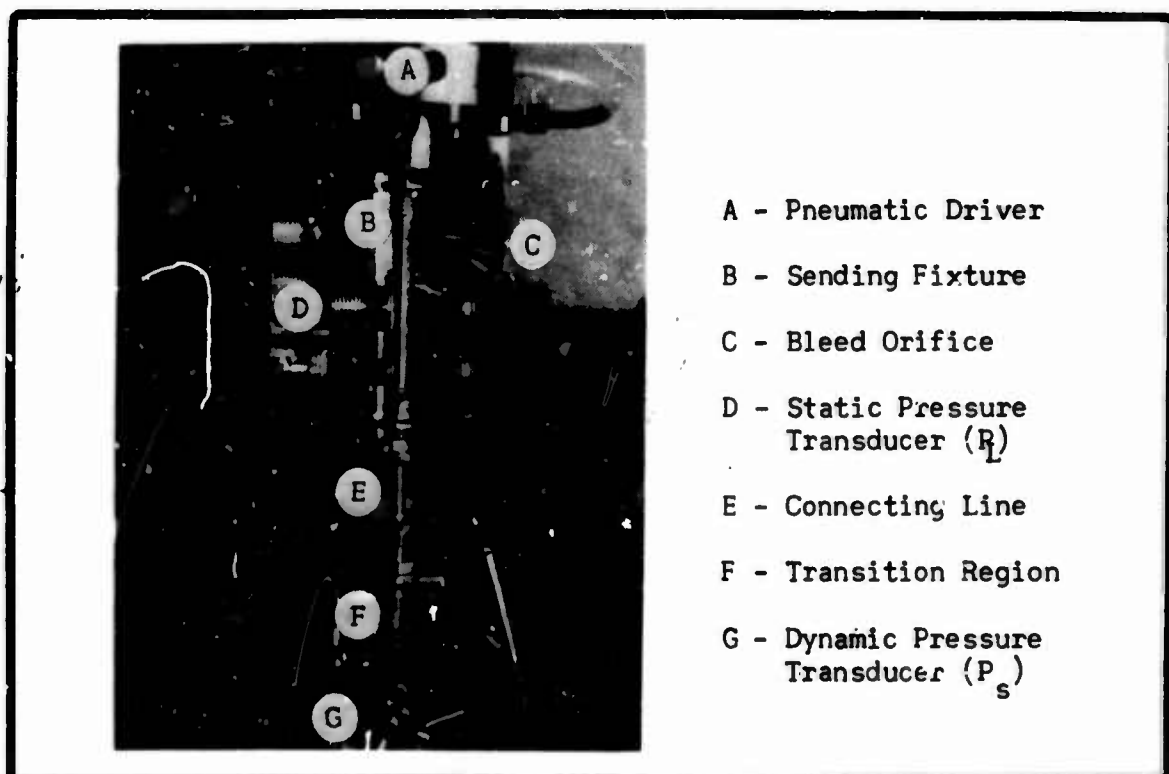
Fig. 3. Sending Fixture and Pneumatic Driver

(P_s) and receiving (P_r) dynamic pressure transducers and the transducer ports were contained in the test fixture. Provision for additional

A - Pneumatic Driver and
    Sending Fixture

B - Dynamic Pressure
    Transducer (P_s)

C - Test Line

D - Dynamic Pressure
    Transducer (P_r)

E - Termination Volume

F - Liquid Fill Tubing
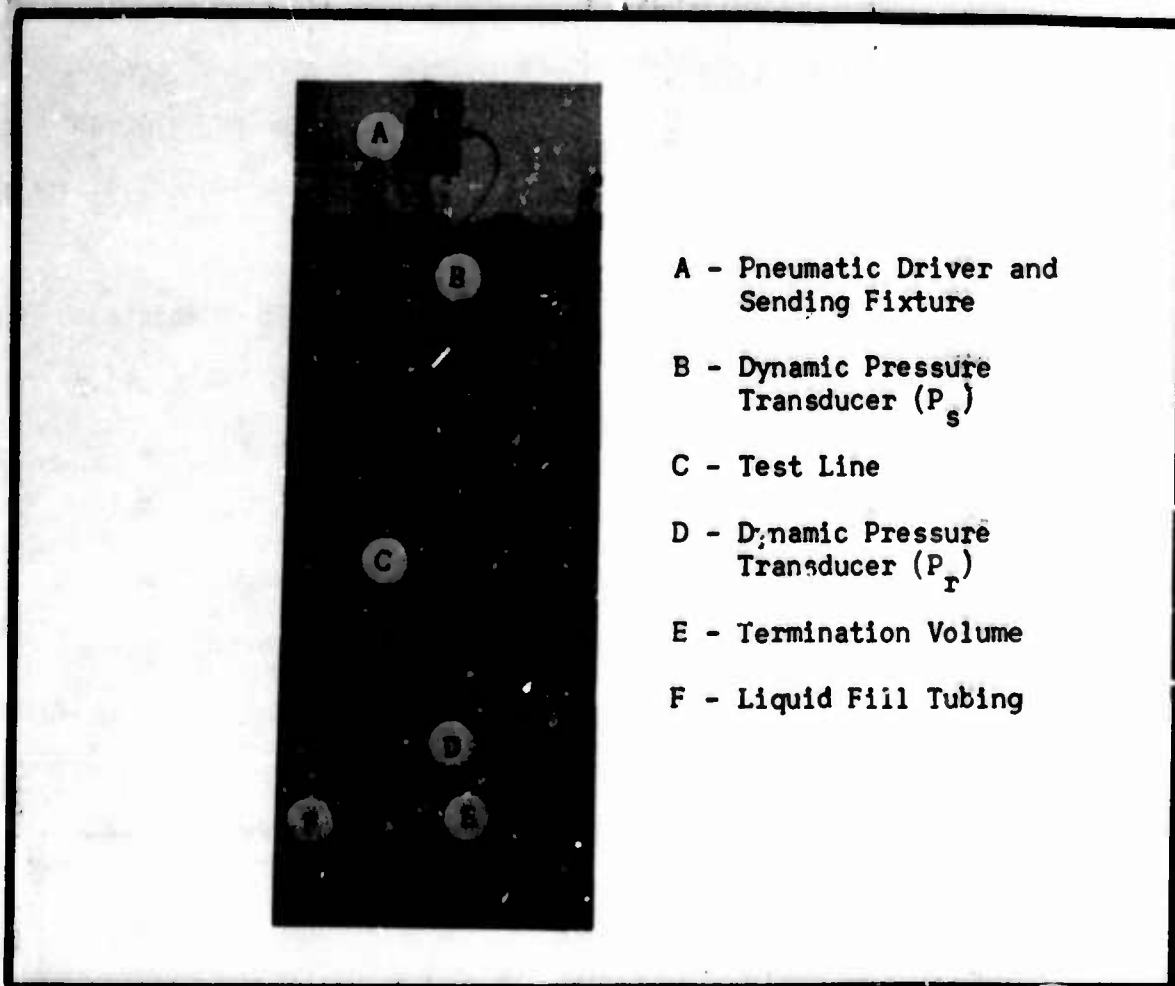
Fig. 4. Rectangular Line Test Fixture

ports was made in the line design, but they were not used in this study.
(See Fig. 4.) The dimensions of the transmission line and terminating
volume are shown in Fig. 5, p. 13. The volume termination was designed
so that the volume could be changed by filling the volume with a liquid
through a fill port located in the bottom of the termination (Fig. 6).
Mercury was used in the series of experiments.

Pneumatic Signal Source

The pneumatic signal source consisted of an electronic signal
generator, high-power amplifier, an electro-pneumatic signal generator
and the sending fixture (Fig. 2). The electronic signal generator
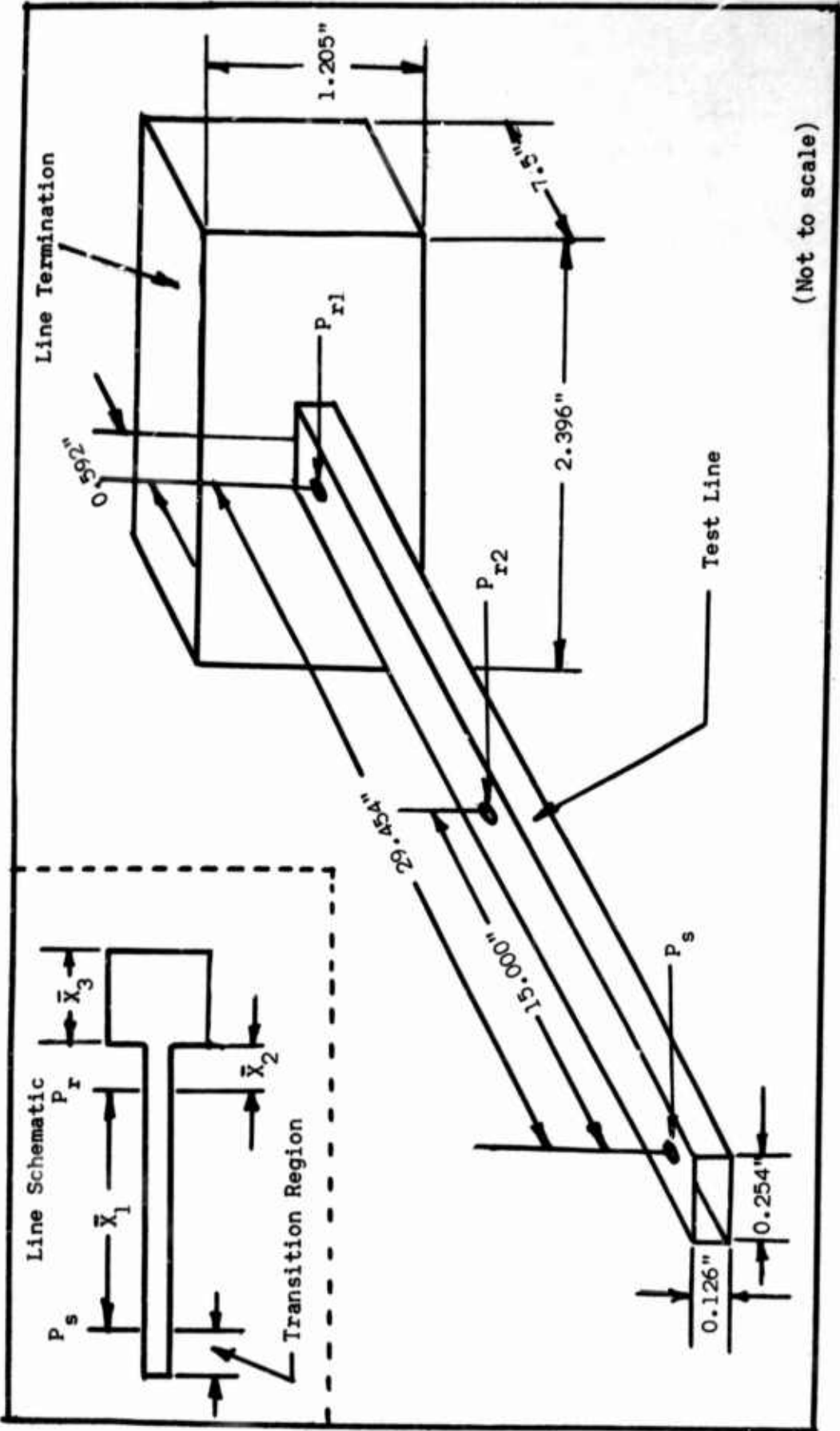
Fig. 5. Test Fixture Interior Dimensions

contained in one of the wave analyzers developed a sinusoidal voltage
which was amplified by a linear amplifier and then by a matched-gain,

A - Pressure
    Transducer (P_r)

B - Volume
    Termination

C - Liquid Level

D - Base Plate

E - Liquid Fill
    Tubing
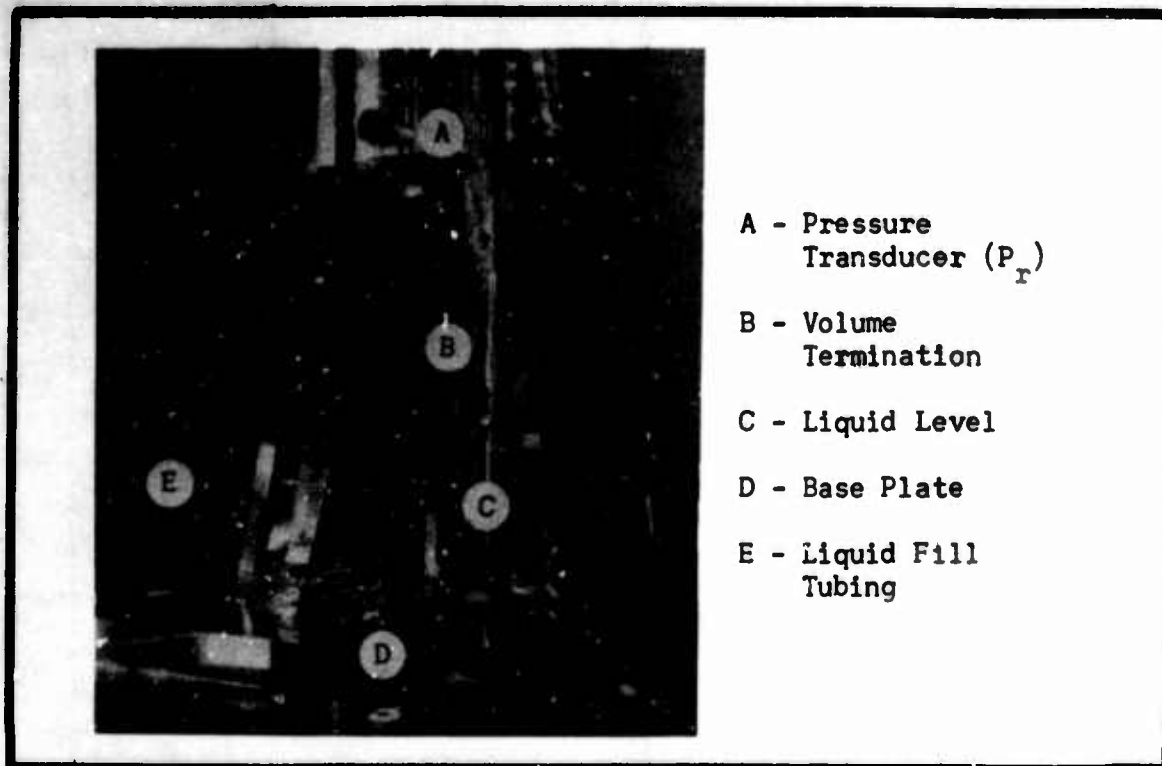
Fig. 6.   Volume Termination

push-pull amplifier in the pneumatic signal generator which in turn
drove a piezoelectric flapper valve in the pneumatic driver head.
Since the pneumatic driver functioned only when a gas flowed through
the flapper valve, it was necessary to provide a bleed orifice in the
sending fixture. With a sinusoidal voltage input to the piezoelectric
disc, the disc oscillated sinusoidally between the orifices, causing a
sinusoidal change (AC) in pressure to be induced on the static line
pressure (DC). The sending fixture also contained the static pressure
transducer (P_L), which measured the line static pressure. The elec-
tronic signal was generated in the electronic wave analyzer at the same
frequency being measured at the dynamic pressure sensing port (P_s)
(Fig. 2).

14

Dimensional Accuracy

The accuracy of the dimensional measurements is critical; this is also discussed by Miller (Ref 14:34). The test fixture base and height measurements were considered accurate to within 0.001 in. ± 0.0005 in. The fixture termination measurements were considered accurate to ± 0.1 in. (Fig. 5).

The Monitoring Equipment

The sinusoidal input voltage frequency was monitored on an electronic counter. The signal voltage was monitored on a vacuum-tube-voltmeter. The output of the static pressure transducer (P_L) was monitored on a differential millivoltmeter. The outputs of the dynamic pressure transducers $(P_s$ and $P_r)$ were amplified in charge amplifiers and sent to two wave analyzers. The wave analyzers were used to determine the fundamental frequency RMS voltage developed by the charge amplifiers. A dual-beam oscilloscope was used to provide a display of the outputs of P_s and P_r. See Fig. 2 for the test equipment schematic. The display was recorded on film at selected frequencies. Another dual-beam oscilloscope was used as linear amplifiers for the outputs of the charge amplifiers. The outputs of both Y-axis amplifiers were fed to the input of the second dual-beam oscilloscope, thereby permitting the display and recording of P_s versus P_r simultaneously (Fig. 7). A mercury thermometer and a precision mercury barometer were used for measuring ambient temperature and pressure. See Fig. 6 for monitoring equipment layout.
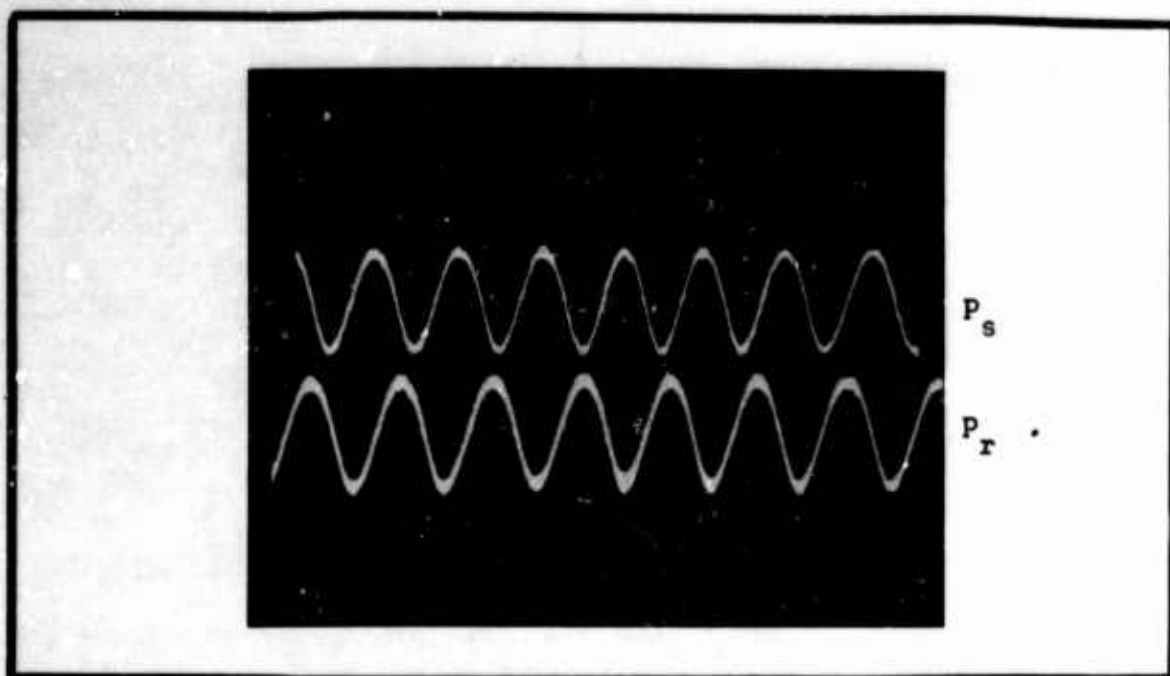
Fig. 7. Typical Dual-Beam
Oscilloscope Display for P_s and P_r

Air Supply

The air used in these tests was laboratory shop air, which was double-filtered and was routed through a settling tank before entering the pneumatic driver head.

A - Pneumatic Drive
    Electronics

B - Air Supply

C - Test Fixture

D - VTVM

E - Millivoltmeter (P_L)

F - Charge Amplifiers

G - Electronic Counter

H - Wave Analyzer (P_s)

I - Wave Analyzer (P_r)

J - Dual-Beam
    Oscilloscope
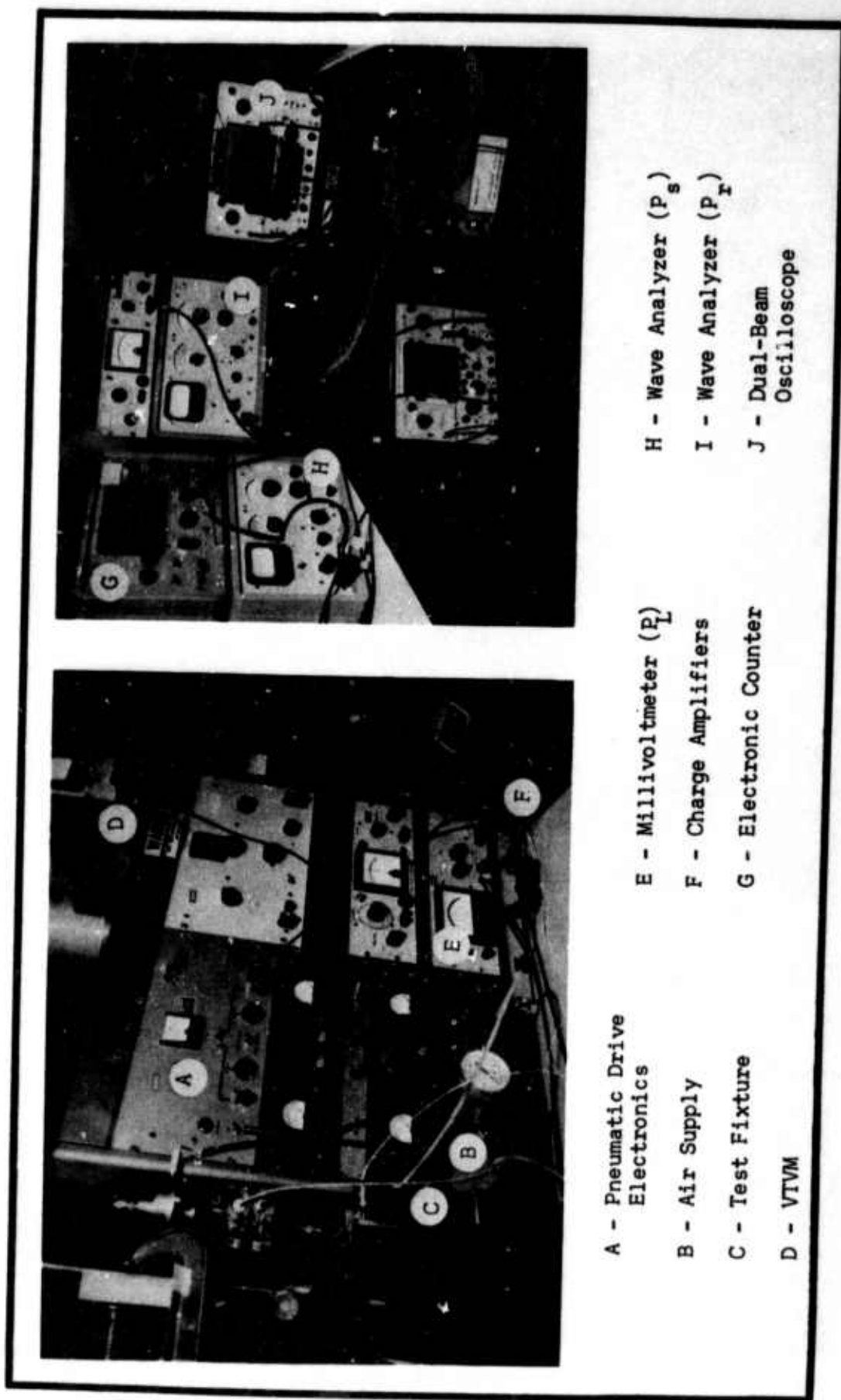
Fig. 8. Monitoring Equipment Layout

17

IV. Experimental Procedures

The objectives outlined in Section I required that data be
obtained experimentally to determine the frequency response of cascaded
rectangular pneumatic lines. The data were required to test the accuracy
of the analytical model for predicting the frequency response of rec-
tangular lines.

General

Once the tests were begun, power was left on all test equipment to
insure stability of the test measurements. Ambient temperature and
pressure readings were taken during each test run and were monitored
for change when each test run lasted longer than an hour. The experi-
mental procedures used in this investigation were similar to the pro-
cedures used by Karam, Wilda, and Miller (Refs 11, 26, 14).

The Cascaded Rectangular Line Tests

The data for the cascaded lines were acquired by measuring the RMS
amplitude of the dynamic input pressure signal (P_s) and the RMS ampli-
tude of the output pressure signal (P_r) at selected locations along the
transmission line (Fig. 4). A computer program was used to reduce the
data by dividing the output dynamic pressure by the input dynamic
pressure and then by calculating the gain in dB. This program was a
subroutine to the general computer program for this investigation as
outlined in Appendix A.

The frequencies at which data were taken were arbitrarily selected.
For some tests data were taken every 10 Hz, and for other tests data

were taken every 25 Hz to 45 Hz. However, for the majority of tests data were taken at points where the frequency response curves exhibited high gain and low gain, i.e., the peaks and valleys in the frequency response curve. The data were taken at 20, 25, and 40 psig and the results of the three runs were plotted with the associated theoretical frequency response curve as calculated using the rectangular transmission line model. A series of tests were also run on blocked rectangular transmission lines and were similar to blocked line investigations by Karam (Ref 11). Discussion of the correlation of data is contained in Section V.

Equipment Considerations

As observed by Karam and by Miller (Refs 11, 14), second harmonic distortion was observed, particularly during the blocked line tests. The wave analyzers were used to measure the outputs of the charge amplifiers at the primary frequency being generated. The wave analyzers were used throughout the frequency range investigated in the series of tests.

Signal Size

The frequency was varied in this study from 10 to 1250 Hz. The sending fixture was the same as used by Karam (Ref 11:15). However, since there was some pressure drop expected in the connecting line between the sending fixture and the test fixture, a new signal size was arbitrarily chosen to be 10 volts RMS applied into the pneumatic driver's push-pull;amplifier. This gave dynamic pressure readings somewhat higher than those quoted by Miller (Ref 14:35).

V. Results and Discussion

Detailed results of the experimental results may be found in Appendices B, C, and D which contain the theoretical frequency response curves and the experimentally determined data points for each curve.

The Rectangular Pneumatic Transmission Line Model

A review of the objectives in Section I shows that a computer program was required which provided solutions to Eqs (2), (5), and (14) and analytical data which predicted the frequency response of volume terminated and blocked rectangular pneumatic lines. Another objective was to experimentally verify the gain equation [Eq (14)].

The rectangular pneumatic transmission line frequency response computer program for the IBM 7094 is described in detail in Appendix A. The program provides solutions to the transmission line distributed parameters at selected frequencies, line pressures, line lengths, and line terminations. A subroutine to the computer program provides solutions to Eq (14) from experimental data. The analytical data and experimental data are then plotted through a computer subroutine on graph paper for direct verification of the theoretical data with the test data.

Correlation of Rectangular Transmission Line Model with Data Presented by Schaedel

For this study, it was considered expedient to compute the distributed impedance and admittance parameters, Eqs (2) and (5) and then compute the gain equation, Eq (14). However, the computer program was checked for correlation with data presented by Schaedel by comparing

the computer output data with the line wave length attenuation graph presented in the paper by Schaedel (Ref 20:51). Since the design aspect ratio of the test line was 0.5 or 2 depending upon how height and base measurements are selected, the computer output data should provide data points which coincide with the 0.5 aspect ratio curve presented by Schaedel (Ref 20:51).

A portion of the Fig. 11 presented by Schaedel (Ref 20:51) is shown in Fig. 9 along with data used from the computer print-out of the solutions to Eq (11). The data was taken at selected gauge pressures and arbitrarily chosen frequencies. Note that ω/ω_v is the frequency ratio described by Schaedel (Ref 20:38). The attenuation per wave length in the line is:

$$(\alpha_1 \gamma) = 54.575 \, \frac{\alpha_1}{\beta_1} \, dB \qquad (20)$$

which is discussed by Schaedel (Ref 20:43) and by Nichols (Ref 17:12). The computer data used from solutions to Eq (11) provide line attenuations and phase shifts per unit length which coincide with the 0.5 and also the 2.0 aspect ratio curve in Fig. 9. As expected the computer program model provides solutions for the distributed impedance and admittance parameters and also computer solutions for α_1 and β_1 which may be used in Eq (20).

T'e Rectangular Transmission Line Model and the Blocked Line

Figure 10 shows a sample plot for a blocked rectangular line. The solid line represents the frequency response as calculated by rectangular pneumatic transmission line computer program, and the x'ᵪ represent the frequency response as calculated from experimental data.
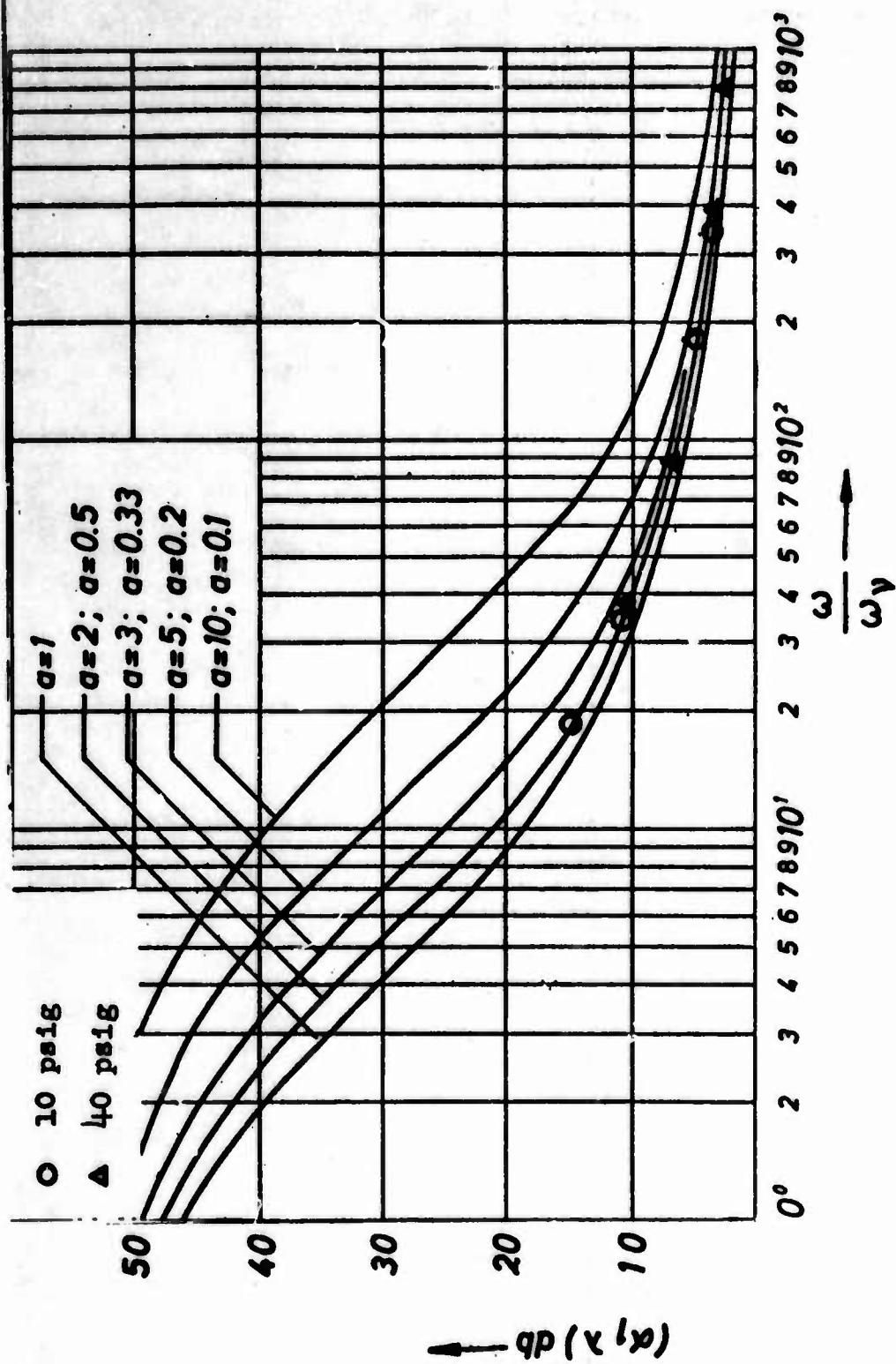
Fig. 9. Computer Data Solutions for Attenuation Per Line Wavelength in dB
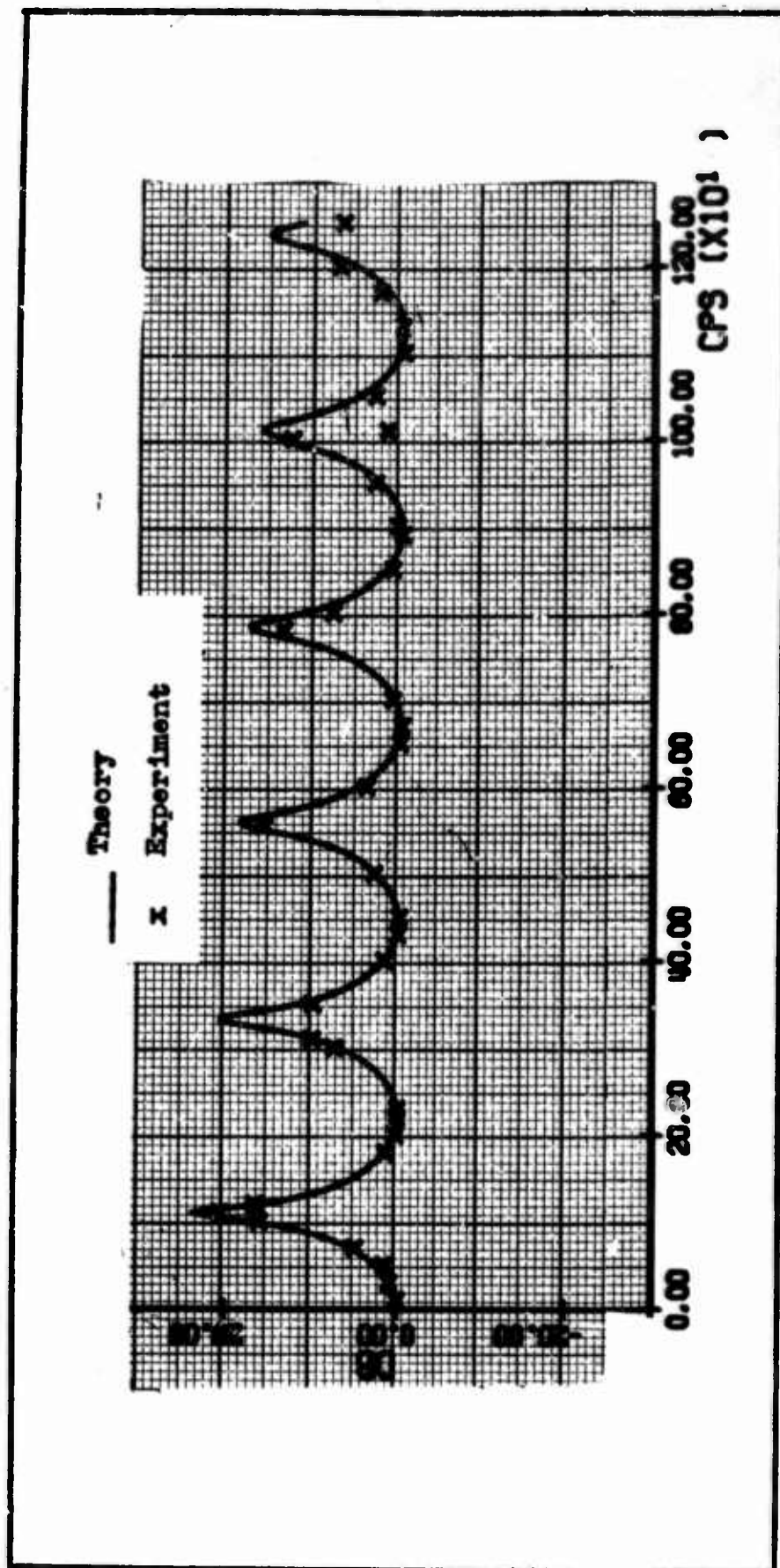
Fig. 10. Correlation of Data Obtained in this Study with the Rectangular Pneumatic
Line Model Program for $\bar{X}_1$ = 29.454 in., $\bar{X}_2$ = 0.592 in., $b_1 = b_2$ = 0.254 in.,
$h_1 = h_2$ = 0.126 in., P_L = 25 psig

Although the plot is similar to the blocked line plots presented by Miller (Ref 14:39), the termination does have an effect on the frequency response. During the experiment it was discovered that it was impossible to accomplish an actual blocked line test because mercury was forced into the receiving transducer (P_r) with the effect that all pressure variations at the receiving transducer (P_r) were damped out and thus not sensed by the transducer.

In the blocked line tests, a short length of line was added beyond the receiving transducer (P_r) to assure that mercury would not be forced into the receiving transducer (P_r). The computer program was designed to treat the additional length of a line as a volume termination when calculating the data to the frequency response curves.

A large deviation was found experimentally at 1010Hz but may have been attributed in part to second harmonic distortion.

An attempt was made to duplicate the experimental test at 1010 Hz, but not all the test conditions could be duplicated, such as the ambient temperature and pressure. A display of the dual-beam oscilloscope was recorded during the test and is shown in Fig. 11. Note how the second harmonics appear to cancel the fundamental at the sending transducer (P_s) and partially at the receiving transducers (P_r). The second harmonic was measured for both the sending (P_s) and receiving (P_r) transducers. Harmonics were noticed to occur more often for the blocked line tests than for the volume-terminated tests. Iberall (Ref 10:92-93) discusses second harmonic distortion caused by nonlinearities of pneumatic lines. Excluding the harmonic distortion problem, the error in gain as calculated by the computer is about 2 dB at 780 Hz, 800 Hz, 1050 Hz, and 1200 Hz. The maximum frequency error is about +10 Hz at
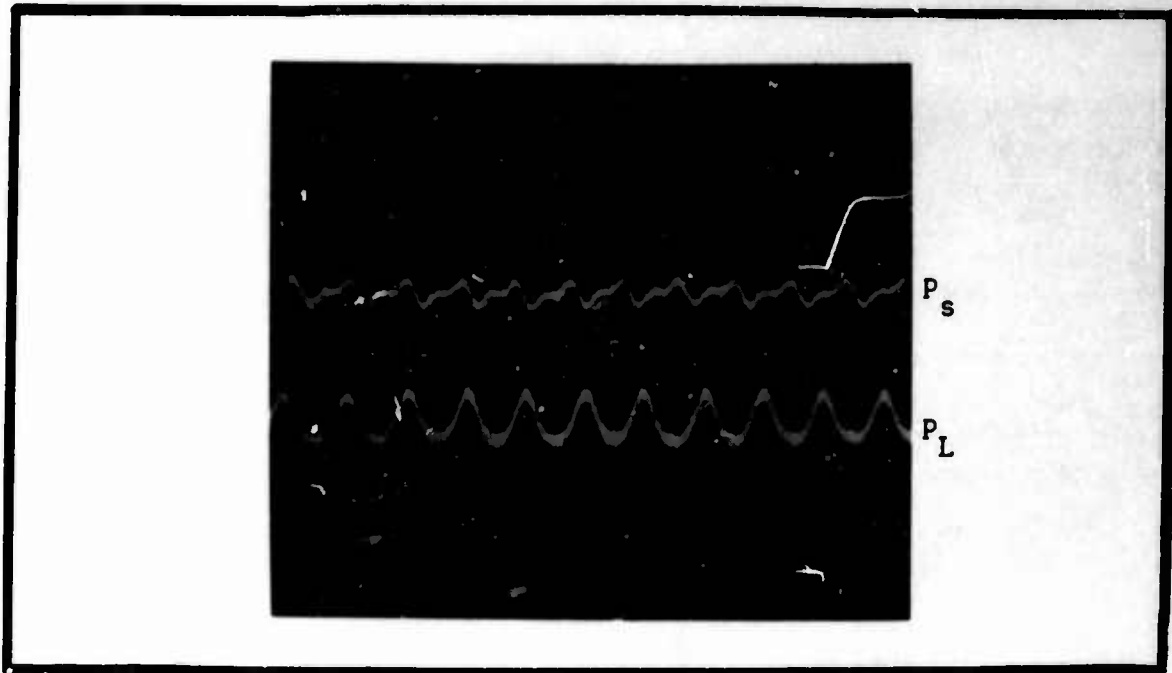
24

Fig. 11. Harmonic Distortion Display at 1010 Hz.
$\bar{X}_1$ = 29.454 in., $\bar{X}_2$ = 0.592 in., $\bar{X}_3$ = 0,
P_L = 25 psig, P_s at 1010 Hz = 4.1 mV,
P_s at 2020 Hz = 2.45 mV, P_r at 1010 Hz =
10.2 mV, P_r at 2020 Hz = 2.5 mV

1200 Hz. These errors are fairly representative, as can be seen in Appendix B. However, some scattering of data is noted, particularly in the 40 psig plots.

As discussed in Section II, both real and imaginary parts of the distributed impedance and admittance are frequency dependent [Eqs (4) and (7)]. Table I lists some of the characteristics for a 29.454 in. long pneumatic transmission line which is terminated in an additional 0.592 in. length of the same line.

By comparing the shape of the frequency response curve (Fig. 9) with the line parameters (Table I), it is noted that for the anti-resonant condition of the line at 10 Hz the line capacitance is much smaller than at resonance which is 1000 Hz. Other resonance peaks

25

Table I

Rectangular Pneumatic Transmission Line Parameters versus Frequency

$b_1 = b_2 = 0.254$ in., $h_1 = h_2 = 0.126$ in.,

$P_L = 25$ psig, Temp. $= 86^\circ F$

Line Parameters	Frequency	
	10 Hz	1000 Hz
R'_s, $\dfrac{psi}{cis}$	$(1.52)(10^{-4})$	$(8.33)(10^{-4})$
L'_s, $\dfrac{psi\text{-}sec}{cis}$	$(6.88)(10^{-4})$	$(5.91)(10^{-2})$
G'_s, $\dfrac{cis}{psi}$	$(3.02)(10^{-3})$	$(2.58)(10^{-2})$
C'_s, $\dfrac{cis\text{-}sec}{psi}$	$(3.97)(10^{-2})$	$(3.66)(10^{0})$
α_{1s}, $\dfrac{nep}{in}$	$(7.77)(10^{-4})$	$(4.92)(10^{-3})$
β_{1s}, $\dfrac{rad}{in}$	$(5.24)(10^{-3})$	$(4.65)(10^{-1})$
C, $\dfrac{in}{sec}$	$(1.198)(10^{4})$	$(1.35)(10^{4})$
C_a, $\dfrac{in}{sec}$	$(1.377)(10^{4})$	$(1.377)(10^{4})$

occur at 110 Hz, 335 Hz, 560 Hz, and 785 Hz. As expected the attenuation per unit length increases for increasing frequency as does the phase velocity. The phase velocity increases from 0.872 c_a at 10 Hz to 0.98 c_a at 1000 Hz. The gain peaks decrease with increasing frequency also attesting to the fact that the attenuation is increasing with increasing frequency. Therefore, a blocked pneumatic transmission line

has a frequency response curve which is similar to an open circuit electrical transmission line. This phenomena is known as the "Ferranti effect" (Ref 23:100).

The Rectangular Pneumatic Transmission Line Model and the Volume-Terminated Line

As discussed in Section II, the rectangular transmission line terminated in a volume was treated as a group of cascaded lines terminated in a blocked rectangular line. The cascaded lines were treated as a series of three lines. Line one was the line under test between the sending dynamic pressure transducer (P_s) and the receiving dynamic pressure transducer (P_r). Line two was the short piece of line between the receiving dynamic pressure transducer (P_r) and transition point of the transmission line under test with the volume-termination. Line three was the rectangular volume-terminated line (Figs. 4 and 5). Thus, the load impedance of line two is the input impedance of line three and the load impedance of line one is the input impedance of line two when terminated in line three. Using Eqs (13) and (14) iteratively solves for the gain of line one. Since the equations defining Z'_s and Y'_s are extremely complicated formulae, it can be seen that it is practically a necessity to use a computer program to provide solutions to the gain equation, Eq. (14). Since dynamic pressure in the line is analogous to voltage (AC), then pressure at any point in the line is directly proportional to the input impedance at that point.

Figures 12, 13, and 14 are typical frequency response curves for volume-terminated lines. The response curves show that the cascaded lines interact as expected. Typically, for the 7.394 in termination (Fig. 12) at 15 Hz the input impedance at the dynamic sending transducer

27

Fig. 12. Correlation of Data Obtained in this Study with the Rectangular Line Model for $\bar{X}_1 = 29.454$ in., $\bar{X}_2 = 0.592$ in., $\bar{X}_3 = 7.394$ in., $b_1 = b_2 = 0.254$ in., $b_3 = 2.396$ in., $h_1 = h_2 = 0.126$ in., $h_3 = 1.205$ in., $P_L = 40$ psig

Fig. 13. Correlation of Data Obtained in This Study with the Rectangular Line Model
for $\bar{X}_1 = 29.454$ in., $\bar{X}_2 = 0.592$ in., $\bar{X}_3 = 3.0$ in., $b_1 = b_2 = 0.254$ in.,
$b_3 = 2.396$ in., $h_1 = h_2 = 0.126$ in., $h_3 = 1.205$ in., $P_L = 40$ psig
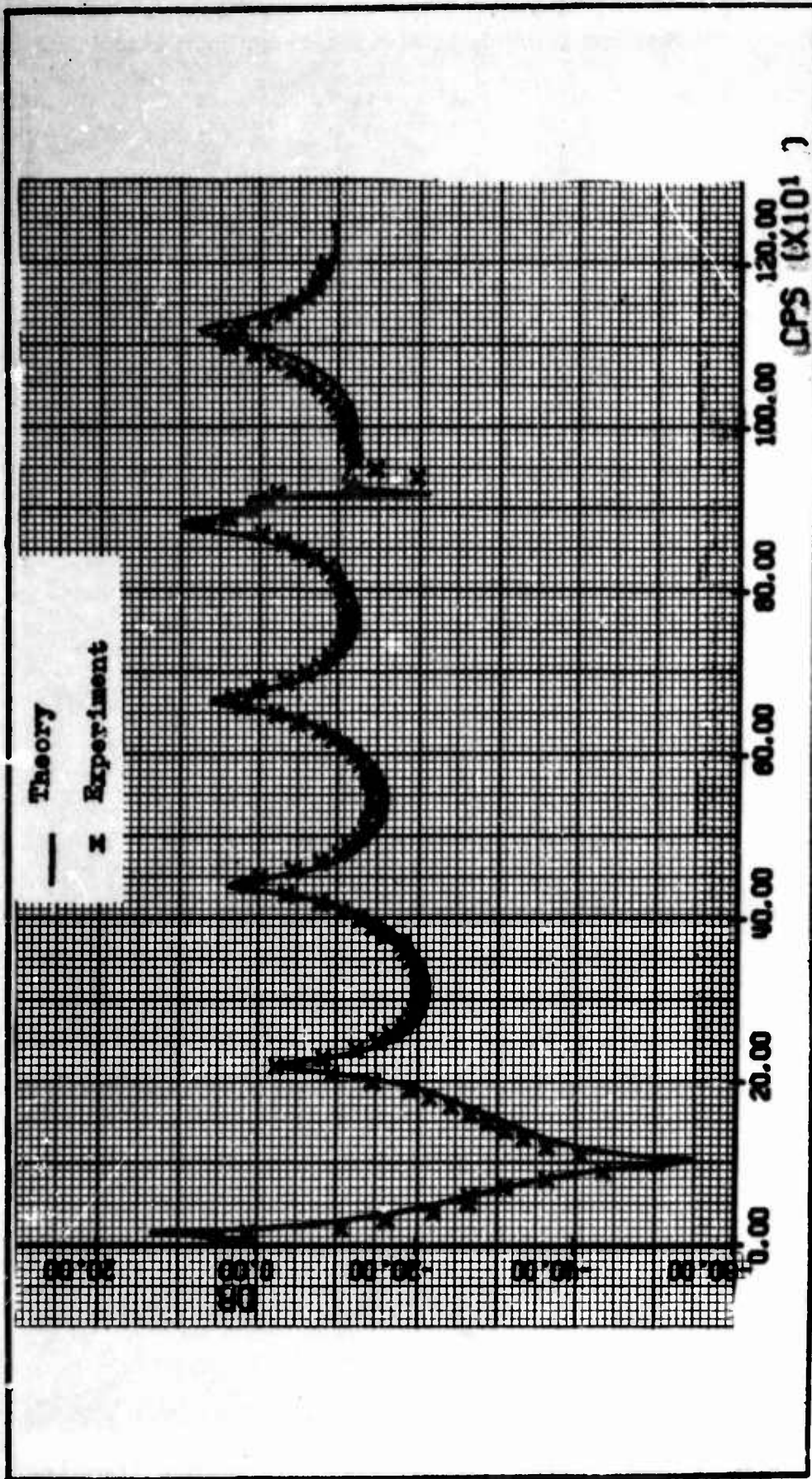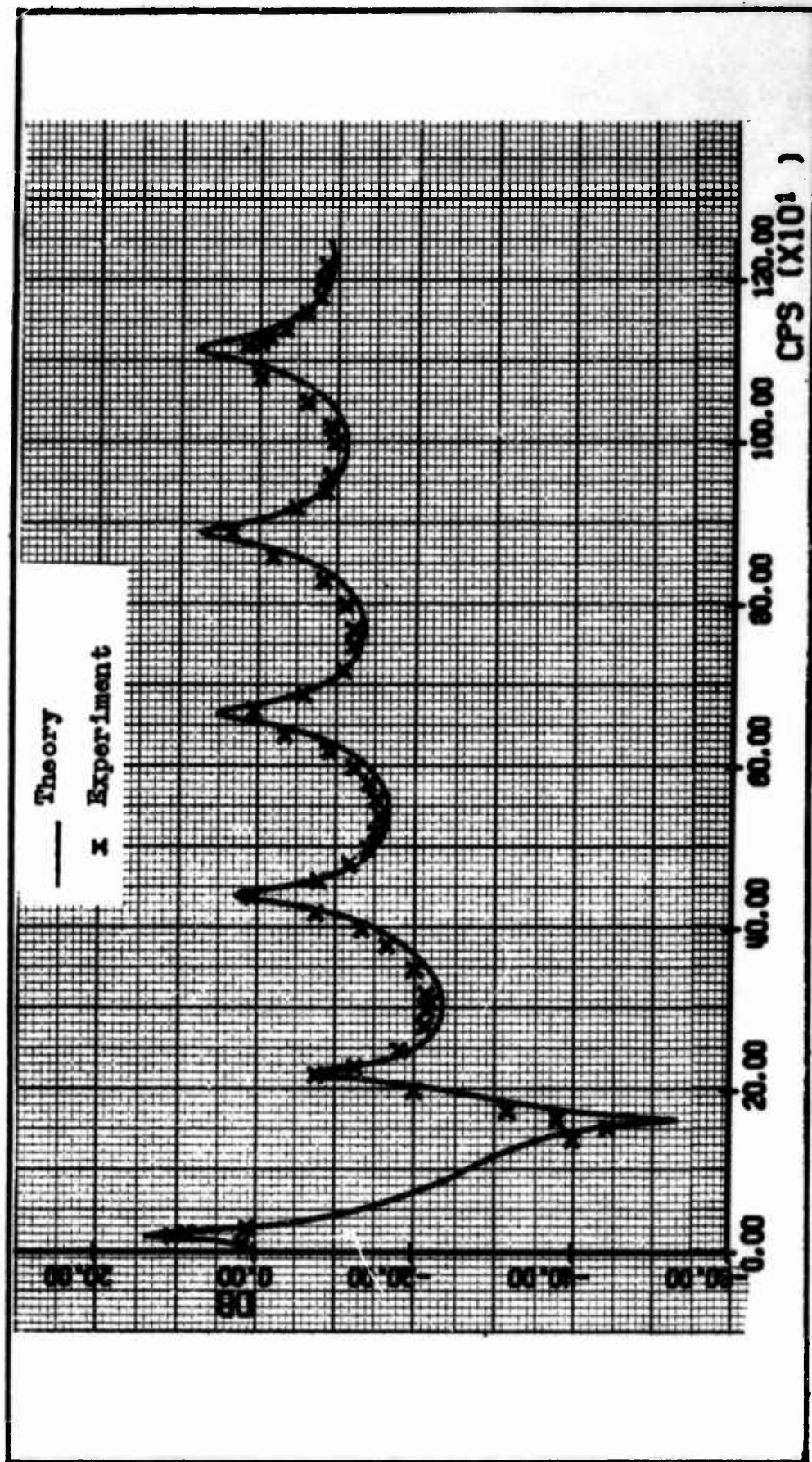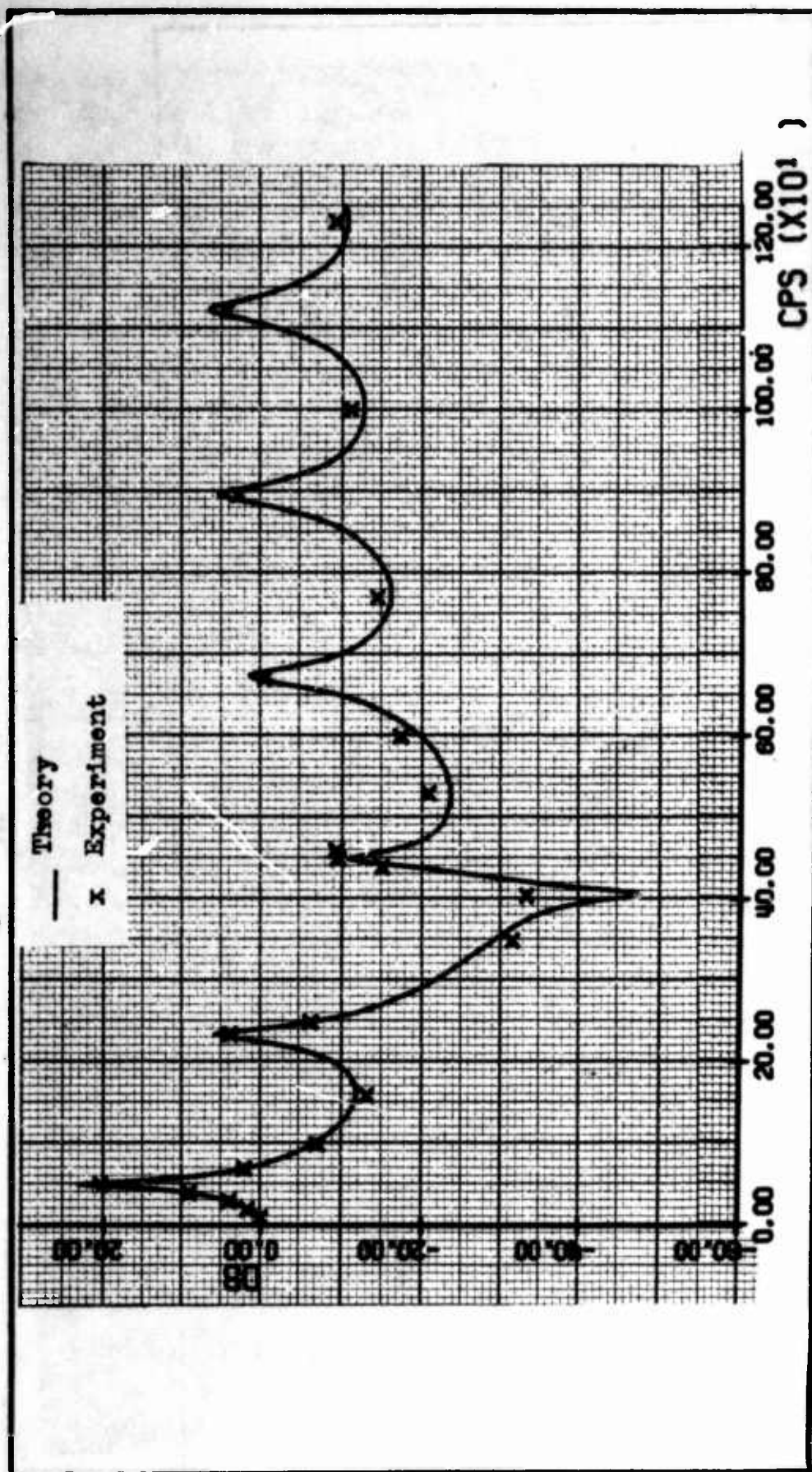
Fig. 14. Correlation of Data Obtained in this Study with the Rectangular Line Model for $\bar{X}_1 = 29.454$ in., $\bar{X}_2 = 0.592$ in., $\bar{X}_3 = 0.5$ in., $b_1 = b_2 = 0.254$ in., $b_3 = 2.396$ in., $h_1 = h_2 = 0.126$ in., $h_3 = 1.205$ in., $P_L = 40$ psig

(P_s) is $(6.20)(10^{-3}) - j(3.71)(10^{-2})$ and the input impedance at the dynamic receiving transducer (P_r) is $(2.32)(10^{-4}) - j(3.62)(10^{-2})$, resulting in a positive gain at 15 Hz. However, at 105 Hz the input impedance to transducer (P_s) is $(8.94)(10^{-1}) - j(5.11)(10^{-3})$ and the input impedance to transducer (P_r) is $(2.46)(10^{-2}) + j(1.88)(10^{-4})$, resulting in a large negative gain at 105 Hz. A similar effect is noted between 915 Hz and 920 Hz. At 915 Hz the input impedance at transducer (P_s) is $(2.31)(10^{-2}) - j(8.4)(10^{-2})$ and the input impedance at transducer (P_r) is $(5.34)(10^{-3}) - j(3.39)(10^{-2})$, resulting in a slight positive gain. At 920 Hz the input impedance at transducer (P_s) is $(2.06)(10^{-2}) - j(4.8)(10^{-2})$ and the input impedance at transducer (P_r) is $(2.28)(10^{-3}) - j(1.83)(10^{-3})$, resulting in a negative gain. These effects noted are the result of the line changing from a capacitive input line at resonance (15 Hz) to a resistive line at antiresonance (105 Hz). Similar effects for varying volume terminations were noted by Miller (Ref 14:43-45) and by Wilda (Ref 26:19-22).

Analysis of Results

The experimental data agree quite closely with the analytically computed data for both blocked and volume-terminated rectangular pneumatic transmission lines. However, scattering of data was observed as noted earlier. With reference to Fig. 12, it was known that the measurement of the termination point must be very accurate. To check the possibility that the measurement may have been incorrect, the termination data for Fig. 10 was varied plus and minus 0.1 in. The frequency response curves in Appendix D depict the results of this variation in parameters study. It was found that a volume termination

31

of 7.3 in. more accurately describes this particular line study than does the nominal 7.394 in. termination which was assumed to be accurate.

As discussed earlier, data scattering may also have been attributed in part to second harmonics; however, this experimental problem could not be predicted in advance of each frequency tested. The pneumatic driver was known to develop strong harmonics at about 400 Hz and 800 Hz plus or minus 50 Hz (Refs 11, 14, and 26). A third source of data scattering was believed to be caused by some erratic readings of the wave analyzers at temperatures above 80°F. Most of the short volume-terminated line experiments and all the blocked-line experiments took place in ambient temperatures above 80°F and relative humidities in excess of 60%.

Although time did not permit additional blocked line tests, the results for both the blocked-line tests and the volume-terminated tests strongly verify the theory as developed by Schaedel and which is used as the model for the computer program.

VI. Conclusions

1. The rectangular pneumatic transmission line theoretical model predicts the small signal frequency response of non-flowing rectangular transmission lines usually within 3 dB over the range of 10 Hz to 1220 Hz. In some cases the model was considered accurate to within 1 dB. The computer model was also shown to accurately predict the following small-signal parameters for rectangular pneumatic lines:

        a. Input impedance

        b. Characteristic impedance

        c. Attenuation constant

        d. Phase constant

        e. Free speed of sound, c_a

        f. Propagation velocity, c

        g. Resonant frequencies

2. The theoretical model was not designed to predict effects of the second harmonics, which were particularly troublesome during the blocked line tests.

3. The accurate measurement of the line termination lengths and also the accurate measurement of the test lines are critical factors in obtaining good agreement between the theoretical model and the experimental data.

VII. Recommendations

1. The rectangular pneumatic transmission line computer program was designed to solve Eqs (2) and (5) by iterative techniques and further analysis should be directed toward:

 a. simplification of Eqs (2) and (5) such that a computer program is not a mandatory requirement to solve the transfer gain equation [Eq (15)]

 b. extension of the computer model study to frequencies above 1250 Hz up to possibly 30,000 Hz.

2. This study considered rectangular lines in cascade; however, further investigations should consider rectangular line tuning devices such as those tested by Miller (Ref 14:32) for circular pneumatic lines. Since most fluidic devices use interconnecting channels which are rectangular in cross section, such a study will assist the designer in properly constructing tuned interconnecting pneumatic lines.

3. A study should be performed which determines the capability of the rectangular pneumatic line parameters for lines very small in cross section, in the ranges of 0.001 in. by 0.003 in. to 0.005 in. by 0.01 in.

4. An investigation should be performed on flowing rectangular pneumatic transmission lines since most fluidic devices require flowing gases for the transfer of information, and the study should include the effects of turbulent flow. The theoretical analysis should also be expanded to include the effects of flow through the rectangular line.

Bibliography

1. Bergh, H., and H. Tijdeman. _Theoretical and Experimental Results for the Dynamic Response of Pressure Measuring Systems._ National Aero- and Astronautical Research Institute Report No. NLR-TR F.238. Amsterdam: National Aero- and Astronautical Research Institute, January 1965.

2. Brown, F. T. "The Transient Response of Fluid Lines." _Journal of Basic Engineering, Trans. ASME_, 84:547-553 (December 1962).

3. D'Azzo, J. J., and C. H. Houpis. _Feedback Control System Analysis and Synthesis_ (Second Edition). New York: McGraw-Hill Book Co., Inc., 1966.

4. Ebert, W. A., and E. M. Sparrow. "Slip Flow in Rectangular and Annular Ducts." ASME Paper 65-FE-20. New York: ASME, March 16, 1965.

5. Eckert, E. R. G., and T. F. Ervine, Jr., _Incompressible Friction Factor, Transition and Hydrodynamic Entrance Length Studies of Ducts with Triangular and Rectangular Cross Sections._ WADC Technical Report 58-85 (AD-151027). Wright-Patterson Air Force Base, Ohio: Wright Air Development Center, April 1957.

6. Guillemin, E. A. _Synthesis of Passive Networks._ New York: John Wiley and Sons, Inc., 1967.

7. Hartig, H. E., and R. F. Lambert. "Attenuation in a Rectangular Slotted Tube of (1,0) Transverse Acoustic Waves." _Journal of the Acoustical Society of America_, 22:42-47 (January 1950).

8. Hilsenrath, J., _et al_. _Tables of Thermal Properties of Gases._ Washington, D. C.: National Bureau of Standards Circular 564, 1955.

9. Houtz, J. Private Communication. Air Force Flight Dynamics Laboratory, Wright-Patterson Air Force Base, Ohio, July 8, 1968.

10. Iberall, A. S. "Attenuation of Oscillatory Pressures in Instrument Lines." _Journal of Research_, 45:85-108 (1950).

11. Karam, J. T., Jr. _The Frequency Response of Blocked Pneumatic Lines._ Unpublished Thesis. Wright-Patterson Air Force Base, Ohio: Air Force Institute of Technology, 1966.

12. Karam, J. T., Jr., and M. E. Franke. "The Frequency Response of Pneumatic Lines." _Journal of Basic Engineering, Trans. ASME_, 89:371-378 (June 1967).

13. Krishnaiyer, R., and T. J. Lechner, Jr. "An Experimental Evaluation of Fluidic Transmission Line Theory." _Advances in Fluidics._ (Edited by F. T. Brown, _et al_). New York: American Society of Mechanical Engineers, 1967.

14. Miller, R. N. Dynamic Characteristics of Blocked, Concentric, Cascaded Pneumatic Transmission Lines. Unpublished Thesis. Wright-Patterson Air Force Base, Ohio: Air Force Institute of Technology, 1968.

15. Moore, R. K. Traveling Wave Engineering. New York: McGraw-Hill Book Co., Inc., 1960.

16. Morse, P. M., and U. K. Ingard. "Linear Acoustic Theory." Encyclopedia of Physics, Acoustics I. Volume XI/1. Berlin: Springer-Verlag, 1961.

17. Nichols, N. B. "The Linear Properties of Pneumatic Transmission Lines." Transactions of the Instrument Society of America, 1:5-14 (January 1962).

18. Pai, S. I. Viscous Flow Theory. Princeton, New Jersey: D. Van Nostrand Company, Inc., 1956.

19. Rohmann, C. P., and E. C. Grogan. "On the Dynamics of Pneumatic Transmission Lines." Transactions of the American Society of Mechanical Engineers, 79:853-874 (May 1957).

20. Schaedel, H. A Theoretical Investigation of Fluidic Transmission Lines with Rectangular Cross Section. Paper K3, Third Cranfield Fluidics Conference, Turin, Italy. Cranfield, Bedford, England: British Hydomechanics Research Association, May 1968.

21. Stephens, R. W. B., and A. E. Bates. Acoustics and Vibrational Physics (Second Edition). London: Edward Arnold, Ltd., 1966.

22. Strutt, J. W. (Lord Rayleigh). The Theory of Sound. Vols. I and II. New York: Dover Publications, 1945.

23. Ware, L. A., and H. R. Reed. Communication Circuits. New York: John Wiley and Sons, Inc., 1949.

24. Watts, G. P. An Experimental Verification of a Computer Program for the Calculation of Oscillatory Pressure Attenuation in Pneumatic Transmission Lines. Los Alamos Scientific Laboratory Report No. LA-3199-MS. New Mexico: Los Alamos Scientific Laboratory of the University of California, November 1964.

25. Westman, H. P., et al. Reference Data for Radio Engineers (ITT) (Fourth Edition). New York: American Book-Shatford Press, Inc., March 1967.

26. Wilda, R. W. Pneumatic Line Dynamics. Unpublished Thesis. Wright-Patterson Air Force Base, Ohio: Air Force Institute of Technology, 1967.

Appendix A

Development of a Rectangular
Pneumatic Transmission Line Model Computer Program

This appendix contains the discussion on the rectangular pneumatic transmission line model computer program. The computer program as written by Houtz (Ref 9) solves through iteration techniques the distributed impedance and admittance equations [Eqs (2) and (5)]. To conserve computer time, an approximation for the complex hyperbolic tangent function was used. It can be shown that (Ref 25:1048)

$$\tanh(x + jy) = \frac{\tanh x + j\tan y}{1 + j\tanh x \tan y} \qquad (A-1)$$

The computer subroutine for the hyperbolic tangent was modified such that for values of x greater than 3, $\tanh x = 1.0$. In order to maintain finite computations, the computer subroutine was directed to ignore values of y whenever

$$y = \frac{2i - 1}{2}\pi, i = (1, 2, 3, \ldots) \qquad (A-2)$$

If y equaled odd multiples of π, then the program was directed to proceed to the next frequency for calculation. This did not occur for the frequencies selected in the cases investigated for this study.

Once the complex impedance and admittance parameters are solved per unit length, the computer program provides solutions to the propagation constant [Eq (11)]. With the propagation constant solved, the computer

program then proceeds to provide solutions to the input impedance at each line, the load impedance at each line, and finally the transfer gain equation for the transmission line undergoing test [Eq (14)].

Although the computer program provides solutions to Eq (14), it can be modified to provide solutions to the general gain equation, Eq (16).

The program is on the remaining pages of this appendix, and the format for the data is on the last page. The format for the data is as follows:

Card 1: Case-number card

Card 2: Minimum gain in dB to be plotted by the Calcomp plotter; gain in dB per inch on the graph

Card 3: Length of transmission line in inches between the dynamic sending transducer (P_s) and the line transition point $(\bar{X}_1 + \bar{X}_2)$; length of the volume termination in inches $(\bar{X}_3)$; length of transmission line in inches between the dynamic receiving transducer (P_r) and the line transition point $(\bar{X}_2)$

Card 4: Base of the transmission line in inches; base of the terminating volume in inches

Card 5: Height of the transmission line in inches; height of the terminating volume in inches.

Card 6: Line pressure in psig

Card 7: Ambient temperature in $^{\circ}F$; ambient pressure in inches of mercury; viscosity in psi-sec; the gas constant, $in^2/sec^2 - {}^{\circ}R$; the specific heat ratio of air; the dimensionless Prandtl number

Card 8: Number of data points; subroutine call identifier for the legend to be plotted by the Calcomp plotter

Card 9:   A maximum of 44 character word printed at the base of the graph by the Calcomp plotter

Card 10 and on: Experimental data--frequency at which data was taken; P_r in millivolts RMS; P_s in millivolts RMS.
The ratio of specific heats for air as used in this study was for air at 40 psig, 80°F, $\gamma = 1.4065$; at 25 psig, 80°F, $\gamma = 1.4047$; and at 10 psig, 80°F, $\gamma = 1.4029$ (Ref 8:59).

Information printed out for each increment of frequency is frequency in Hz, R_s', L_s', C_s', G_s', α_1, β_1, ω_ν, ω_T, transmission line and the terminating volume. The transfer gain for the line undergoing test and the input impedance Z_i, and characteristic impedance Z_o for each line are also printed out. The adiabatic speed of sound c_a is printed out for the specific case under study.

```
$IBFTC SQMLRE  M94,,XR7,DECK
      DATA TPI/6.2831853/
      DIMENSION BCDX(9), BCDY(1), DB(1000), OMG(1000), DATA(600)
      DATA BLANK/6H      /
      DATA DECI/6H DB /
      DATA CPS/6H CPS /
      DATA FH/1250./
      NMAX=600
      CALL PLOTS(DATA,NMAX)
1     READ(5,100)ICAS
100   FORMAT(6I12)
      IF (ICAS) 501,501,2
2     READ(5,105)DBLO,DBHI
      READ(5,105)DI1,DI2,DI3
105   FORMAT(6E12.0)
      READ(5,105)ABASE1,ABASE2
      READ(5,105)AHGT1,AHGT2
      READ(5,105)PL
      READ(5,105)TF,PG,AMU,RE,GAM,SIG
      DO 4 I=1,8
4     BCDX(I)=BLANK
      BCDY(1)=DECI
      BCDX(9)=CPS
      IDT=6
      IF (PG.LT.20.) GO TO 5
      PG=.4912*PG
5     NPG=0
      ICT=1
      IND=1
      N=0
      PBR=PL+PG
      TBR=TF+460.
      RHO=PBR/(RE*TBR)
      ARG1=PBR*GAM/RHO
      CA=SQRT(ARG1)
```

Fig. A-1. Computer Program for
The Rectangular Transmission Line Model

```
QTCA=.25*CA
FN1=QTCA/DI1
FN2=QTCA/DI2
ANU=AMU/RHO
AR1=ABASE1*AHGT1
AR2=ABASE2*AHGT2
EPS=1./PBR
SMA1=AHGT1/ABASE1
SMA2=AHGT2/ABASE2
TEMP=4.*ANU
WGM1=TEMP/AR1
WGM2=TEMP/AR2
TEMP=TEMP/(SIG*SIG)
WNU1=TEMP/AR1
WNU2=TEMP/AR2
KKND=2
IF (DI2.NE.0.) GO TO 8
IF (DI3.NE.0.) GO TO 8
KKND=1
IDT=13
AR2=0.
WGM2=0.
WNU2=0.
ABASE2=0.
AHGT2=0.
DW=5.
Y=0.
N=N+1
Y=Y+DW
W=TPI*Y
CALL INTGR(ITM,Y)
CALL ZSER(ITM,AZN1,BZN1,AMU,AR1,SMA1,W,WGM1,IERR)
GO TO (40,42),IERR
CONTINUE
CALL YSER(ITM,AYN1,BYN1,AMU,AR1,SMA1,W,WNU1,GAM,EPS,IERR)
```

```
8
40
42
```

Fig. A-1. Computer Program for
The Rectangular Transmission Line Model
(Continued)

41

```
         GO TO (40,44),IERR
   44    CONTINUE
C
C        SQRT(Z * Y)
C
         CALL CMPMP(TEMP1,TEMP2,AZN1,BZN1,AYN1,BYN1)
         CALL RTCMP(AN1,BTN1,TEMP1,TEMP2)
         AMD1=TPI/BTN1
C
C        SQRT(Z /.Y)
C
         CALL CMPDV(TEM1,TEM2,AZN1,BZN1,AYN1,BYN1)
         CALL RTCMP(AZRN1,BZRN1,TEM1,TEM2)
         GO TO (46,48),KKND
   46    TEM3=AN1*DI1
         TEM4=BTN1*DI1
         CALL APCOSH(TEM7,TEM8,TEM3,TEM4)
         TEM3=1.
         TEM4=0.
         CALL CMPDV(TEM1,TEM2,TEM3,TEM4,TEM7,TEM8)
         GO TO 54
   48    CALL ZSER(ITM,AZN2,BZN2,AMU,AR2,SMA2,W,WGM2,IERR)
         GO TO (40,50),IERR
   50    CONTINUE
         CALL YSER(ITM,AYN2,BYN2,AMU,AR2,SMA2,W,WNU2,GAM,EPS,IERR)
         GO TO (40,52),IERR
   52    CONTINUE
         CALL CMPMP(TEMP3,TEMP4,AZN2,BZN2,AYN2,BYN2)
         CALL RTCMP(AN2,BTN2,TEMP3,TEMP4)
         AMD2=TPI/BTN2
         CALL CMPDV(TEM3,TEM4,AZN2,BZN2,AYN2,BYN2)
         CALL RTCMP(AZRN2,BZRN2,TEM3,TEM4)
         TEMP=AN2*DI2
         CALL HCOSX(ARG1,TEMP)
         CALL HSINX(ARG2,TEMP)
```

Fig. A-1. Computer Program for
The Rectangular Transmission Line Model
(Continued)

```
        TEM5=BTN2*DI2
        TEMP=COS(TEM5)
        TEM1=ARG1*TEMP
        TEM3=ARG2*TEMP
        TEMP=SIN(TEM5)
        TEM2=ARG2*TEMP
        TEM4=ARG1*TEMP
        CALL CMPDV(ARG1,ARG2,TEM1,TEM2,TEM3,TEM4)
        CALL CMPMP(AZIN2,BZIN2,AZRN2,BZRN2,ARG1,ARG2)
C   BEGIN CALCULATION OF ZIN N1
        CALL CALZIN(AZIN1,BZIN1,AZRN1,BZRN1,AZIN2,BZIN2,AN1,DI1,BTN1)
C   BEGIN CALCULATION OF ZIN N2
        CALL CALZIN(AZIN3,BZIN3,AZRN1,BZRN1,AZIN2,BZIN2,AN1,DI3,BTN1)
C   BEGIN CALCULATION OF P2 / P1
        TEMP=BTN1*(DI1-DI3)
        CSBI1=COS(TEMP)
        SNBI1=SIN(TEMP)
        TEMP=AN1*(DI1-DI3)
        CALL HCOSX(ARG1,TEMP)
        CALL HSINX(ARG2,TEMP)
        TEM1=ARG1*CSBI1
        TEM2=ARG2*SNBI1
        CALL CMPDV(TEM7,TEM8,AZIN3,BZIN3,AZIN1,BZIN1)
        CALL CMPMP(TEM3,TEM4,AZIN3,BZIN3,AZRN1,BZRN1)
        TEM5=ARG2*CSBI1
        TEM6=ARG1*SNBI1
        CALL CMPDV(TEM7,TEM8,AZIN3,BZIN3,AZRN1,BZRN1)
        CALL CMPMP(TEM1,TEM2,TEM7,TEM8,TEM5,TEM6)
        TEM1=TEM3-TEM1
        TEM2=TEM4-TEM2
54      TEMP=TEM1*TEM1+TEM2*TEM2
        RTP=SQRT(TEMP)
        GP=20.*ALOG10(RTP)
        IF (N.LT.ICT) GO TO 55
        ICT=ICT+IDT
```

Fig. A-1. Computer Program for
The Rectangular Transmission Line Model
(Continued)

```
      NPG=NPG+1
      WRITE(6,601)ICAS,NPG
  601 FORMAT(1H1,10X,23HTRANSMISSION LINE STUDY,10X,5HCASE I3,57X,8HPAGE
     1 NO .,I3)
      WRITE(6,801)PL,TF,PG,AR1,AR2
  801 FORMAT(1H0, 8X, 4HPL =E12.4, 3X, 4HTF =E12.4, 3X, 4HPA =E12.4, 3X,
     1 4HA1 =E12.4, 3X,4HA2 =E12.4)
      WRITE(6,805)AMU,RE,GAM,SIG,CA
  805 FORMAT(    9X, 4HMU =E12.4, 3X, 4HRE =E12.4, 2X, 5HGMA =E12.4, 2X
     1, 5HSGA =E12.4, 3X, 4HCA =E12.4)
      WRITE(6,807)FN1,FN2,DI1,DI2,DI3
  807 FORMAT(    8X, 5HFN1 =E12.4, 2X, 5HFN2 =E12.4, 2X, 5HL 1 =E12.4,
     1,2X, 5HL 2 =E12.4, 2X, 5HL 3 =E12.4)
      WRITE(6,811)ANU,EPS,WGM1,WGM2,WNU1,WNU2
  811 FORMAT( 9X, 4HNU =E12.4, 2X, 5HEPS =E12.4, 1X,6HWG 1 =E12.4, 1X,
     1 6HWG 2 =E12.4, 1X, 6HWT 1 =E12.4, 1X, 6HWT 2 =E12.4)
      WRITE(6,809)ABASE1,ABASE2,AHGT1,AHGT2
  809 FORMAT( 9X, 4HB1 =E12.4, 3X, 4HB2 =E12.4, 3X, 4HH1 =E12.4, 3X,
     1 4HH2 =E12.4)
   55 GO TO (58,56),KKND
   56 WRITE(6,901)Y,AMD1,AMD2,GP
  901 FORMAT(1H0,13X, 6HFREQ =1PE12.4, 2X,11HLAMBDA N1 =1PE12.4, 2X,
     111HLAMBDA N2 =1PE12.4, 9X, 4HGP =1PE12.4)
      WRITE(6,903)AN1,AN2,BTN1,BTN2
  903 FORMAT(10X, 10HALPHA N1 =1PE12.4, 3X,10HALPHA N2 =1PE12.4, 4X,9HBE
     1TA N1 =1PE12.4, 4X, 9HBETA N2 =1PE12.4)
      WRITE(6,904)AZN1,BZN1,AZRN2,BZN2
  904 FORMAT(13X, 7HZ N 1 =1PE12.4, 4X, 9HJ Z N 1 =1PE12.4, 6X, 7HZ N 2
     1=1PE12.4, 4X, 9HJ Z N 2 =1PE12.4)
      WRITE(6,906)AYN1,BYN1,AYN2,BYN2
  906 FORMAT(13X, 7HY N 1 =1PE12.4, 4X, 9HJ Y N 1 =1PE12.4, 6X, 7HY N 2
     1=1PE12.4, 4X, 9HJ Y N 2 =1PE12.4)
      WRITE(6,905)AZRN1,BZRN1,AZRN2,BZRN2
  905 FORMAT(12X, 8HZ O N1 =1PE12.4, 3X,10HJ Z O N1 =1PE12.4, 5X,8HZ O N
     12 =1PE12.4, 3X,10HJ Z O N2 =1PE12.4)
```

Fig. A-1. Computer Program for
The Rectangular Transmission Line Model
(Continued)

44

```
      WRITE(6,907)AZIN1,BZIN2,AZIN2,BZIN2
907   FORMAT(11X, 9HZ IN N1 =1PE12.4, 2X,11HJ Z IN N1 =1PE12.4, 4X,9HZ I
     1N N2 =1PE12.4, 2X,11HJ Z IN N2 =1PE12.4)
      WRITE(6,909)AZIN3,BZIN3
909   FORMAT(11X, 9HZ IN N3 =1PE12.4, 2X, 11HJ Z IN N3 =1PE12.4)
      GO TO 59
58    WRITE(6,951)Y,AMD1,GP
951   FORMAT(1H0, 13X, 6HFREQ =1PE12.4, 2X, 11HLAMBDA N1 =1PE12.4, 2X,
     1 4HGP =1PE12.4)
      WRITE(6,953)AN1,BTN1
953   FORMAT(10X,10HALPHA N1 =1PE12.4, 4X, 9HBETA N1 =1PE12.4)
      WRITE(6,955)AZN1,BZN1,AYN1,BYN1
955   FORMAT(13X, 7HZ N 1 =1PE12.4, 4X, 9HJ Z N 1 =1PE12.4, 6X,
     1 7HY N 1 =1PE12.4, 4X, 9HJ Y N 1 =1PE12.4)
59    DB(N)=GP
      OMG(N)=Y
      IF (Y.LT.FH) GO TO 40
      YMIN=DBLO
      DY=DBHI
      XMIN=0.
      DX=200.
      MLR=0
62    MLR=MLR+1
      READ(5,100)NPTS,LSMB
      READ(5,101)(BCDX(I),I=1,8)
101   FORMAT(12A6)
      GO TO (65,68),MLR
65    CALL AXIS(0.,0.,BCDY,6,9.,90.,YMIN,DY,10.)
      CALL AXIS(0.,0.,BCDX,-54,6.25,0.,XMIN,DX,10.)
      OMG(N+1)=XMIN
      DB(N+1)=YMIN
      OMG(N+2)=DX
      DB(N+2)=DY
      CALL LINE(OMG,DB,N,1,0,4)
68    LCT=0
```

Fig. A-1. Computer Program for
The Rectangular Transmission Line Model
(Continued)

```
      DO 70 I=1,NPTS
      IF (I.LT.LCT) GO TO 60
      LCT=LCT+50
      NPG=NPG+1
      WRITE(6,205)(BCDX(J),J=1,8),NPG
  205 FORMAT(1H1, 10X, 13HPRESSURE DATA, 5X, 8A6, 5X, 8HPAGE NO I3)
      WRITE(6,207)
  207 FORMAT(1H0, 10X, 1HN, 4X, 4HFREQ, 10X, 2HP1, 10X, 2HP2, 10X, 2HGP/
     11H0)
   60 READ(5,103)FREQ,P1,P2
  103 FORMAT(3E12.0)
      GP=20.*ALOG10(P1/P2)
      WRITE(6,209)I,FREQ,P1,P2,GP
  209 FORMAT(7X, I5, 4F12.5)
      DB(I)=GP
      OMG(I)=FREQ
   70 CONTINUE
      N=NPTS
      OMG(N+1)=XMIN
      DB(N+1)=YMIN
      OMG(N+2)=DX
      DB(N+2)=DY
      CALL LINE(OMG,DB,N,1,-1,LSMB)
      GO TO (62,91),MLR
   91 CALL PLOT(10.0,0.,-3)
      GO TO 1
  501 CALL PLOTE
      STOP
      END
$IBFTC AC    M94,XR7,DECK
      SUBROUTINE RTCMP(X,Y,A,B)
      CALL ANGL(TEMP,A,B)
      TEMP=.5*TEMP
      Y=A*A+B*B
      X=SQRT(Y)
```

Fig. A-1.   Computer Program for
The Rectangular Transmission Line Model
(Continued)

46

```
      X=SQRT(X)
      Y=X*SIN(TEMP)
      X=X*COS(TEMP)
      RETURN
      END
$IBFTC AB      M94,XR7,DECK
      SUBROUTINE CMPMP(X,Y,A1,A2,B1,B2)
      X=A1*B1-A2*B2
      Y=A1*B2+A2*B1
      RETURN
      END
$IBFTC AD      M94,XR7,DECK
      SUBROUTINE CMPDV(C1,C2,A1,A2,B1,B2)
      TEMP=B1*B1+B2*B2
      C1=A1*B1+A2*B2
      C1=C1/TEMP
      C2=B1*A2-A1*B2
      C2=C2/TEMP
      RETURN
      END
$IBFTC AE      M94,XR7,DECK
      SUBROUTINE HSINX(ARG,X)
      A=EXP(X)
      B=EXP(-X)
      A=A-B
      ARG=.5*A
      RETURN
      END
$IEFTC AF      M94,XR7,DECK
      SUBROUTINE HCOSX(ARG,X)
      A=EXP(X)
      B=EXP(-X)
      A=A+B
      ARG=.5*A
      RETURN
```

Fig, A-1. Computer Program for
The Rectangular Transmission Line Model
(Continued)

```
      END
$IBFTC AG       M94,XR7,DECK
      SUBROUTINE ANGL(C,A,B)
      DATA PI/3.1415926/
      C=ABS(B/A)
      C=ATAN(C)
      IF (A.GT.0.) GO TO 5
      IA=1
      GO TO 7
   5  IA=0
   7  IF (B.GT.0.) GO TO 10
      IB=2
      GO TO 15
  10  IB=0
  15  IA=IA+IB+1
      GO TO (35,30,25,20),IA
  20  C=C-PI
      GO TO 35
  25  C=-C
      GO TO 35
  30  C=PI-C
  35  RETURN
      END
$IEFTC INTG     M94,XR7,DECK
      SUBROUTINE INTGR(JK,ARG)
      TST=ARG/1000.
      IF (TST.LT.1.) GO TO 5
      JK=10
      GO TO 40
   5  TST=ARG/500.
      IF (TST.LT.1.) GO TO 10
      JK=8
      GO TO 40
  10  TST=ARG/100.
      IF (TST.LT.1.) GO TO 15
```

Fig. A-1.   Computer Program for
The Rectangular Transmission Line Model
(Continued)

48

```
        JK=6
        GO TO 40
15      JK=4
40      RETURN
        END
$IBFTC SERZ    M94,XR7,DECK
        SUBROUTINE ZSER(J,AREL,AIMJ,U,A,TNA,FRQ,FGGM,IERR)
        AREL=0.
        AIMJ=0.
        DO 10 K=1,J
        CALL YSUM(K,TNA,FRQ,FQGM,ART,BRT,IERR)
        GO TO (40,8),IERR
8       AREL=AREL+ART
        AIMJ=AIMJ+BRT
10      CONTINUE
        TEM3=AREL
        TEM4=AIMJ
        TEM1=2.*U/(A*A*TNA)
        TEM2=0.
        CALL CMPDV(AREL,AIMJ,TEM1,TEM2,TEM3,TEM4)
40      RETURN
        END
$IBFTC SERY    M94,XR7,DECK
        SUBROUTINE YSER(J,AREL,AIMJ,U,A,TNA,FRQ,FQT,GAM,EPS,IERR)
        TEMP=FRQ*A*EPS
        AREL=0.
        AIMJ=0.
        DO 10 K=1,J
        CALL YSUM(K,TNA,FRQ,FQT,ART,BRT,IERR)
        GO TO (40,8),IERR
8       AREL=AREL+ART
        AIMJ=AIMJ+BRT
10      CONTINUE
        TEM1=2.*TNA*(GAM-1.)*FRQ*TEMP/(FQT*GAM)
        AREL=AREL*TEM1
```

Fig. A-1. Computer Program for
The Rectangular Transmission Line Model
(Continued)

```
         AIMJ=AIMJ*TEM1+TEMP
40       RETURN
         END
$IBFTC SUMY    M94,XR7,DECK
         SUBROUTINE YSUM(I,SMA,OMG,OGT,TEM1,TEM2,IERR)
         DATA PI/3.1415926/
         ALPI=(FLOAT(2*I)-1.)*.5*PI
         ALPSQ=ALPI*ALPI
         OMGR=OMG/OGT
         SMAOM=SMA*OMGR
         TEM1=SMAOM
         TEM2=ALPSQ
         CALL RTCMP(TEM3,TEM4,TEM2,TEM1)
         TEM1=1./SMA
         TEM5=TEM3*TEM1
         TEM6=TEM4*TEM1
         CALL APTANH(TEM1,TEM2,TEM5,TEM6,IERR)
         GO TO (40,30),IERR
30       CONTINUE
         CALL CMPDV(TEM7,TEM8,TEM1,TEM2,TEM5,TEM6)
         TEM7=1.-TEM7
         TEM8=-TEM8
         TEM3='ALPSQ*ALPSQ
         TEM4=ALPSQ*SMAOM
         CALL CMPDV(TEM1,TEM2,TEM7,TEM8,TEM3,TEM4)
40       RETURN
         END
$IBFTC HTNAPX M94,XR7,DECK
         SUBROUTINE APTANH(A,B,C,D,IER)
         IER=2
         IF (C.LT.8.) GO TO 10
         A=1.
         B=0.
         GO TO 30
10       IF (C.GT.-8.) GO TO 12
```

Fig. A-1. Computer Program for
The Rectangular Transmission Line Model
(Continued)

```
      A=-1.
      B=0.
      GO TO 30
   12 X=TANH(C)
   15 Y=SIN(D)/COS(D)
      A=ABS(Y)
      IF (A.LT.50.) GO TO 20
      IER=1
      GO TO 30
   20 TEM1=X
      TEM2=Y
      TEM3=1.
      TEM4=X*Y
      CALL CMPDV(A,B,TEM1,TEM2,TEM3,TEM4)
   30 RETURN
      END
$IBFTC TSTST    M94,XR7,DECK
      SUBROUTINE APCOSH(A,B,X,Y)
      CALL HCOSX(TEM1,X)
      CALL HSINX(TEM2,X)
      A=TEM1*COS(Y)
      B=TEM2*SIN(Y)
      IF (B.GE.0.) GO TO 10
      B=-B
   10 RETURN
      END
$IBFTC AI       M94;XR7,DECK
      SUBROUTINE CALZIN(AZIN1,BZIN1,AZRN1,BZRN1,AZIN2,BZIN2,AN1,DI1,
     1BTN1)
      TEMP=AN1*DI1
      CALL HCOSX(ARG1,TEMP)
      CALL HSINX(ARG2,TEMP)
      TEMP=BTN1*DI1
      CSBI1=COS(TEMP)
      SNBI1=SIN(TEMP)
```

Fig. A-1. Computer Program for
The Rectangular Transmission Line Model
(Continued)

```
ZR=0.
CALL CMPMP(TEM1,TEM2,AZIN2,BZIN2,ARG1,ZR)
CALL CMPMP(TEM3,TEM4,AZRN1,BZRN1,ARG2,ZR)
CALL CMPMP(TEM5,TEM6,AZIN2,BZIN2,ARG2,ZR)
CALL CMPMP(TEM7,TEM8,AZRN1,BZRN1,ARG1,ZR)
A1=TEM1+TEM3
B1=TEM2+TEM4
A2=TEM5+TEM7
B2=TEM6+TEM8
CALL CMPMP(TEM1,TEM2,A1,B1,CSBI1,ZR)
CALL CMPMP(TEM5,TEM6,A2,B2,CSBI1,ZR)
CALL CMPMP(TEM7,TEM8,A1,B1,ZR,SNBI1)
CALL CMPMP(TEM3,TEM4,A2,B2,ZR,SNBI1)
TEM3=TEM3+TEM1
TEM4=TEM4+TEM2
TEM7=TEM7+TEM5
TEM8=TEM8+TEM6
CALL CMPDV(TEM1,TEM2,TEM3,TEM4,TEM7,TEM8)
CALL CMPMP(AZIN1,BZIN1,TEM1,TEM2,AZRN1,BZRN1)
RETURN
END
```

Fig. A-1.   Computer Program for
The Rectangular Transmission Line Model
(Continued)

52

```
140
-0.80000E+02+0.20000E+02
+0.30046E+02+0.10000E+01+0.59150E+00
+0.25300E+00+0.23960E+01
+0.12600E+00+0.12050E+01
+0.40000E+02
+0.82000E+02+0.29217E+02+0.26756E-08+0.24711E+06+0.14065E+01+0.84142E+00
                          20                                         4
FADA-RL-1.0-40-080468
15.      15.2     12.5
25.       9.6      5.3
35.       8.25     1.15
45.       8.3      4.1
160.      1.95    18.7
220.      1.1      3.35
225.      1.03     2.45
230.      0.93     2.62
290.      0.54    38.5
330.      0.92    26.5
445.      4.45     5.75
540.      3.       7.
640.      4.85    12.3
670.      3.45     2.78
690.      3.22     5.3
770.      8.4     39.
890.      3.85     2.78
1000.    10.6     35.5
1120.     8.25     4.85
1230.     9.95    28.5
```

Fig. A-1. Computer Program for
The Rectangular Transmission Line Model
(Continued)

Appendix B

Plots of Experimentally Obtained Frequency Response Points for Blocked Rectangular Pneumatic Lines Correlated with The Frequency Response Curves as Solved by the Rectangular Pneumatic Transmission Model Computer Program

This appendix contains the experimental data taken from a series of tests for blocked rectangular pneumatic lines. The data include the frequency response curve for each case as solved by the rectangular pneumatic transmission line model computer program. The x's are the experimentally determined data points, and the smooth curve is the computer solutions to the transfer gain equations.

The distance between the dynamic sending transducer (P_s) and the dynamic receiving transducer (P_r) is $\bar{X}_1$ in inches. The distance from the receiving dynamic transducer (P_r) to the blocked point of the transmission line is $\bar{X}_2$ in inches. The base is b in inches with the subscript identifying the line. The height is h in inches with the subscript identifying the line.
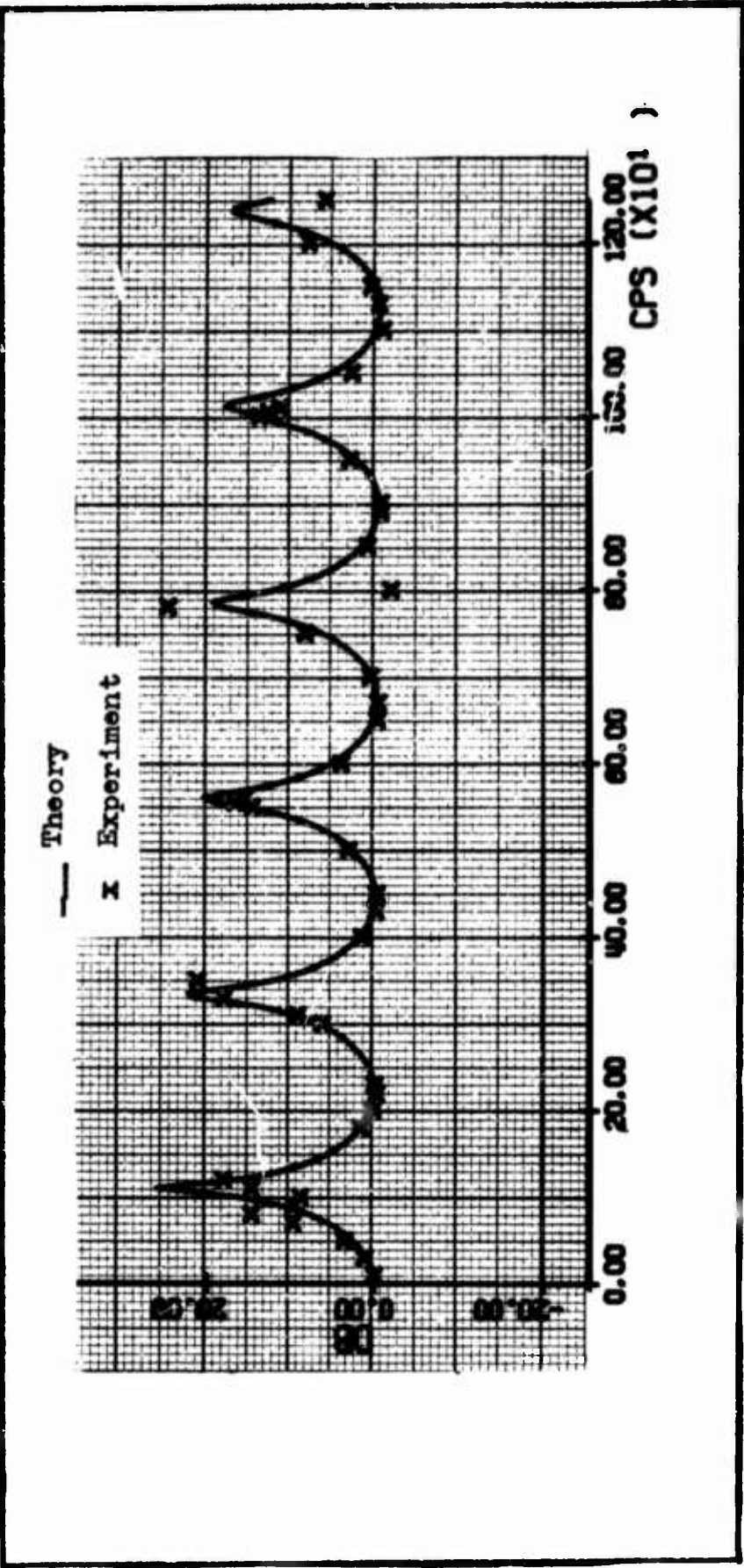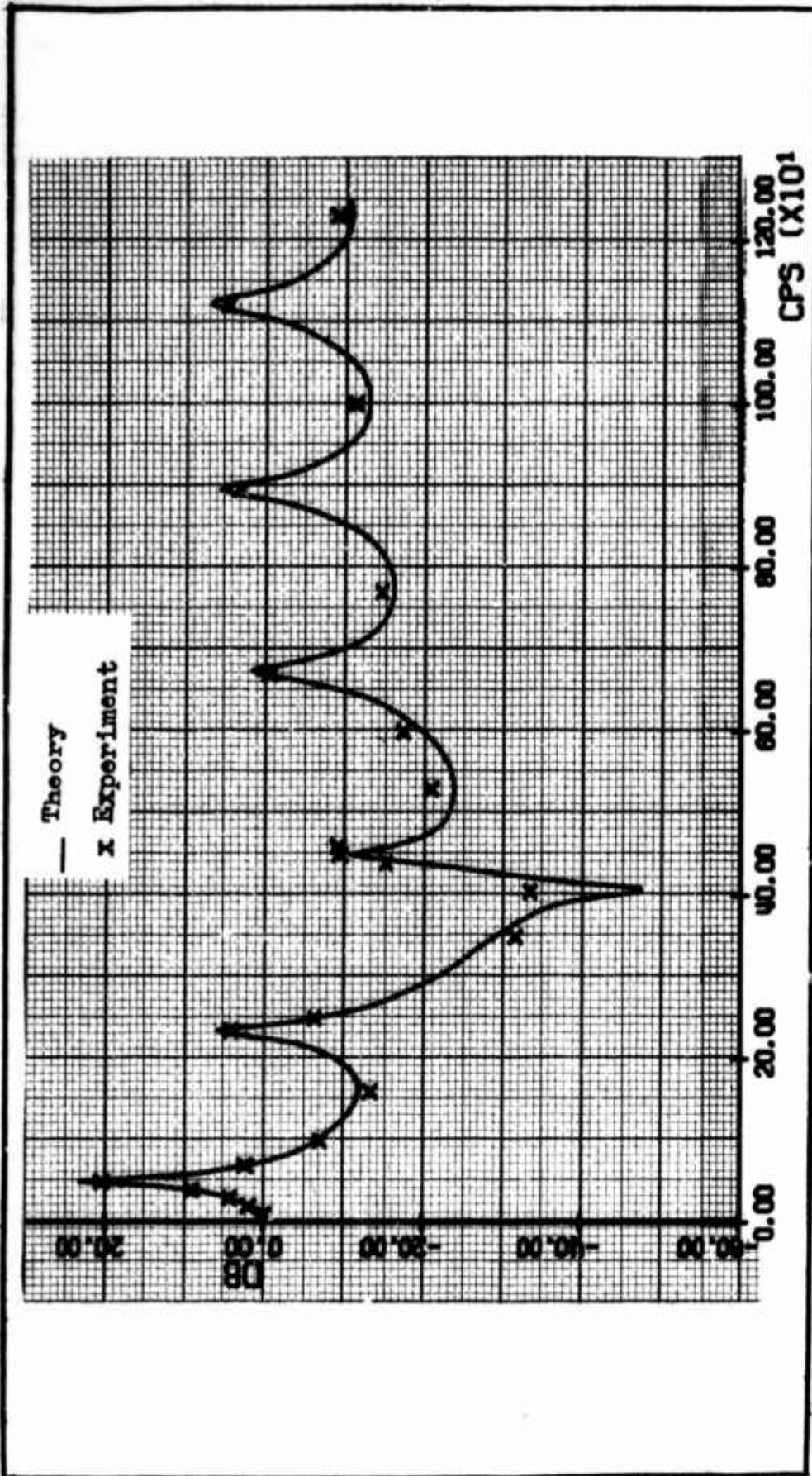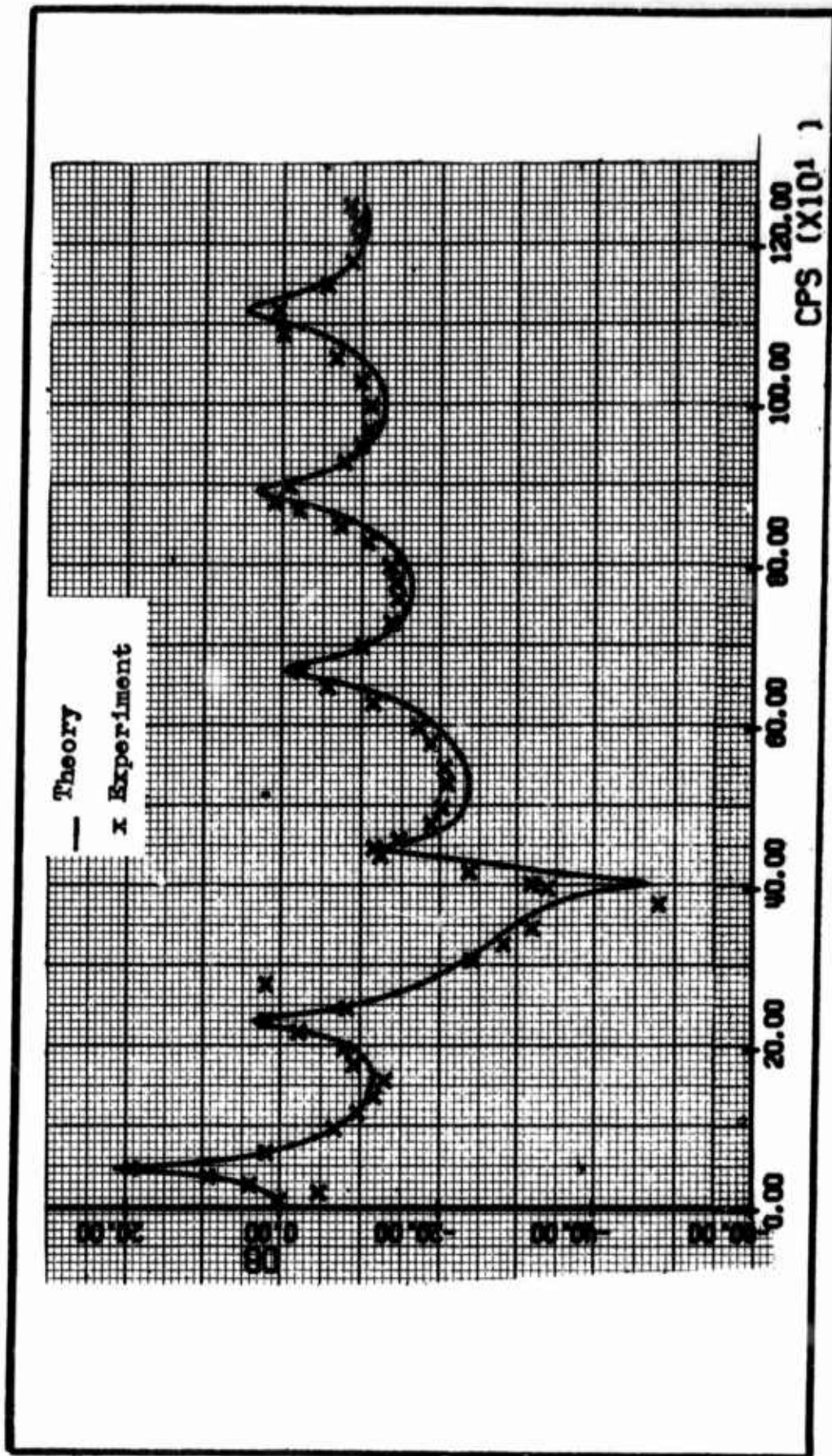
Fig. B-1. Correlation of Data Obtained in this Study with the Rectangular Pneumatic Line Model for $\bar{X}_1 = 29.454$ in., $\bar{X}_2 = 0.592$ in., $b_1 = b_2 = 0.254$ in., $h_1 = h_2 = 0.126$ in., $P_L = 40$ psig
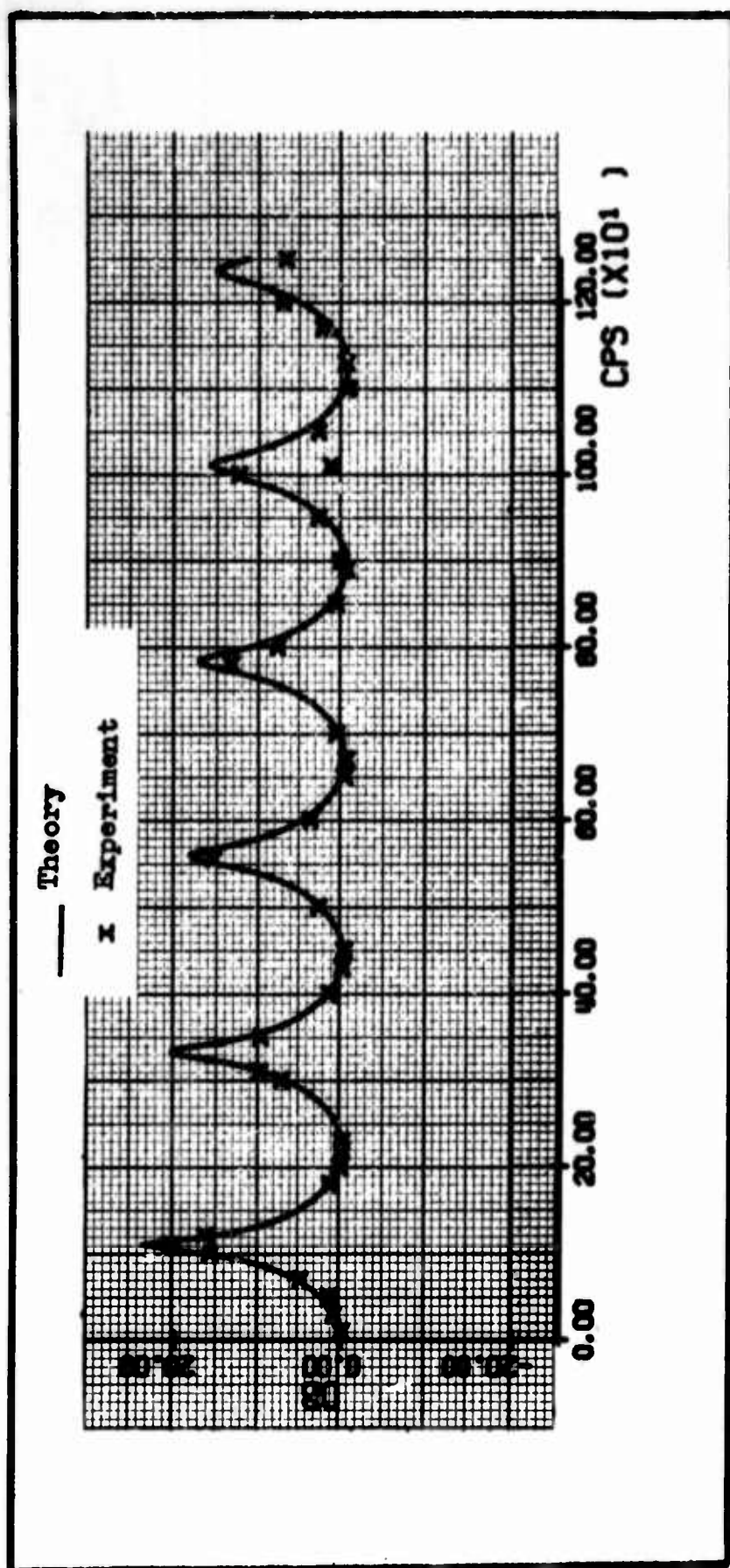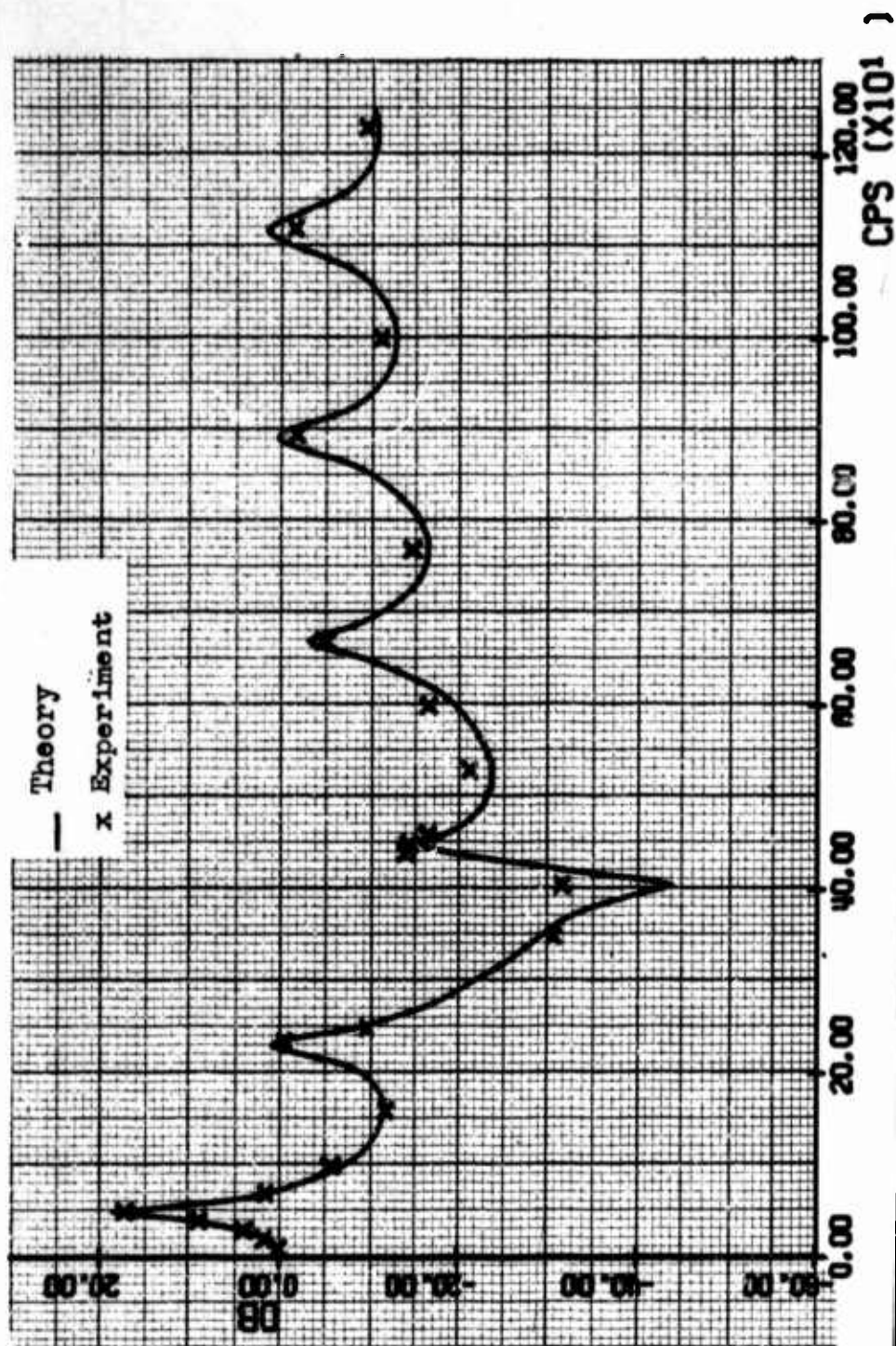
Fig. B-2. Correlation of Data Obtained in this Study with the Rectangular Pneumatic Line Model for $\bar{X}_1 = 29.454$ in., $\bar{X}_2 = 0.592$ in., $b_1 = b_2 = 0.254$ in., $h_1 = h_2 = 0.125$ in., $P_L = 25$ psig
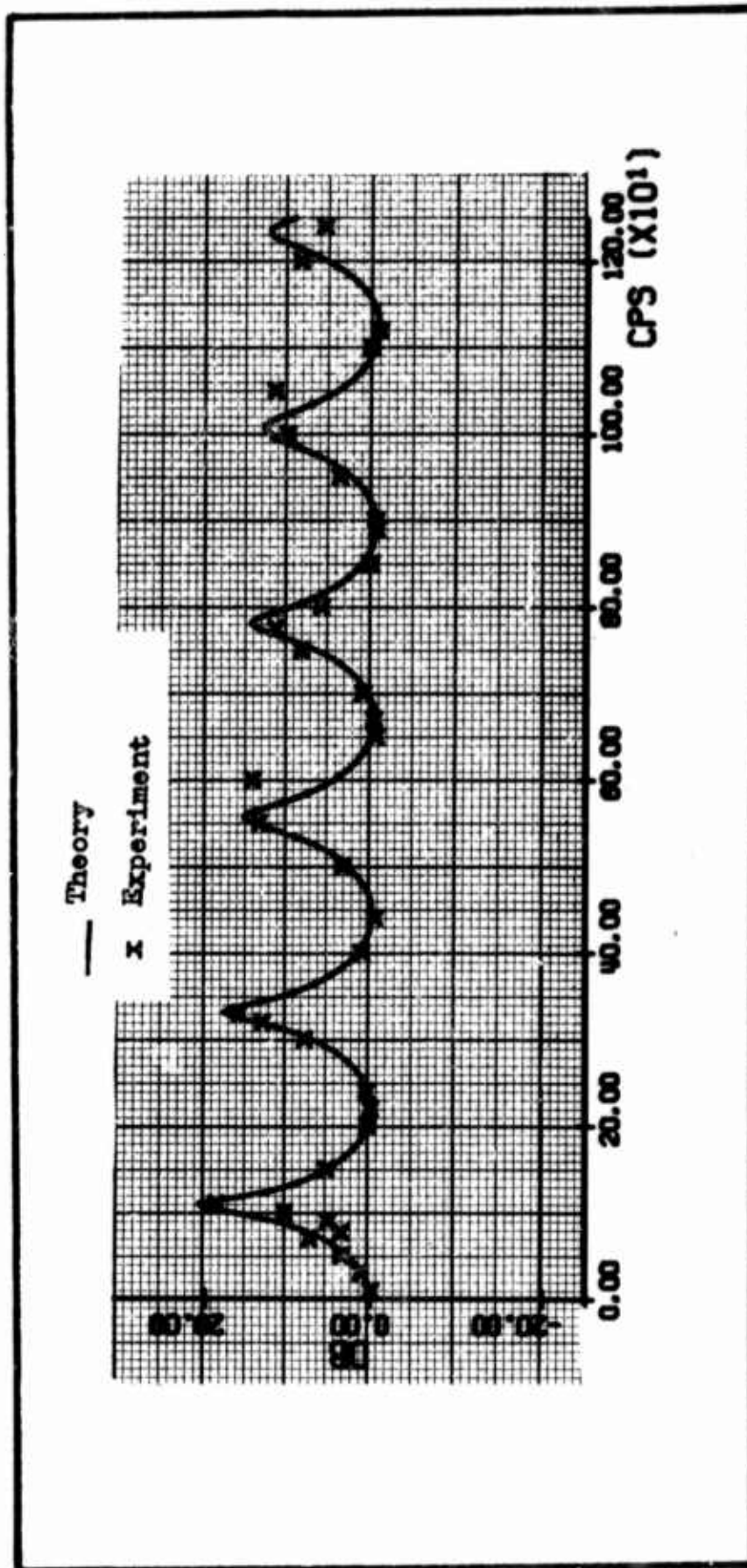
Fig. 3-3. Correlation of Data Obtained in this Study with the Rectangular Pneumatic Line Model for $\bar{X}_1 = 29.454$ in., $\bar{X}_2 = 0.592$ in., $b_1 = b_2 = 0.254$ in., $h_1 = h_2 = 0.126$ in., $P_L = 10$ psig
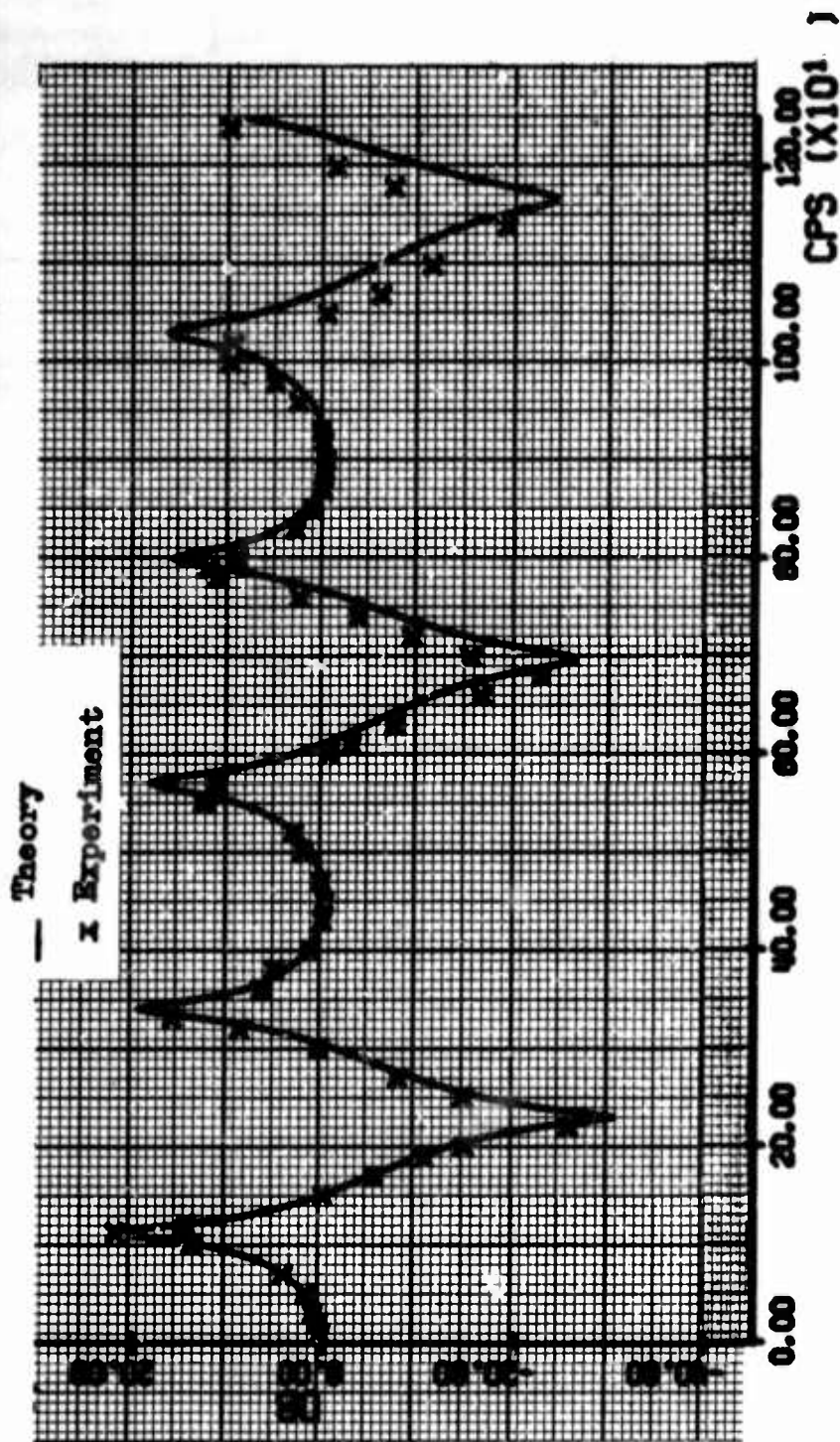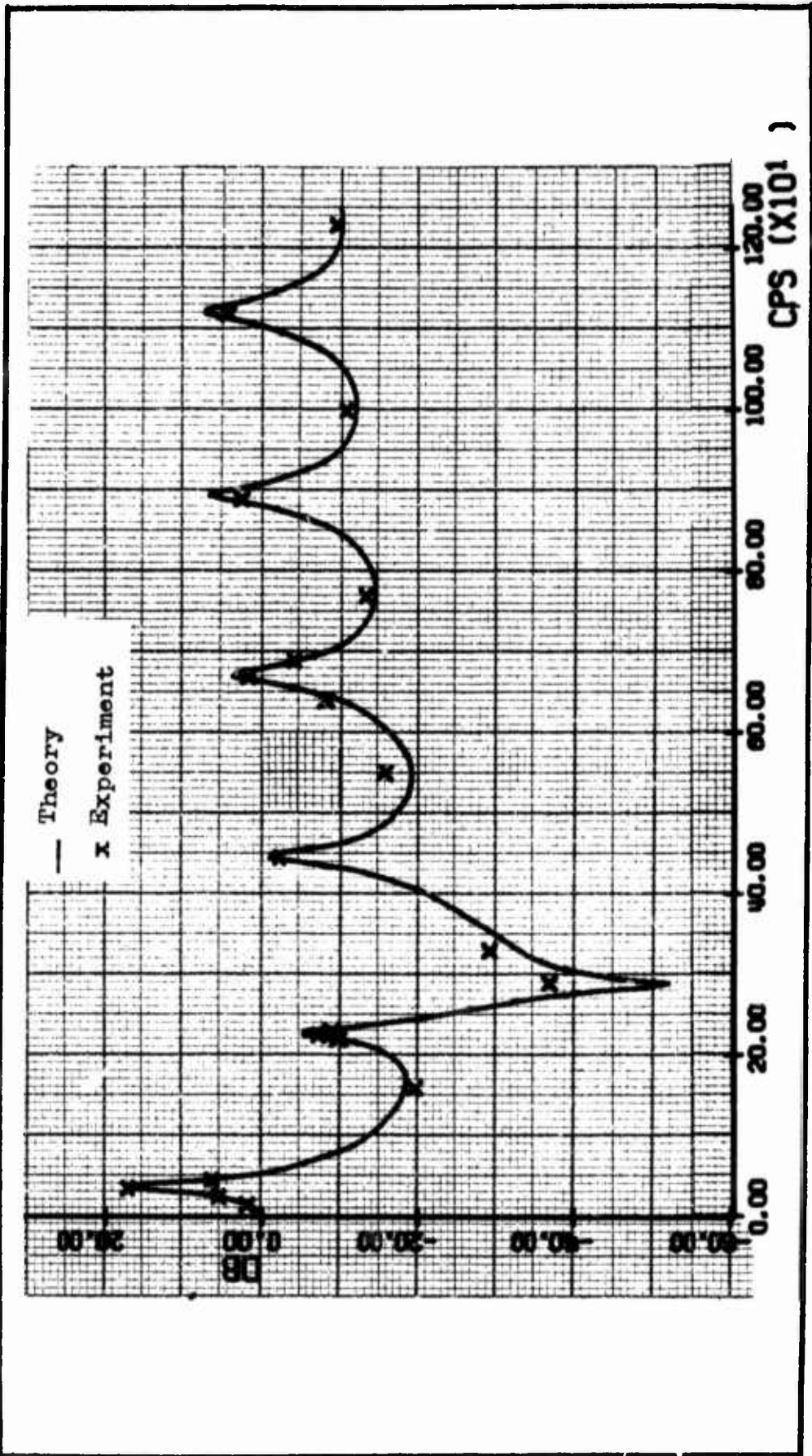
Fig. B-4. Correlation of Data Obtained in This Study with the Rectangular Pneumatic Line Model for $\bar{X}_1 = 15.0$ in., $\bar{X}_2 = 14.454$ in., $b_1 = b_2 = 0.254$ in., $h_1 = h_2 = 0.126$ in., $P_L = 40$ psig
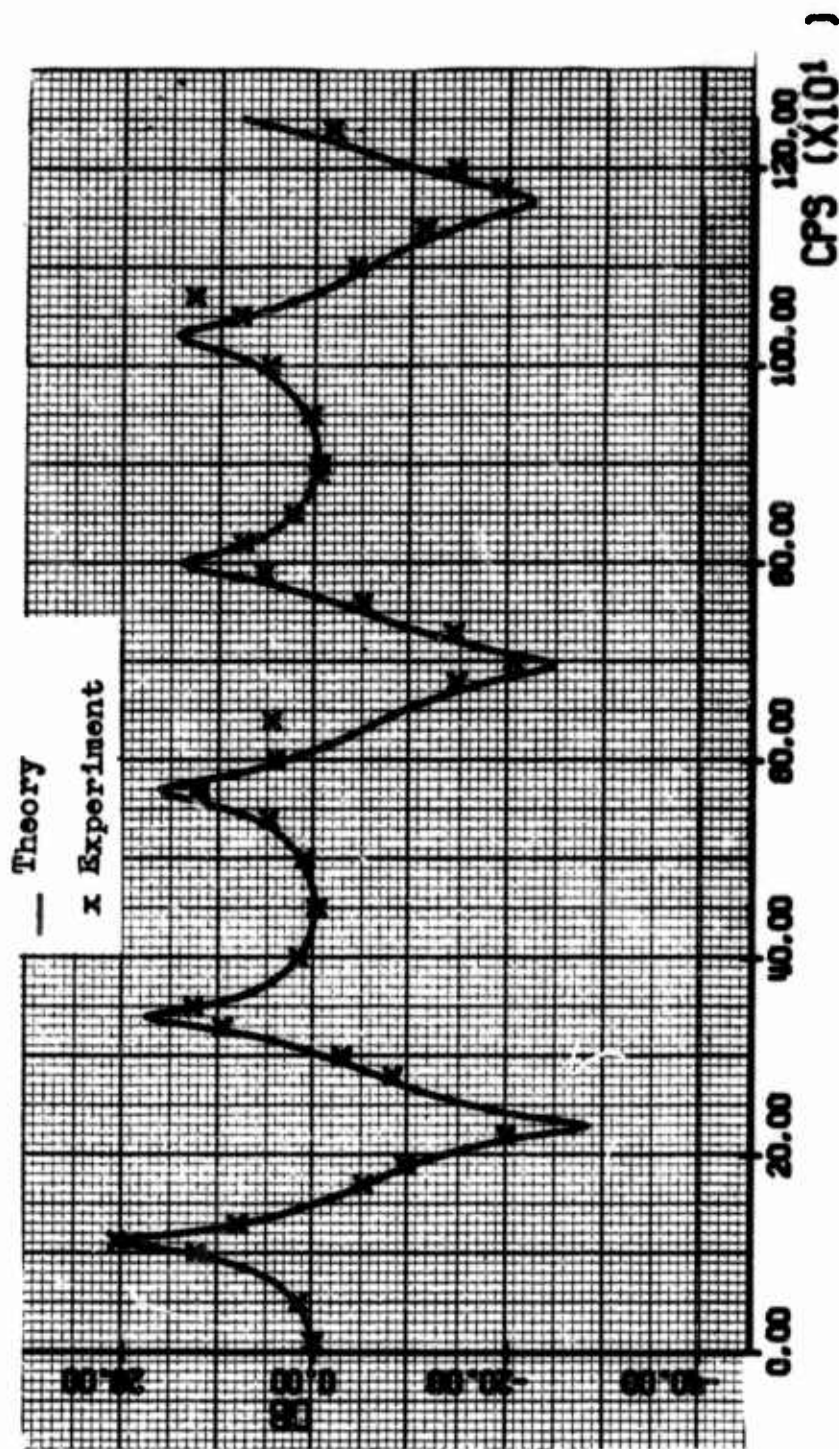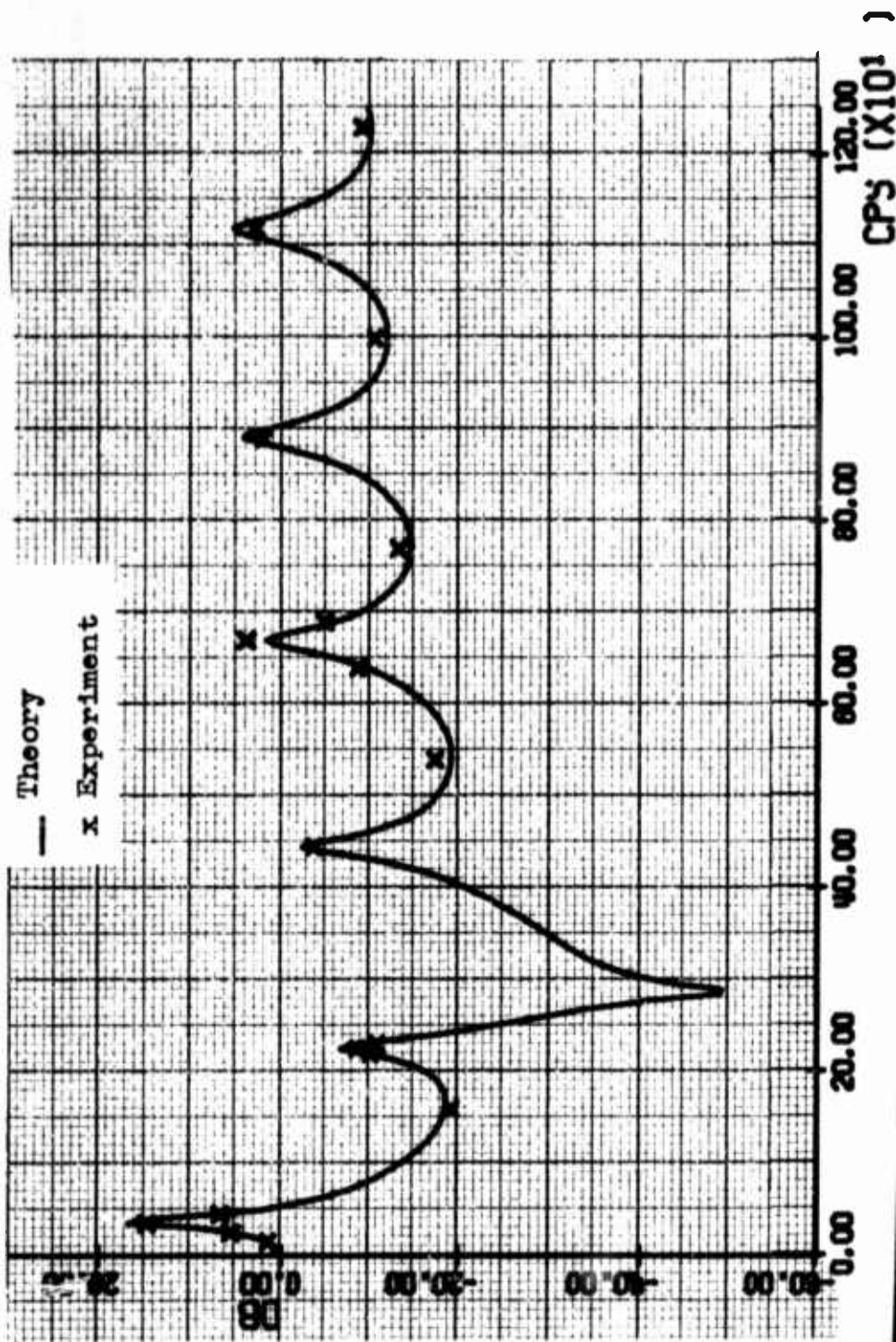
Fig. B-5. Correlation of Data Obtained in this Study with the Rectangu-
lar Pneumatic Line Model for $\bar{X}_1 = 15.0$ in., $\bar{X}_2 = 14.454$ in.,
$b_1 = b_2 = 0.254$ in., $h_1 = h_2 = 0.126$ in., $P_L = 25$ psig
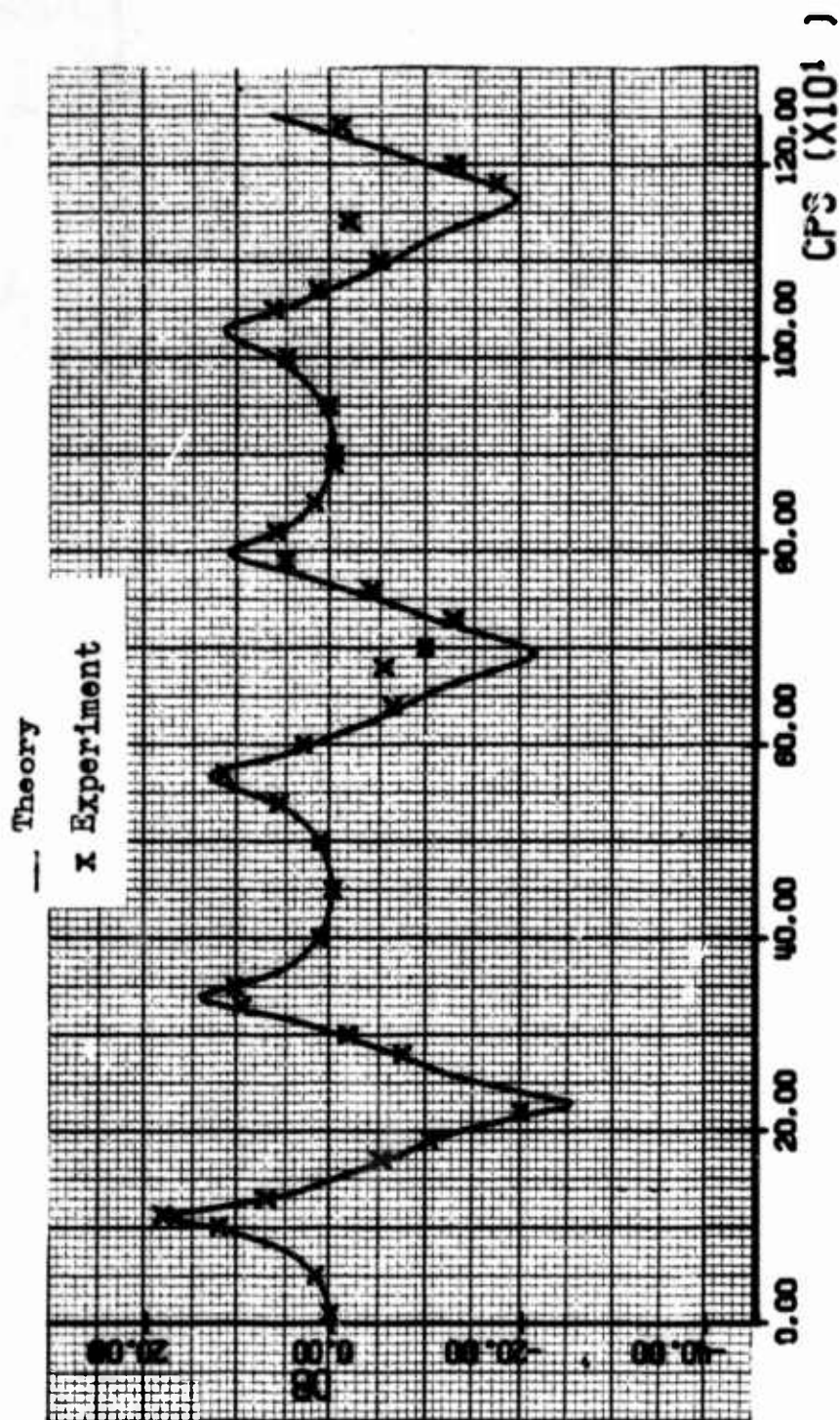
Fig. B-6. Correlation of Data Obtained in this Study with the Rectangu-
lar Pneumatic Line Model for $\bar{X}_1 = 15.0$ in., $\bar{X}_2 = 14.454$ in.,
$b_1 = b_2 = 0.254$ in., $h_1 = h_2 = 0.126$ in., $P_L = 10$ psig

Appendix C

Plots of Experimentally Obtained Frequency Response Points for

Volume-Terminated Rectangular Pneumatic Lines

Correlated with The Frequency Response Curves as Solved by

The Rectangular Pneumatic Transmission Line Model Computer Program

This appendix contains the experimental data taken from a series of tests for volume-terminated rectangular pneumatic transmission lines. The data include the frequency response curve for each case as solved by the rectangular pneumatic transmission line model computer program. The x's are the experimentally determined data points, and the smooth curve is the computer solution to the transfer gain equation.

The distance between the dynamic sending transducer (P_s) and the dynamic receiving transducer (P_r) is $\bar{X}_1$ in inches. The distance from the dynamic receiving transducer (P_r) to the point at which the transmission line transitions to the volume-terminated line is $\bar{X}_2$ in inches. The length of the volume-terminated line is $\bar{X}_3$ in inches. The base is b in inches with the subscript identifying the line. The height is h in inches with the subscript identifying the line.

As discussed in Section V, the measurement of the termination length was considered to be in error by as much as $\pm$ 0.1 inch. The effects of measuring the volume termination length in error by $\pm$ 0.1 in. are shown in Appendix D.
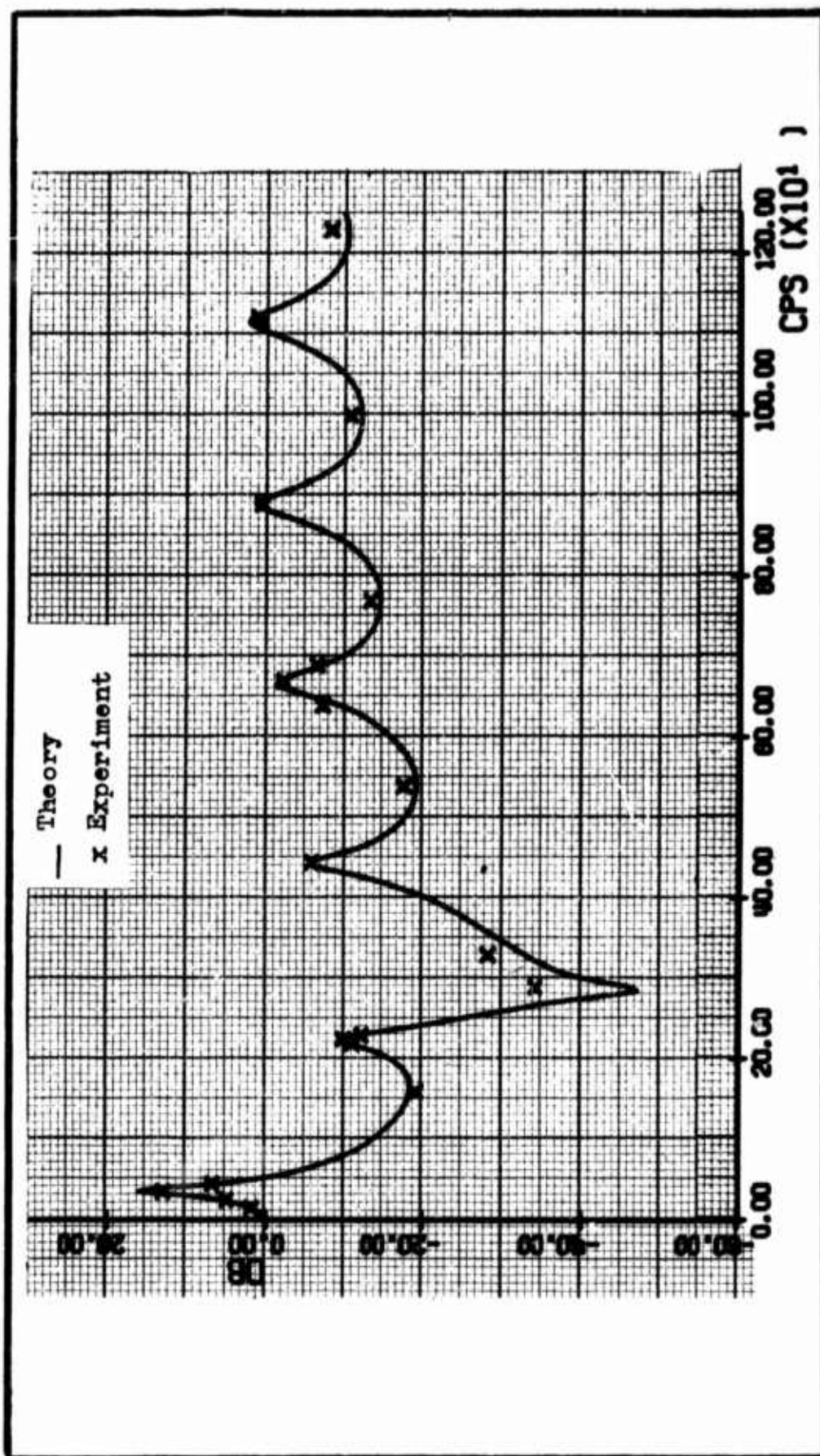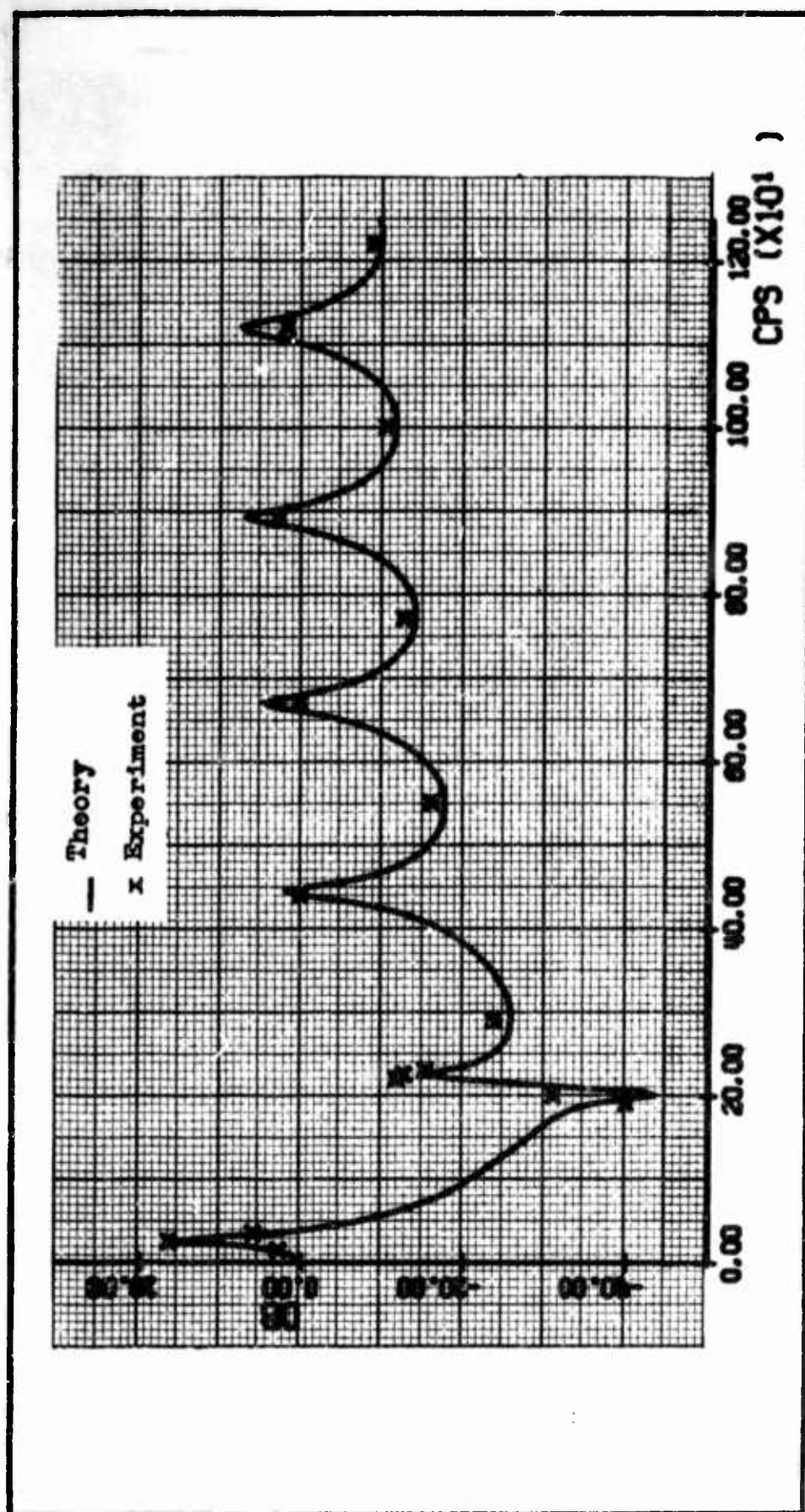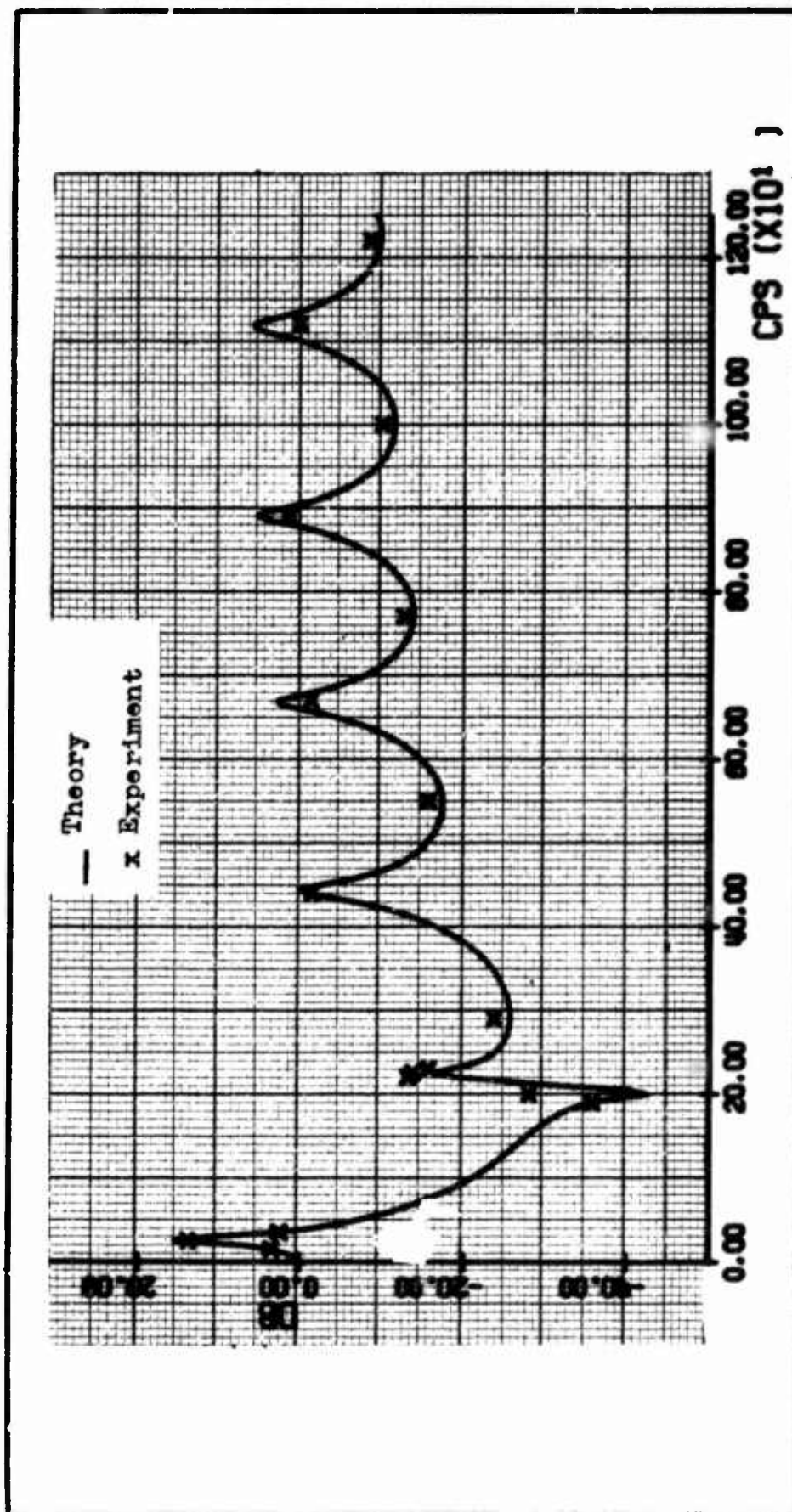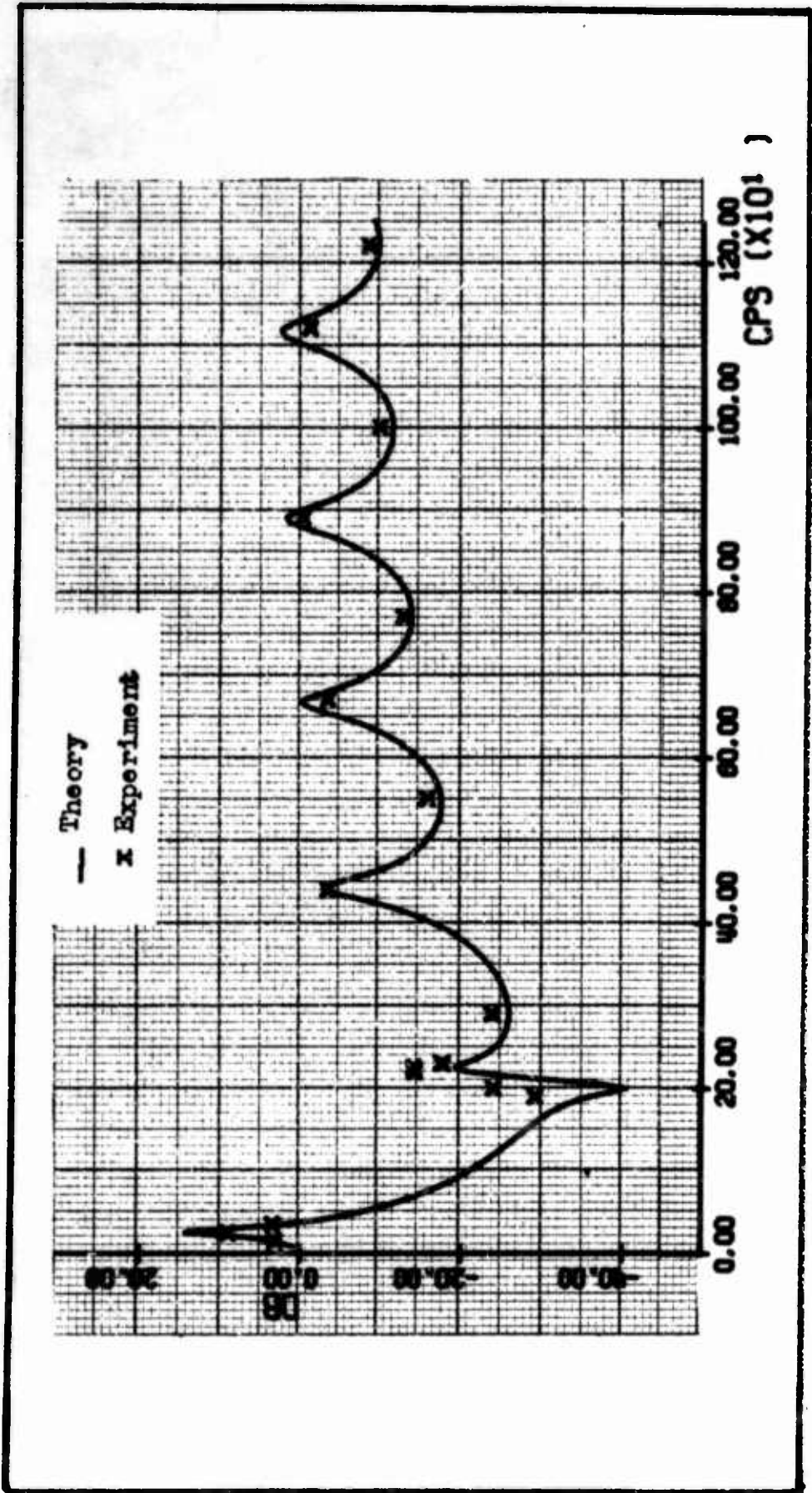
Fig. C-1. Correlation of Data Obtained in This Study with the Rectangular Line Model

for $\bar{X}_1 = 29.454$ in., $\bar{X}_2 = 0.592$ in., $\bar{X}_3 = 0.5$ in., $b_1 = b_2 = 0.254$ in.,

$b_3 = 2.396$ in., $h_1 = h_2 = 0.126$ in., $h_3 = 1.205$ in., $P_L = 40$ psig
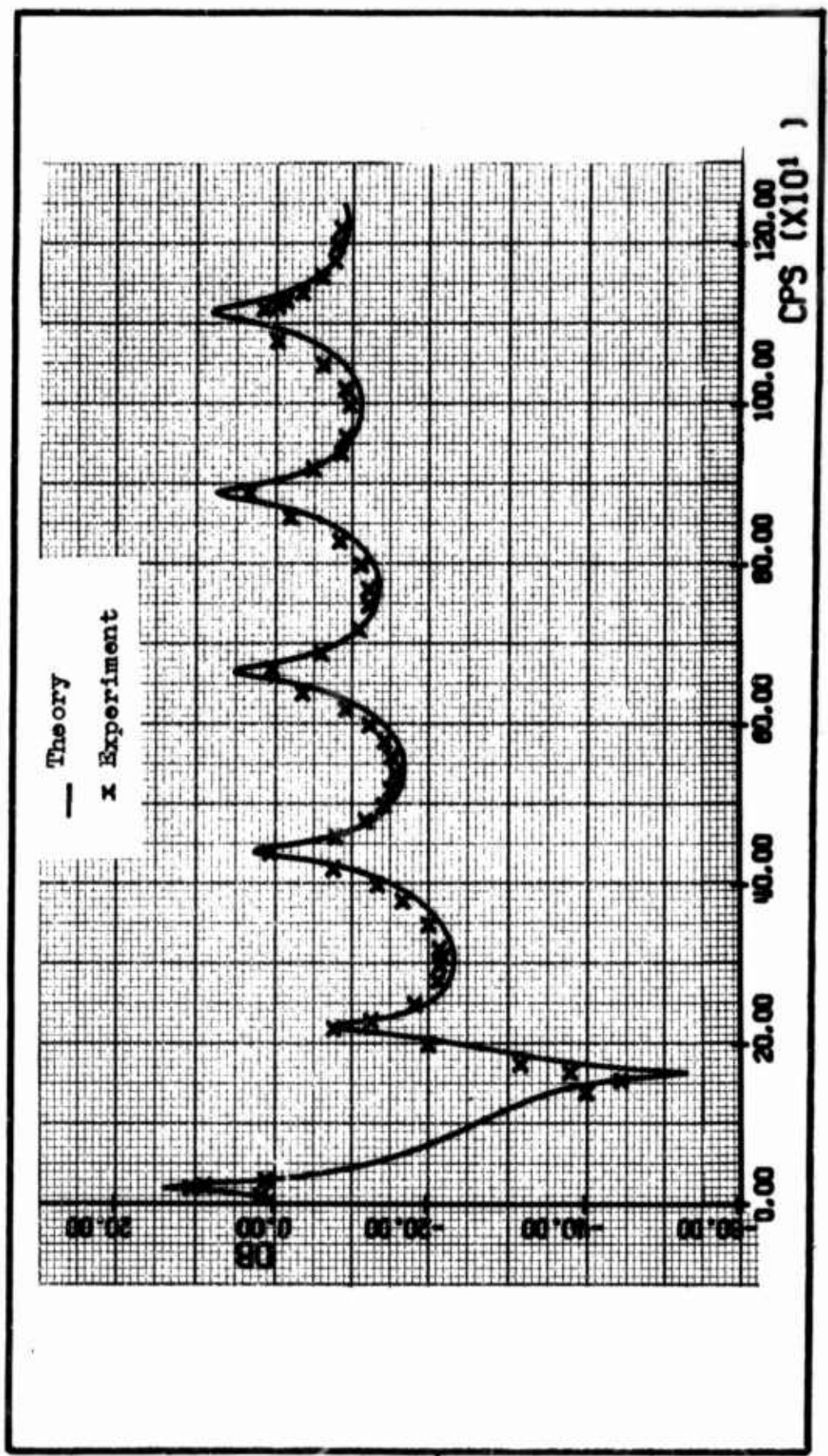
Fig. C-2. Correlation of Data Obtained in This Study with the Rectangular Line Model for $\bar{X}_1 = 29.454$ in., $\bar{X}_2 = 0.592$ in., $\bar{X}_3 = 0.5$ in., $b_1 = b_2 = 0.254$ in., $b_3 = 2.396$ in., $h_1 = h_2 = 0.126$ in., $h_3 = 1.205$ in., $P_L = 25$ psig
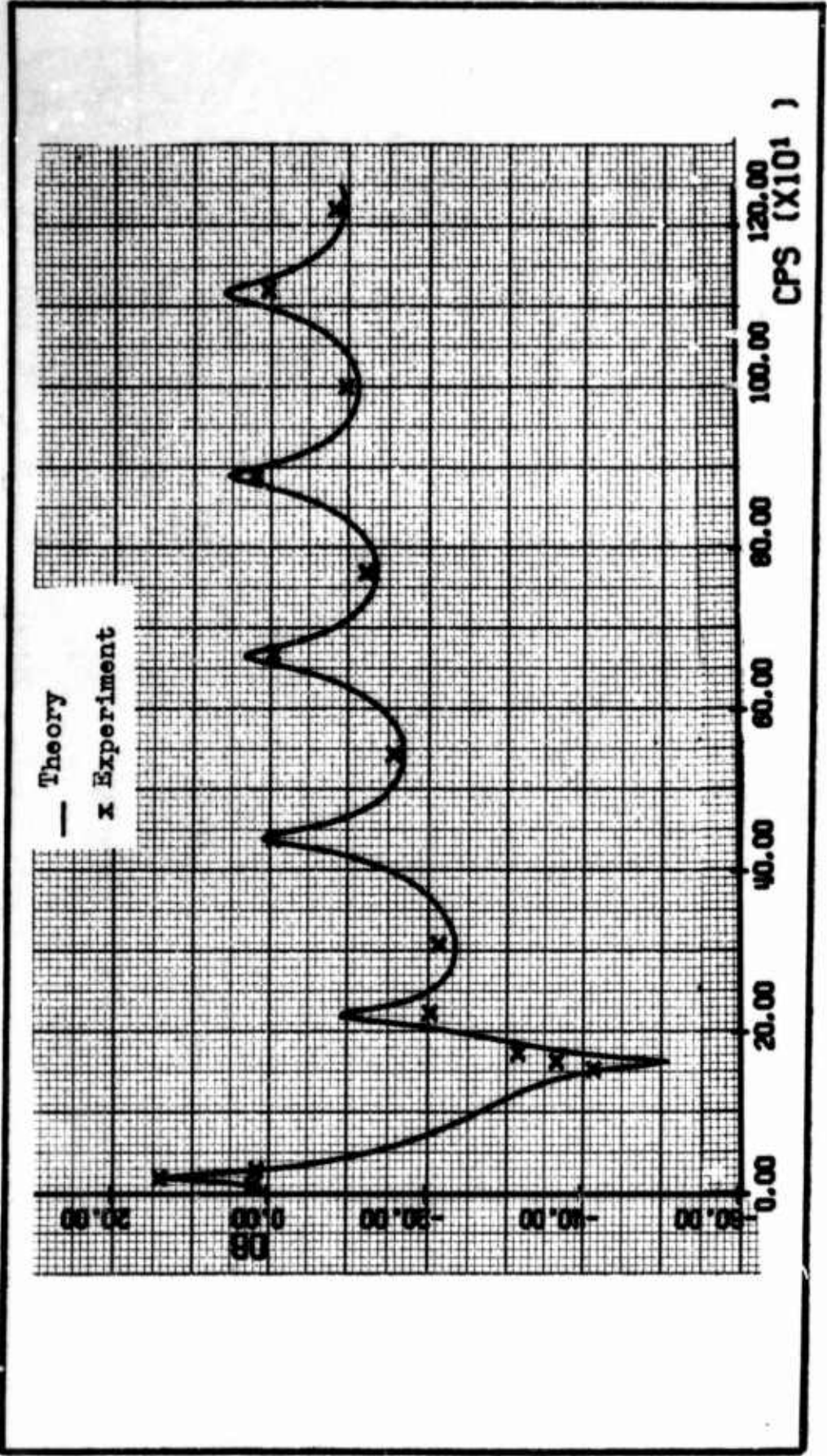
Fig. C-3. Correlation of Data Obtained in This Study with the Rectangular Line Model for $\bar{X}_1 = 29.454$ in., $\bar{X}_2 = 0.592$ in., $\bar{X}_3 = 0.5$ in., $b_1 = b_2 = 0.254$ in., $b_3 = 2.396$ in., $h_1 = h_2 = 0.126$ in., $h_3 = 1.205$ in., $P_L = 10$ psig

Fig. C-4. Correlation of Data Obtained in This Study with the Rectangular Line Model
for $\bar{X}_1 = 29.454$ in., $\bar{X}_2 = 0.592$ in., $\bar{X}_3 = 1.0$ in., $b_1 = b_2 = 0.254$ in.,
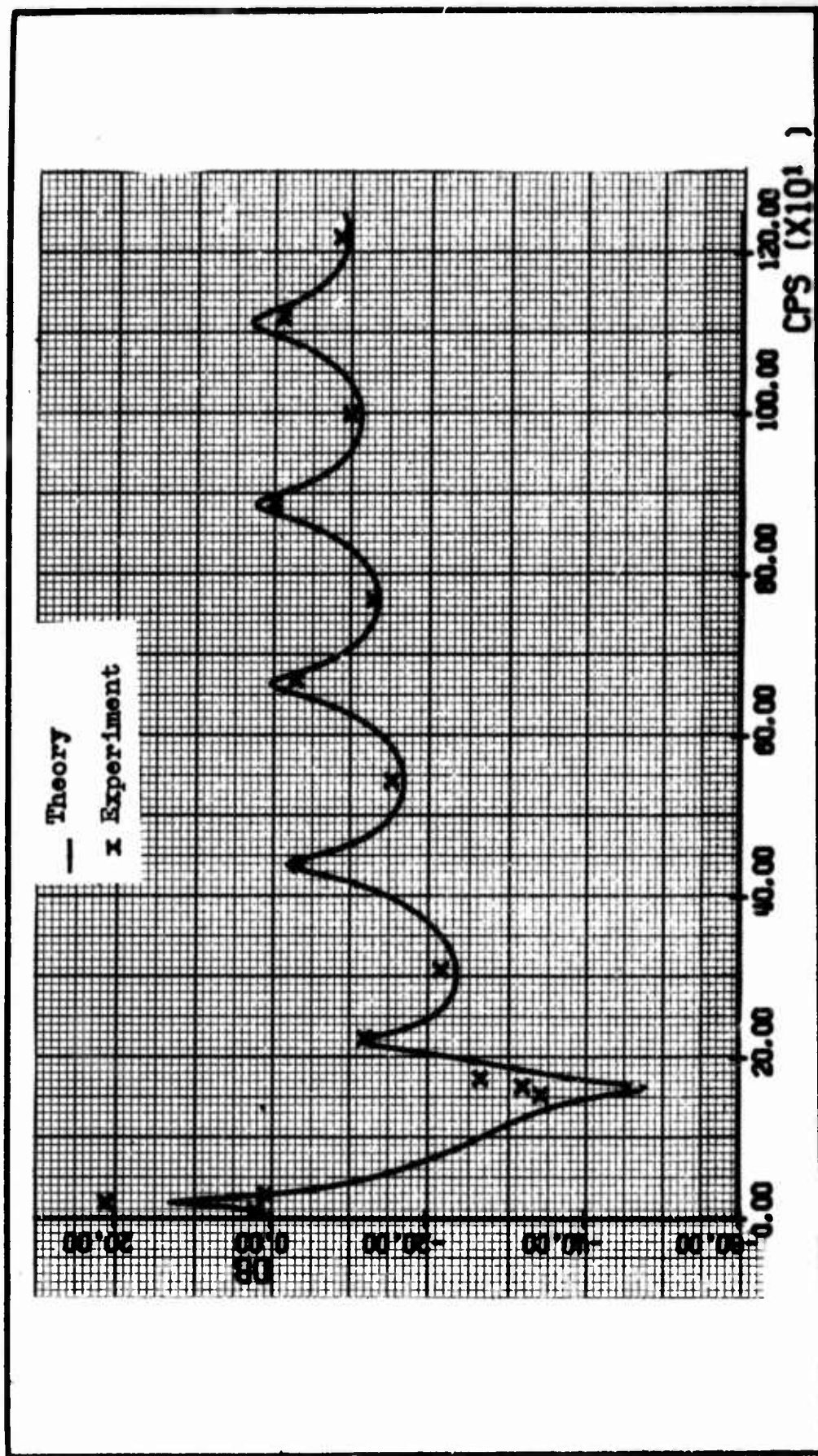$b_3 = 2.396$ in., $h_1 = h_2 = 0.126$ in., $h_3 = 1.205$ in., $P_L = 40$ psig

Fig. C-5. Correlation of Data Obtained in This Study with the Rectangular Line Model for $\bar{X}_1 = 29.454$ in., $\bar{X}_2 = 0.592$ in., $\bar{X}_3 = 1.0$ in., $b_1 = b_2 = 0.254$ in., $b_3 = 2.396$ in., $h_1 = h_2 = 0.126$ in., $h_3 = 1.205$ in., $P_L = 25$ psig

Fig. C-6. Correlation of Data Obtained in This Study with the Rectangular Line Model
for $\bar{X}_1 = 29.454$ in., $\bar{X}_2 = 0.592$ in., $\bar{X}_3 = 1.0$ in., $b_1 = b_2 = 0.254$ in.,
$b_3 = 2.396$ in., $h_1 = h_2 = 0.126$ in., $h_3 = 1.205$ in., $P_L = 10$ psig
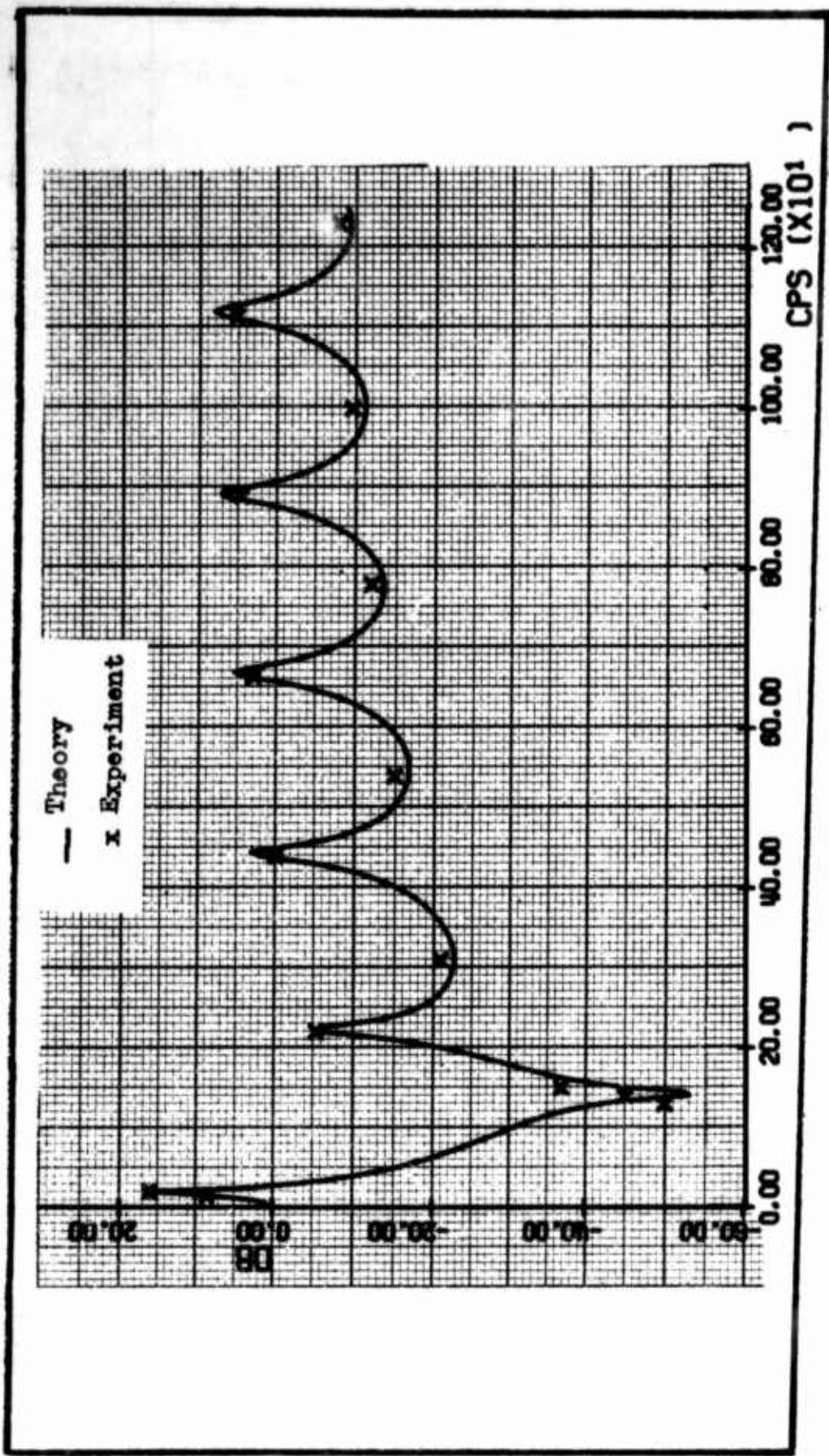
Fig. C-7. Correlation of Data Obtained in This Study with the Rectangular Line Model
for $\bar{X}_1$ = 29.454 in., $\bar{X}_2$ = 0.592 in., $\bar{X}_3$ = 2.0 in., $b_1 = b_2$ = 0.254 in.,
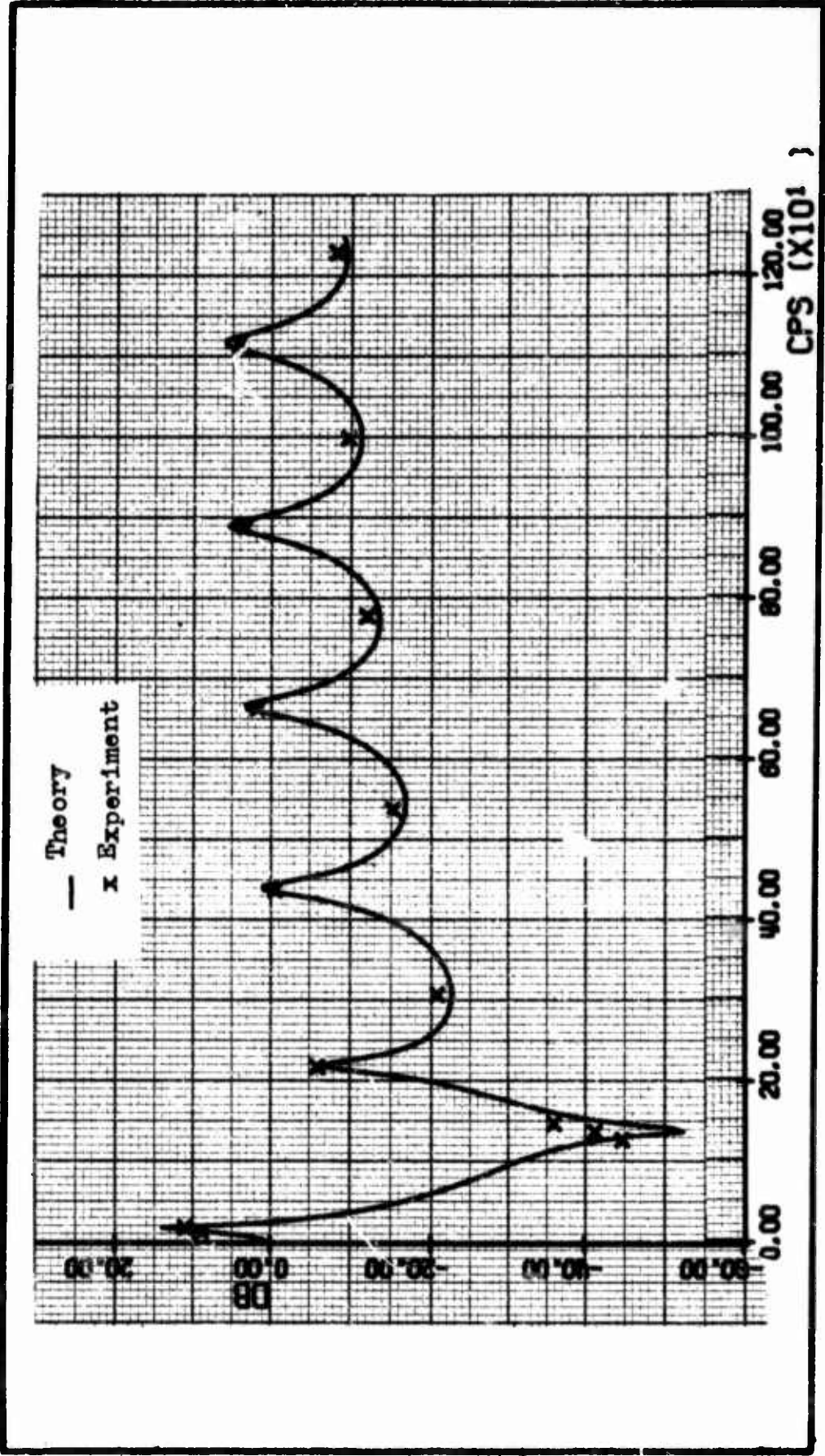b_3 = 2.396 in., $h_1 = h_2$ = 0.126 in., h_3 = 1.205 in., P_L = 40 psig

Fig. C-8. Correlation of Data Obtained in This Study with the Rectangular Line Model for $\bar{X}_1$ = 29.454 in., $\bar{X}_2$ = 0.592 in., $\bar{X}_3$ = 2.0 in., $b_1 = b_2$ = 0.254 in., b_3 = 2.396 in., $h_1 = h_2$ = 0.126 in., h_3 = 1.205 in., P_L = 25 psig
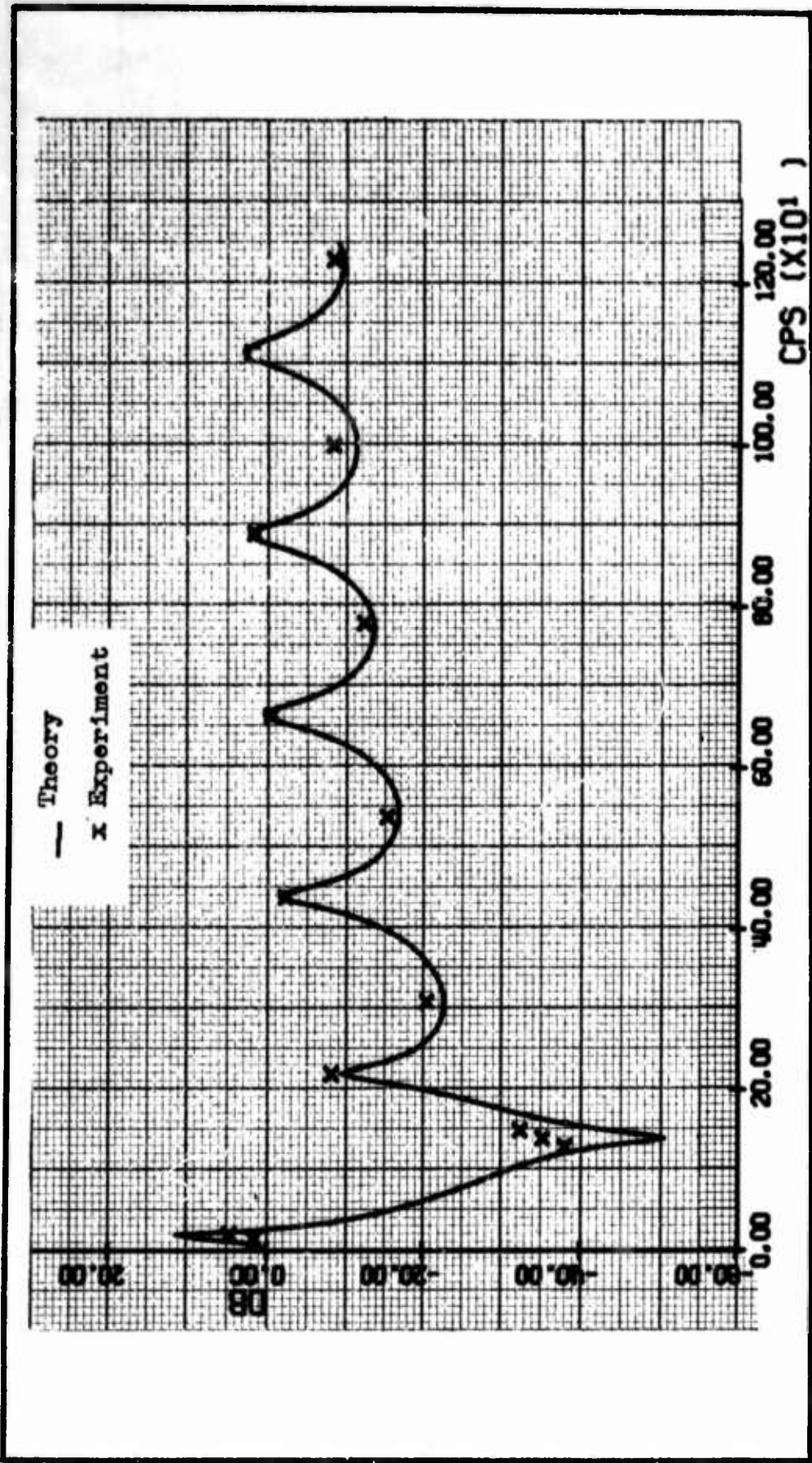
Fig. C-9. Correlation of Data Obtained in This Study with the Rectangular Line Model for $\bar{X}_1 = 29.454$ in., $\bar{X}_2 = 0.592$ in., $\bar{X}_3 = 2.0$ in., $b_1 = b_2 = 0.254$ in., $b_3 = 2.396$ in., $h_1 = h_2 = 0.126$ in., $h_3 = 1.205$ in., $P_L = 10$ psig

Fig. C-10. Correlation of Data Obtained in This Study with the Rectangular Line Model for $X_1 = 29.454$ in., $X_2 = 0.592$ in., $X_3 = 3.0$ in., $b_1 = b_2 = 0.254$ in., $b_3 = 2.396$ in., $h_1 = h_2 = 0.126$ in., $h_3 = 1.205$ in., $P_L = 40$ psig
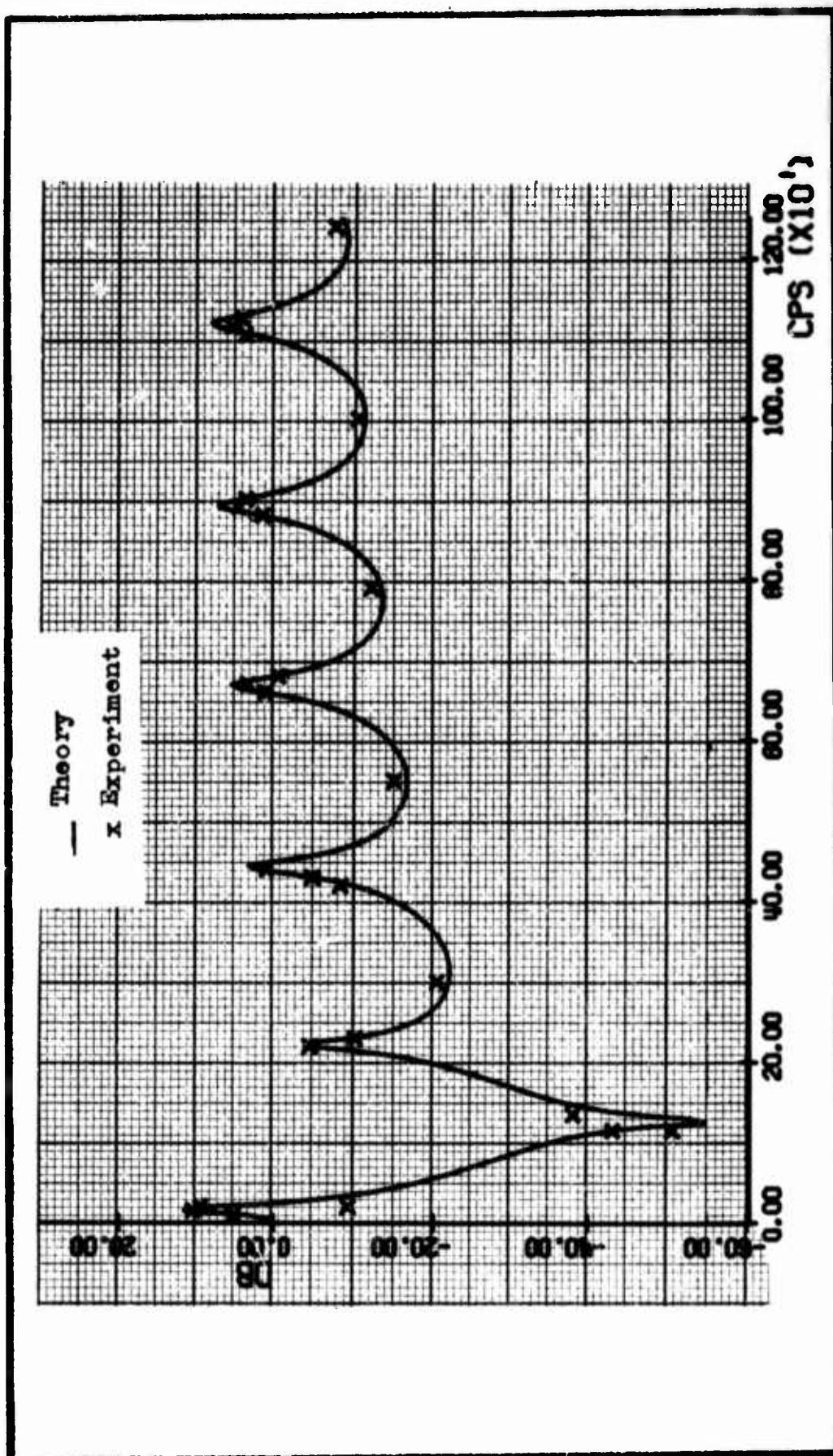
Fig. C-11. Correlation of Data Obtained in This Study with the Rectangular Line Model for $\bar{X}_1 = 29.454$ in., $\bar{X}_2 = 0.592$ in., $\bar{X}_3 = 3.0$ in., $b_1 = b_2 = 0.254$ in., $b_3 = 2.396$ in., $h_1 = h_2 = 0.126$ in., $h_3 = 1.205$ in., $P_L = 25$ psig
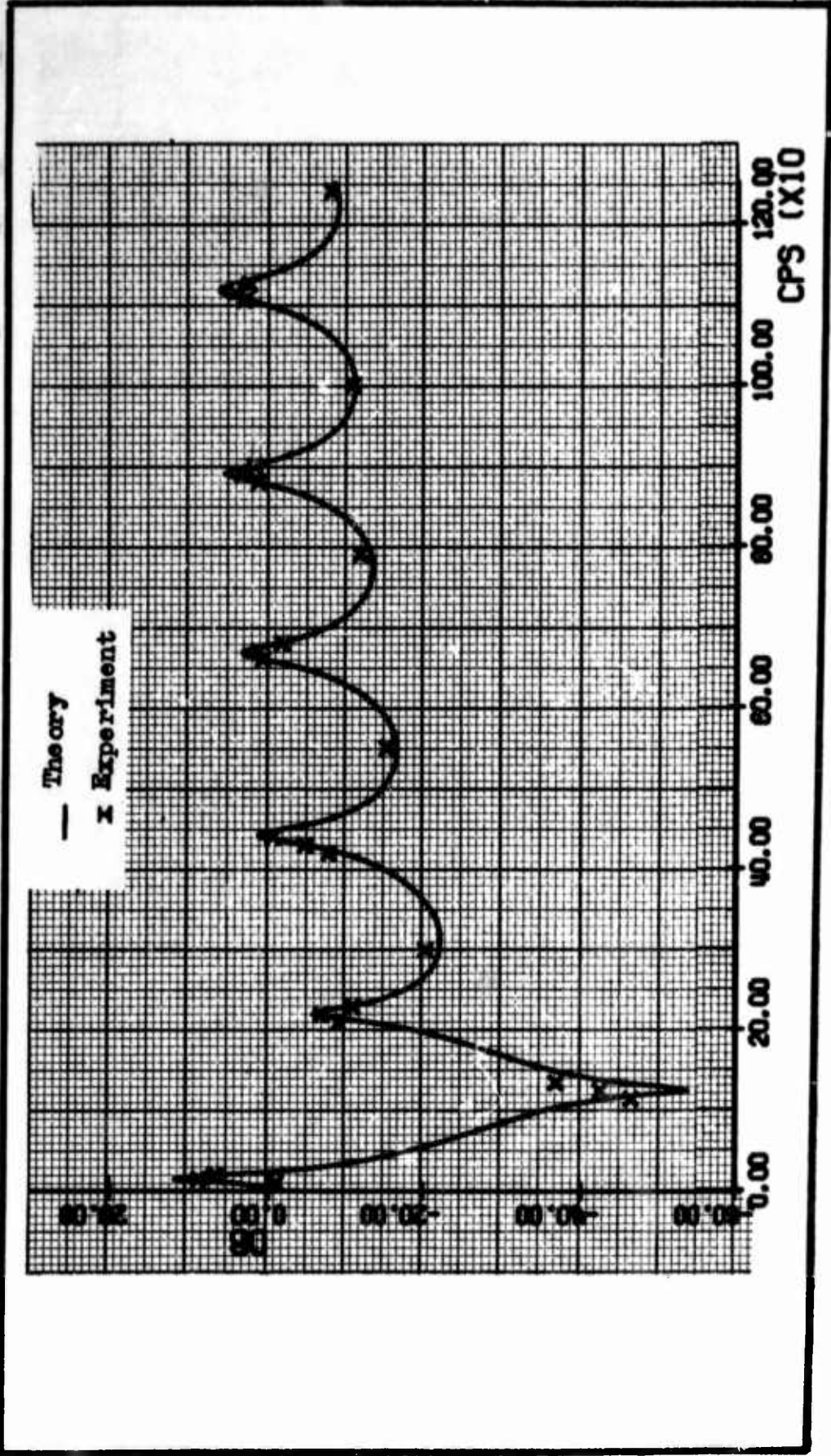
Fig. C-12. Correlation of Data Obtained in This Study with the Rectangular Line Model for $\bar{X}_1$ = 29.454 in., $\bar{X}_2$ = 0.592 in., $\bar{X}_3$ = 3.0 in., b_1 = b_2 = 0.254 in., b_3 = 2.396 in., h_1 = h_2 = 0.126 in., h_3 = 1.205 in., P_L = 10 psig

Fig. C-13. Correlation of Data Obtained in This Study with the Rectangular Line Model for $\bar{X}_1$ = 29.454 in., $\bar{X}_2$ = 0.592 in., $\bar{X}_3$ = 4.0 in., $b_1 = b_2$ = 0.254 in., b_3 = 2.396 in., $h_1 = h_2$ = 0.126 in., h_3 = 1.205 in. P_L = 40 psig

Fig. C-14. Correlation of Data Obtained in This Study with the Rectangular Line Model for $\bar{X}_1 = 29.454$ in. $\bar{X}_2 = 0.592$ in., $\bar{X}_3 = 4.0$ in., $b_1 = b_2 = 0.254$ in., $b_3 = 2.396$ in., $h_1 = h_2 = 0.126$ in., $h_3 = 1.205$ in., $P_L = 25$ psig
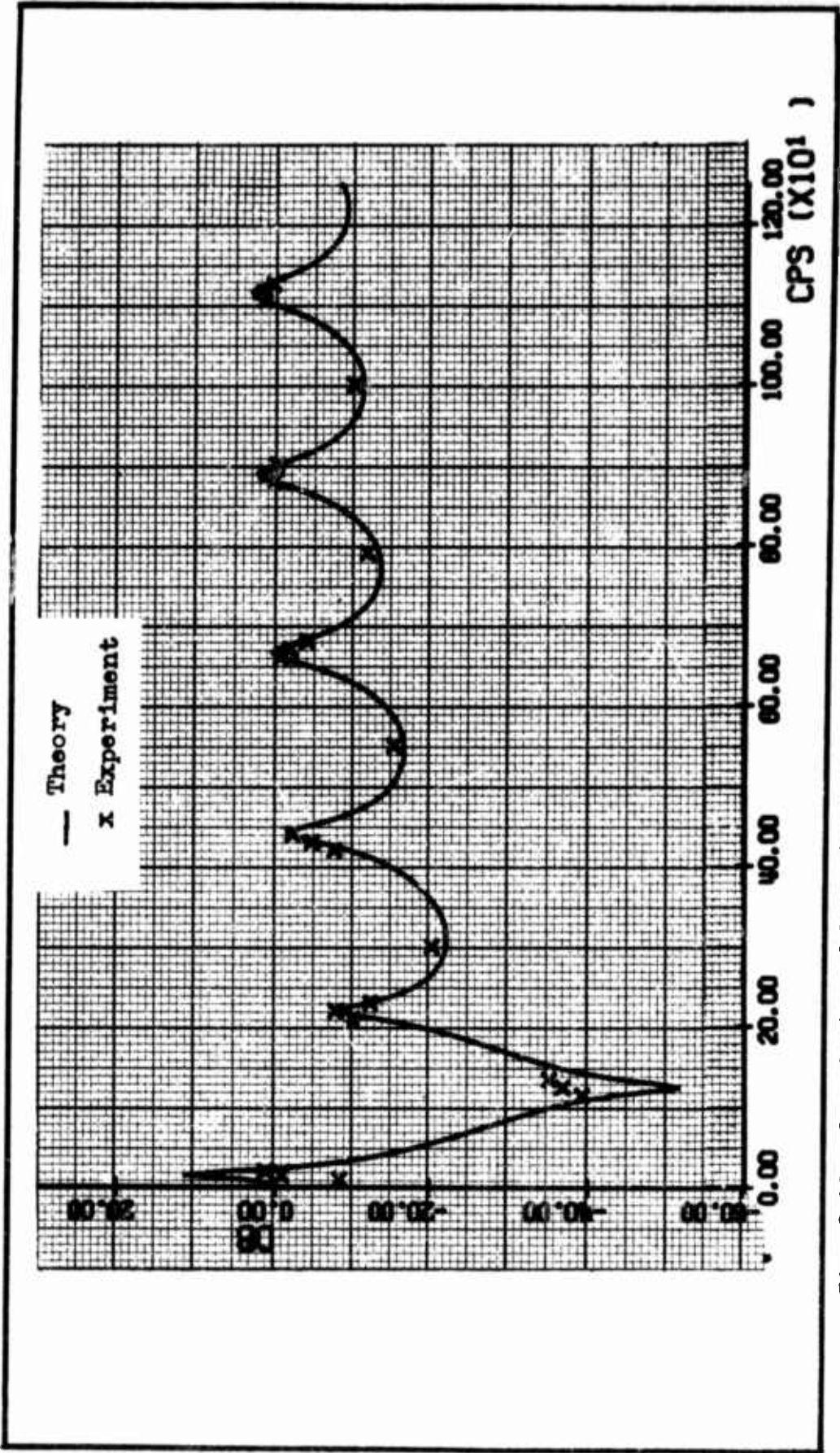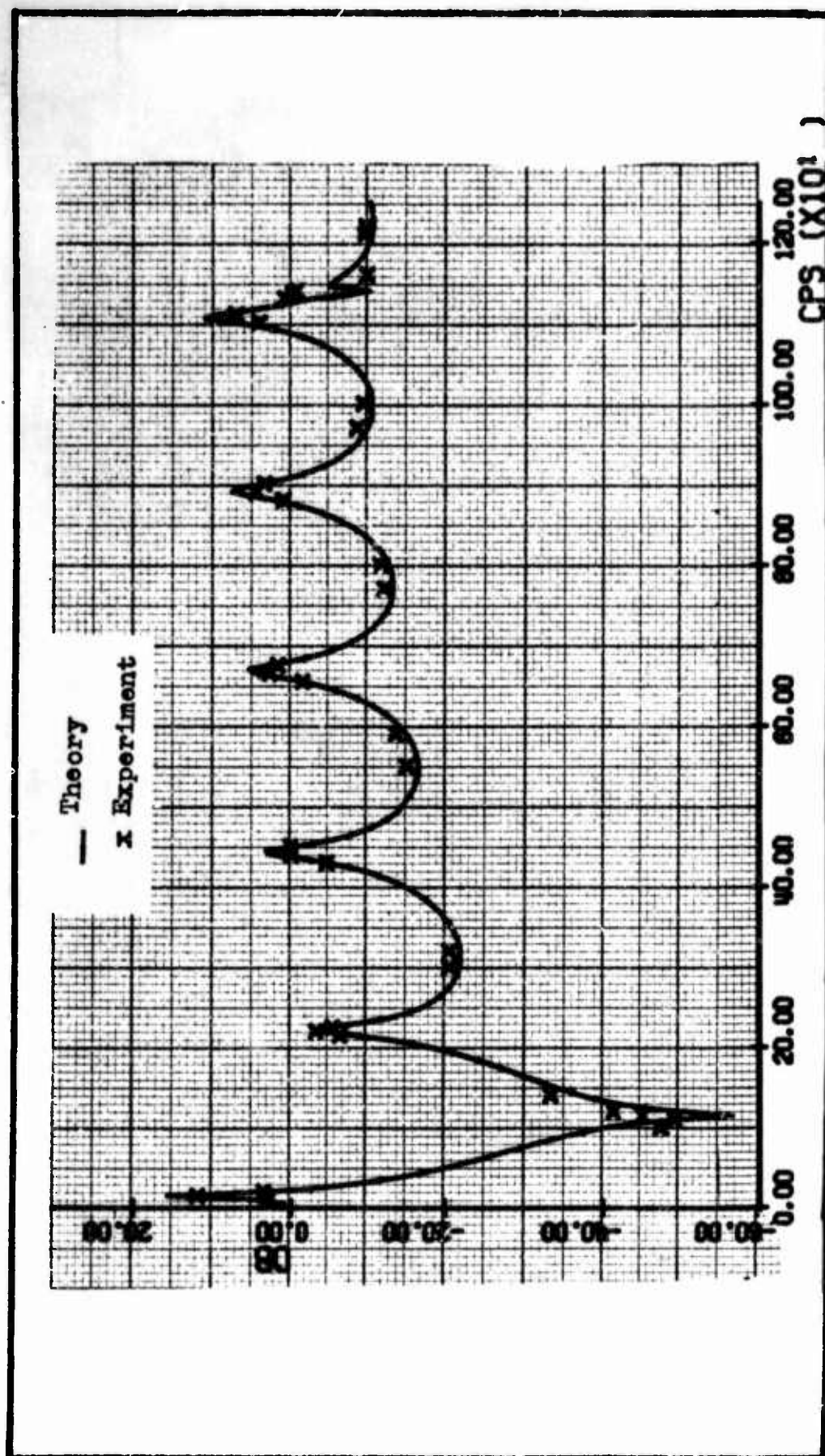
Fig. C-15. Correlation of Data Obtained in this Study with the Rectangular Line Model for $\bar{X}_1 = 29.454$ in., $\bar{X}_2 = 0.592$ in., $\bar{X}_3 = 4.0$ in., $b_1 = b_2 = 0.254$ in., $b_3 = 2.396$ in., $h_1 = h_2 = 0.126$ in., $h_3 = 1.205$ in., $P_L = 10$ psig

Fig. C-16. Correlation of Data Obtained in this Study with the Rectangular Line Model for $\bar{X}_1 = 29.454$ in., $\bar{X}_2 = 0.592$ in., $\bar{X}_3 = 5.0$ in., $b_1 = b_2 = 0.254$ in., $b_3 = 2.396$ in., $h_1 = h_2 = 0.126$ in., $h_3 = 1.205$ in., $P_L = 40$ psig
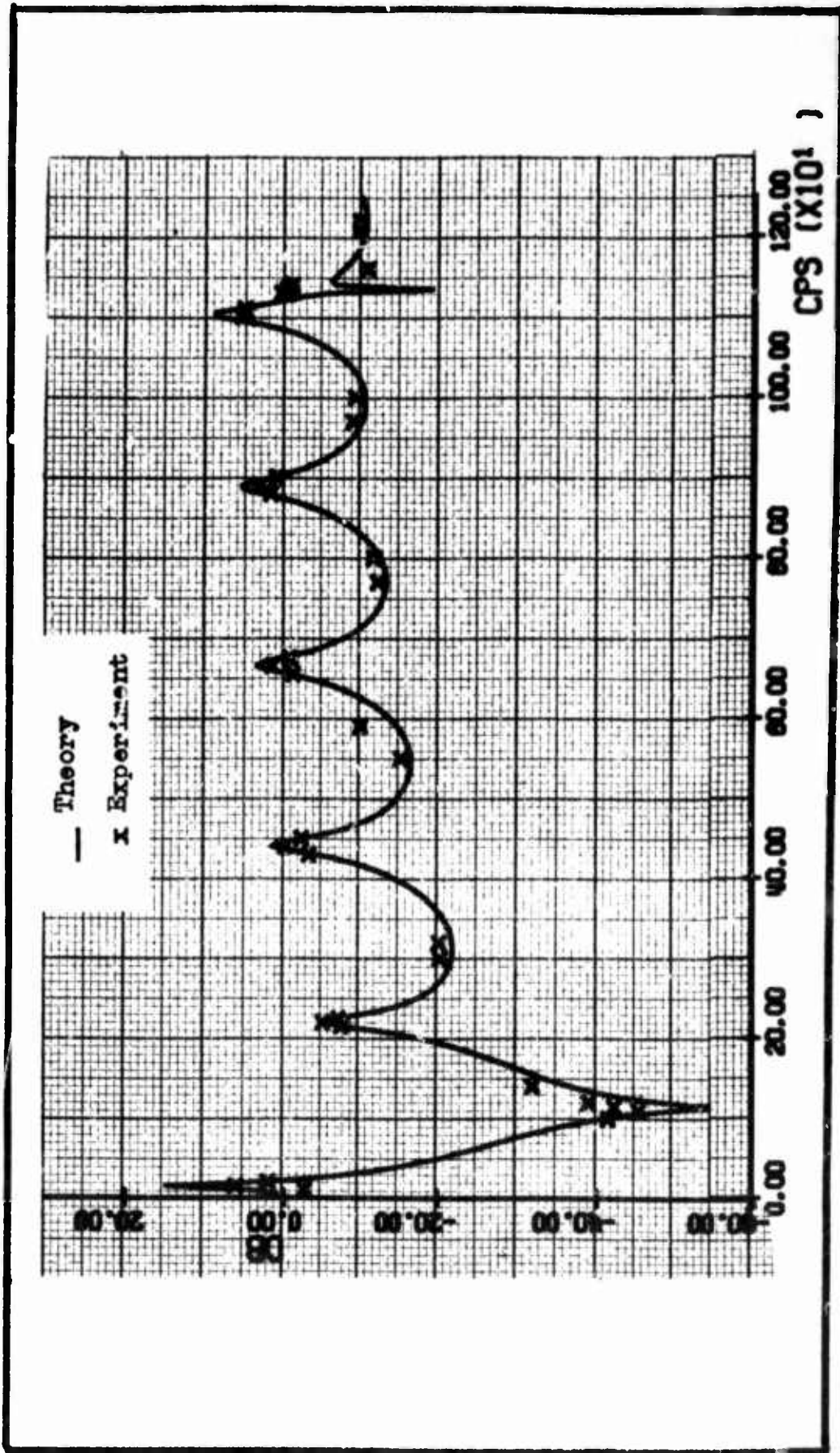
Fig. C-17. Correlation of Data Obtained in this Study with the Rectangular Line Model for $\bar{X}_1 = 29.454$ in., $\bar{X}_2 = 0.592$ in., $\bar{X}_3 = 5.0$ in., $b_1 = b_2 = 0.254$ in., $b_3 = 2.396$ in., $h_1 = h_2 = 0.126$ in., $h_3 = 1.205$ in., $P_L = 25$ psig
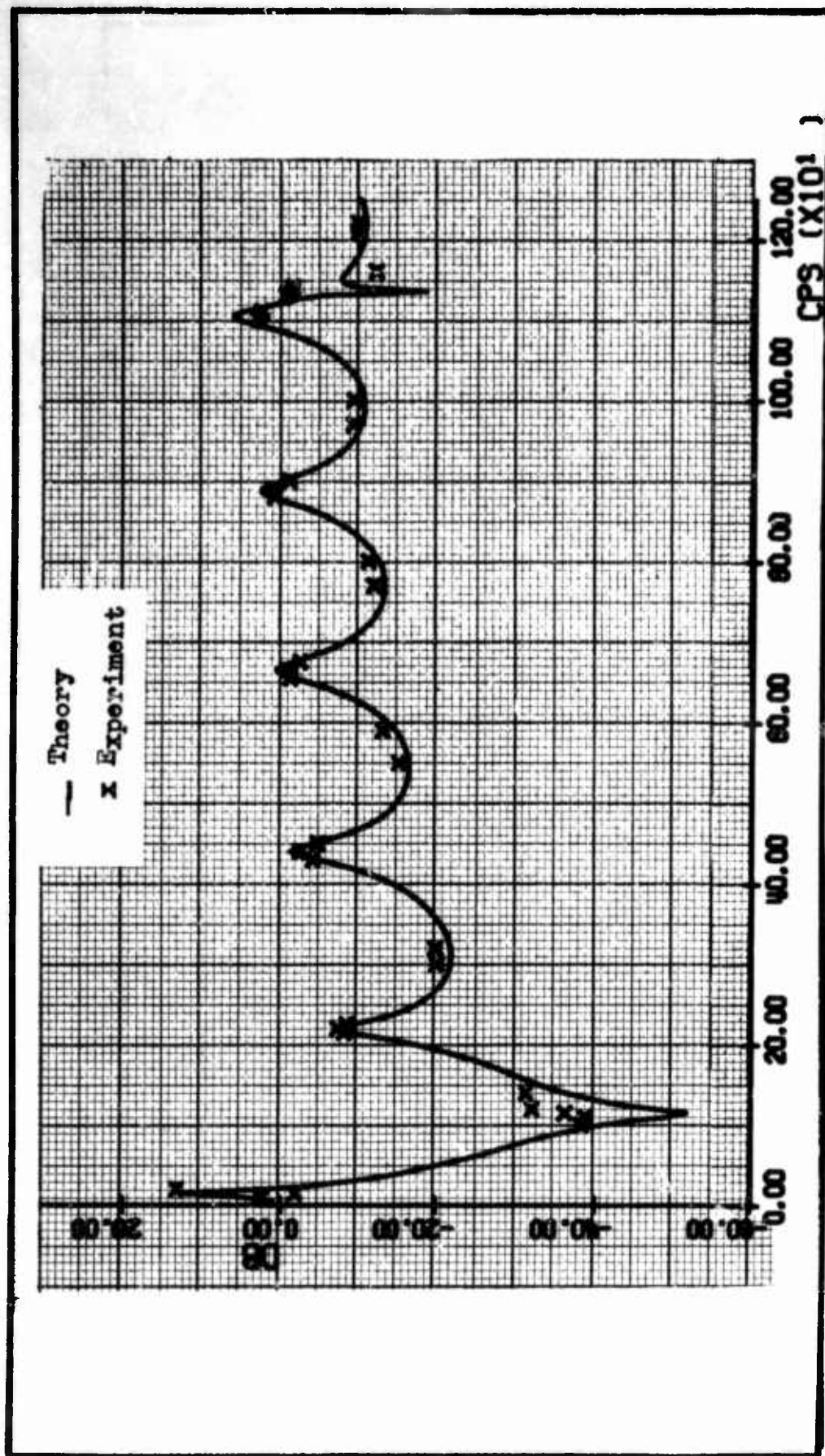
Fig. C-18. Correlation of Data Obtained in this Study with the Rectangular Line Model for $\bar{X}_1 = 29.454$ in., $\bar{X}_2 = 0.592$ in., $\bar{X}_3 = 5.0$ in., $b_1 = b_2 = 0.254$ in., $b_3 = 2.396$ in., $h_1 = h_2 = 0.126$ in., $h_3 = 1.205$ in., $P_L = 10$ psig

Fig. C-19. Correlation of Data Obtained in this Study with the Rectangular Line Model for $\bar{X}_1 = 29.454$ in., $\bar{X}_2 = 0.592$ in., $\bar{X}_3 = 6.0$ in., $b_1 = b_2 = 0.254$ in., $b_3 = 2.396$ in., $h_1 = h_2 = 0.126$ in., $h_3 = 1.205$ in., $P_L = 40$ psig
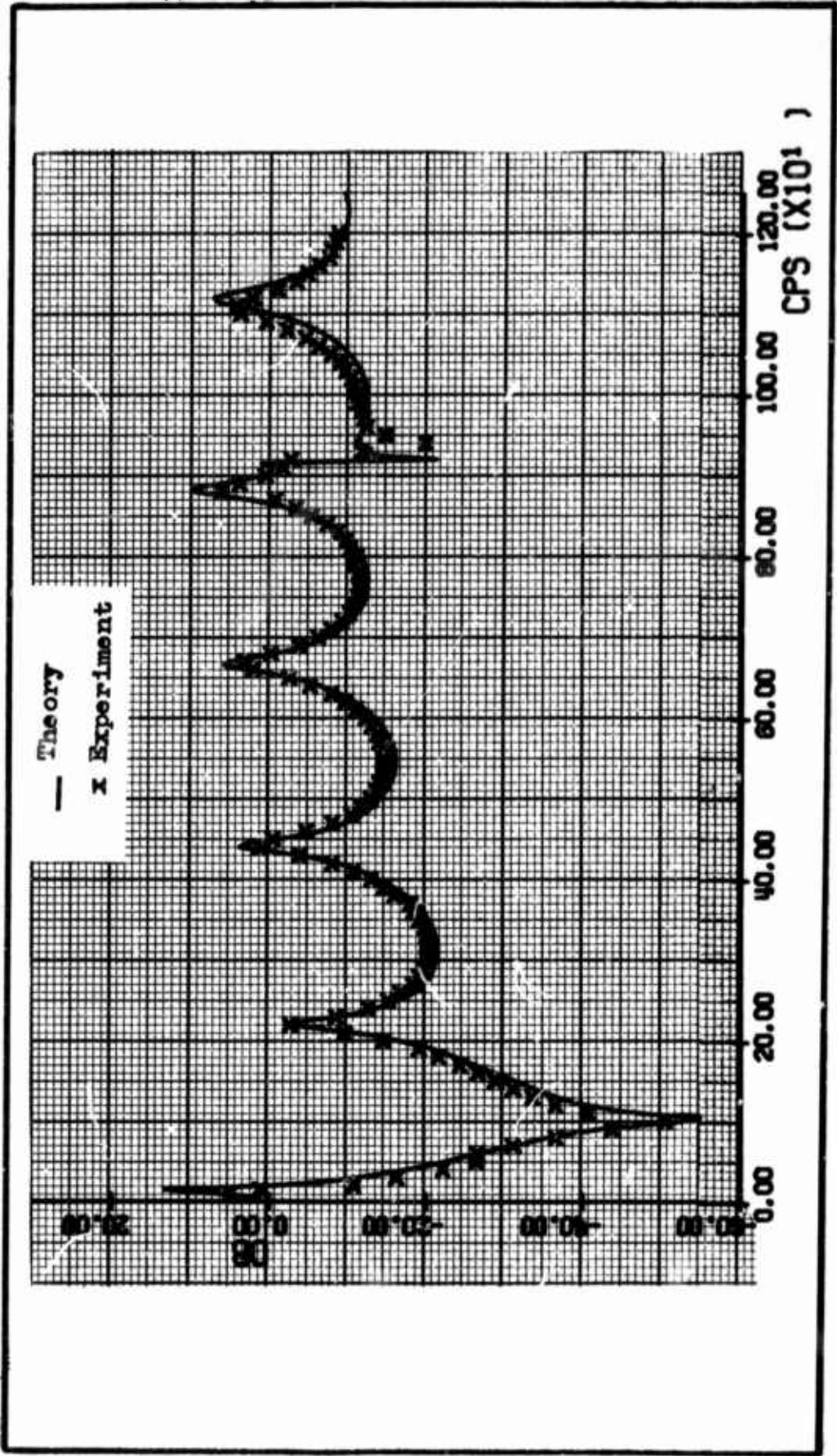
Fig. C-20. Correlation of Data Obtained in this Study with the Rectangular Line Model for $\bar{X}_1 = 29.454$ in., $\bar{X}_2 = 0.592$ in., $\bar{X}_3 = 6.0$ in., $b_1 = b_2 = 0.254$ in., $b_3 = 2.396$ in., $h_1 = h_2 = 0.126$ in., $h_3 = 1.205$ in., $P_L = 25$ psig
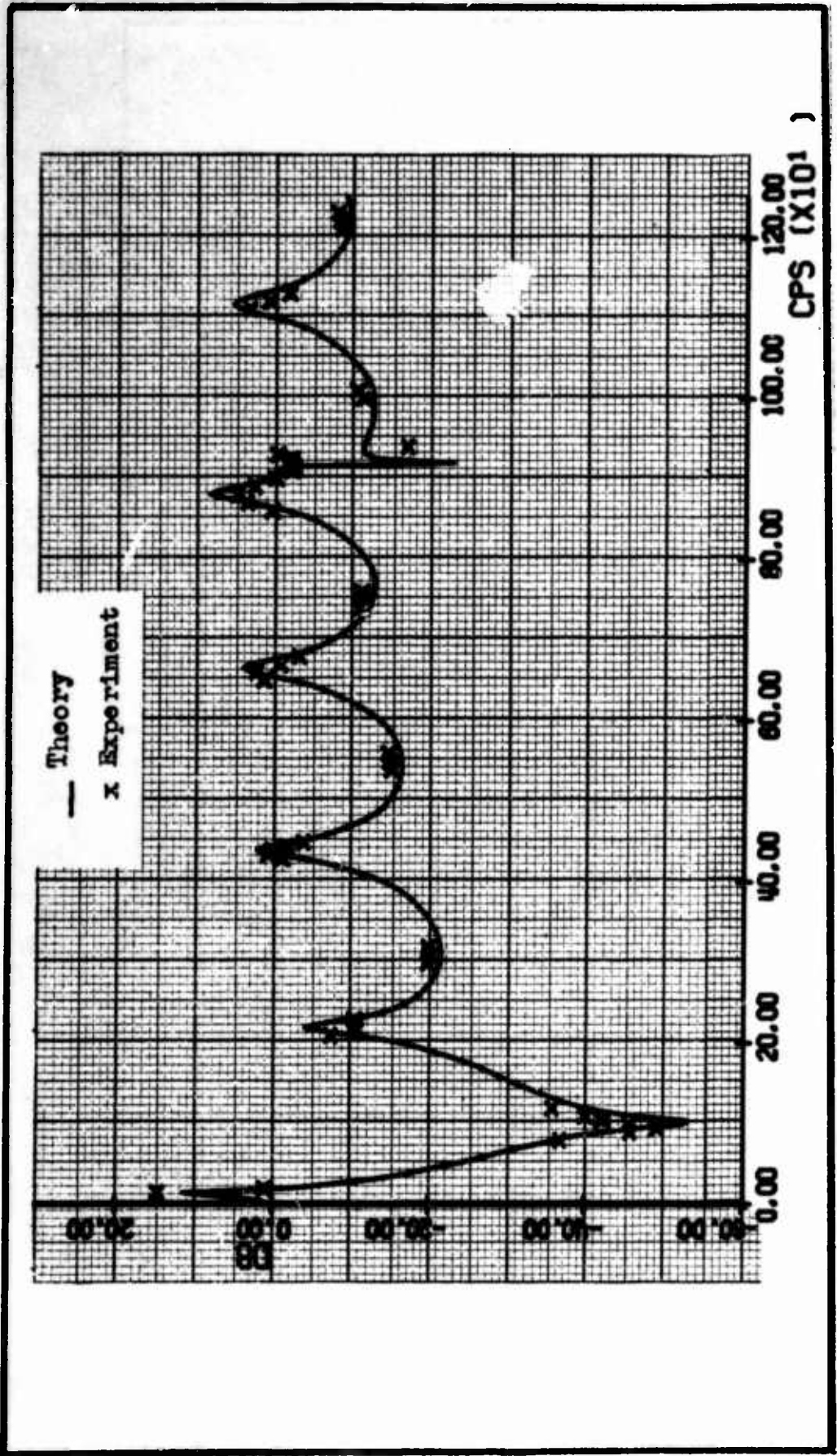
Fig. C-21. Correlation of Data Obtained in this Study with the Rectangular Line Model
for $\bar{X}_1 = 29.454$ in., $\bar{X}_2 = 0.592$ in., $\bar{X}_3 = 6.0$ in., $b_1 = b_2 = 0.254$ in.,
$b_3 = 2.396$ in., $h_1 = h_2 = 0.126$ in., $h_3 = 1.205$ in., $P_L = 10$ psig

Fig. C-22. Correlation of Data Obtained in this Study with the Rectangular Line Model for $\bar{X}_1 = 29.454$ in., $\bar{X}_2 = 0.592$ in., $\bar{X}_3 = 7.394$ in., $b_1 = b_2 = 0.254$ in., $b_3 = 2.396$ in., $h_1 = h_2 = 0.126$ in., $h_3 = 1.205$ in., $P_L = 40$ psig
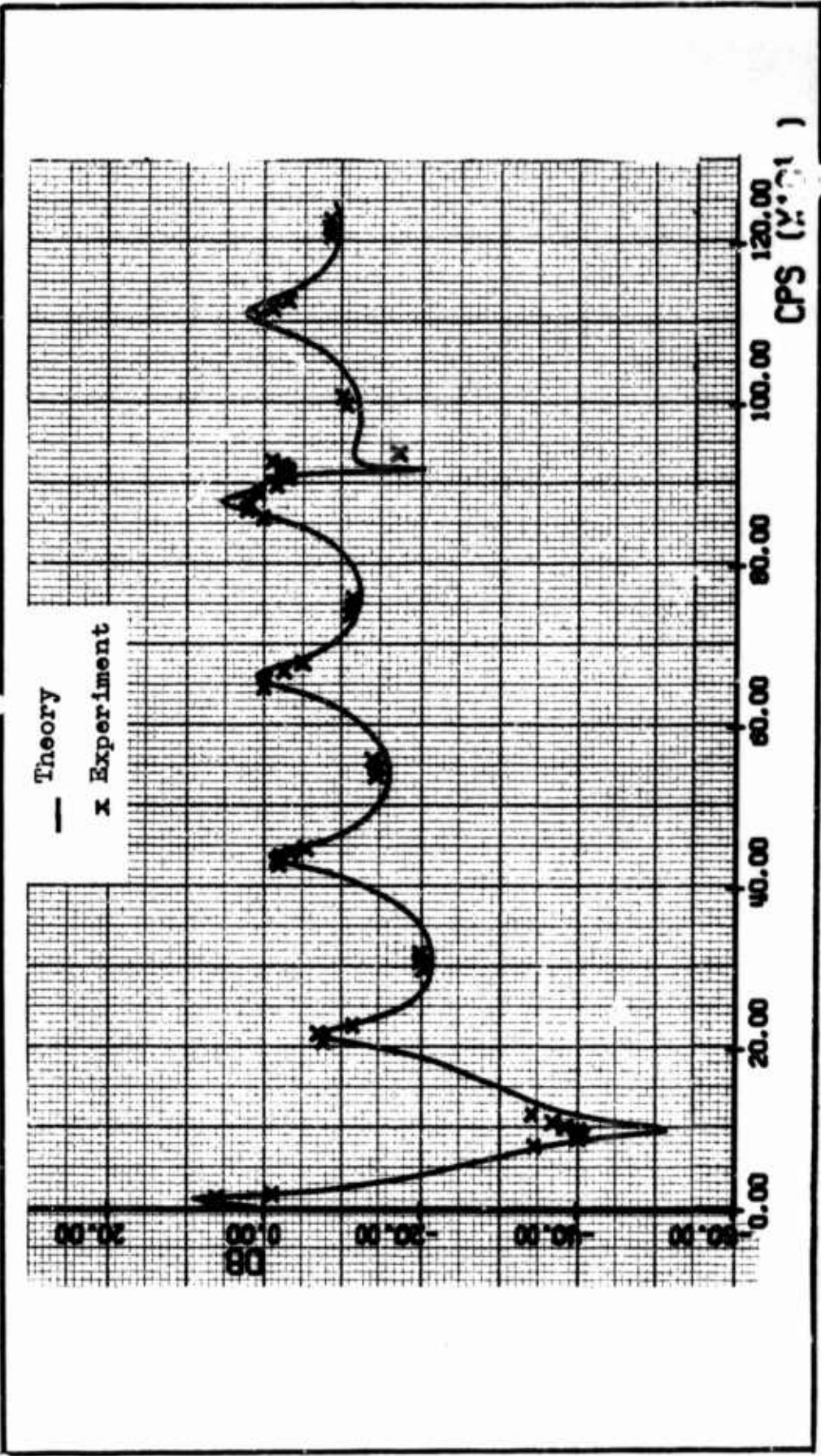
Fig. C-23. Correlation of Data Obtained in this Study with the Rectangular Line Model
for $\bar{X}_1 = 29.454$ in., $\bar{X}_2 = 0.592$ in., $\bar{X}_3 = 7.394$ in., $b_1 = b_2 = 0.254$ in.,
$b_3 = 2.396$ in., $h_1 = h_2 = 0.126$ in., $h_3 = 1.205$ in., $P_L = 25$ psig

Fig. C-24. Correlation of Data Obtained in this Study with the Rectangular Line Model for $\bar{X}_1$ = 29.454 in., $\bar{X}_2$ = 0.592 in., $\bar{X}_3$ = 7.394 in., b_1 = b_2 = 0.254 in., b_3 = 2.396 in., h_1 = h_2 = 0.126 in., h_3 = 1.205 in., P_L = 10 psig

Appendix D

Plots of Experimentally Obtained Frequency Response Points

for Volume-Terminated Rectangular Pneumatic Lines

Correlated with the Frequency Response Curves

as Solved by the Rectangular Pneumatic Transmission Line Model

Computer Program which Includes the

Volume-Terminated Length as a Variation in Parameter

This appendix contains the experimental data taken from the same test depicted in Figs. 10 and C-22. The test is for a volume-terminated rectangular pneumatic transmission line at 40 psig with a termination length considered to be 7.394 in.

The variation in the termination length is the variation in parameter while holding all other data, including experimental data, constant. The data include the frequency response curve for each case as solved by the rectangular pneumatic transmission line model computer program.

As discussed in Section III, the transfer gain equation is sensitive to accurate length measurements of the pneumatic lines. It was believed that the accuracy in determining the fluid level in the volume termination of the test fixture described in Section III could not be measured with any better accuracy than ±0.1 inch. Therefore, the termination length of 7.394 inches as marked on the termination volume test fixture at a test pressure of 40 psig was chosen as a representative case to demonstrate the sensitivity of the transfer gain equation

to line length inaccuracies. The termination length of 7.394 in. was marked on the test fixture, and an attempt was made during the test to place the mercury level as near the mark as possible. Also, it was desired to search for the most accurate length which seemed to provide the best curve fit.

The termination length of 7.394 in. was varied ± 0.1 in. from the nominal value. It was found that a termination length of 7.3 in. describes best the experimental data as computed by the computer program (See Fig. D-1).
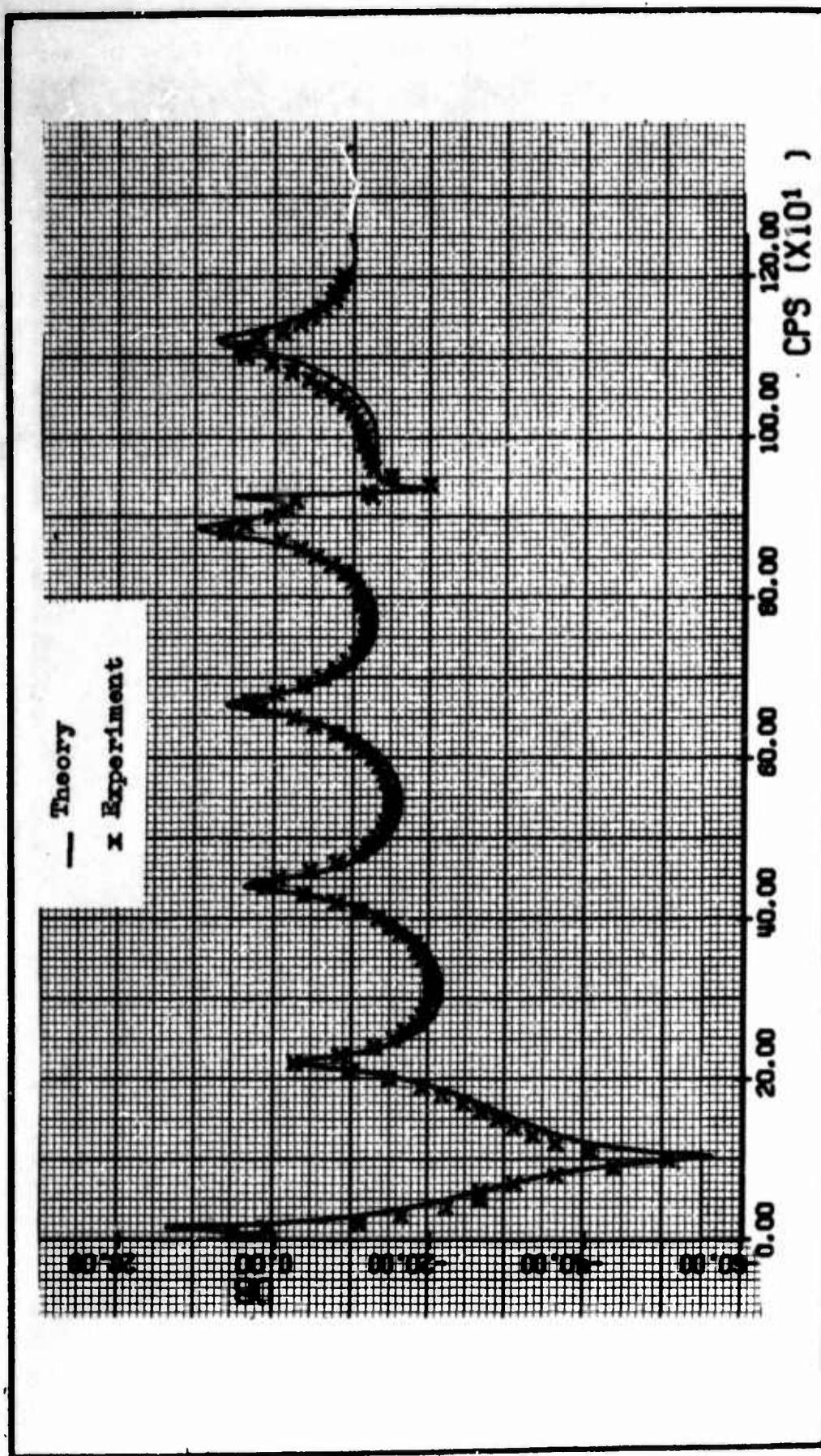
Fig. D-1. Data is the Same as Fig. C-22 Except that $\bar{X}_3 = 7.3$ in.
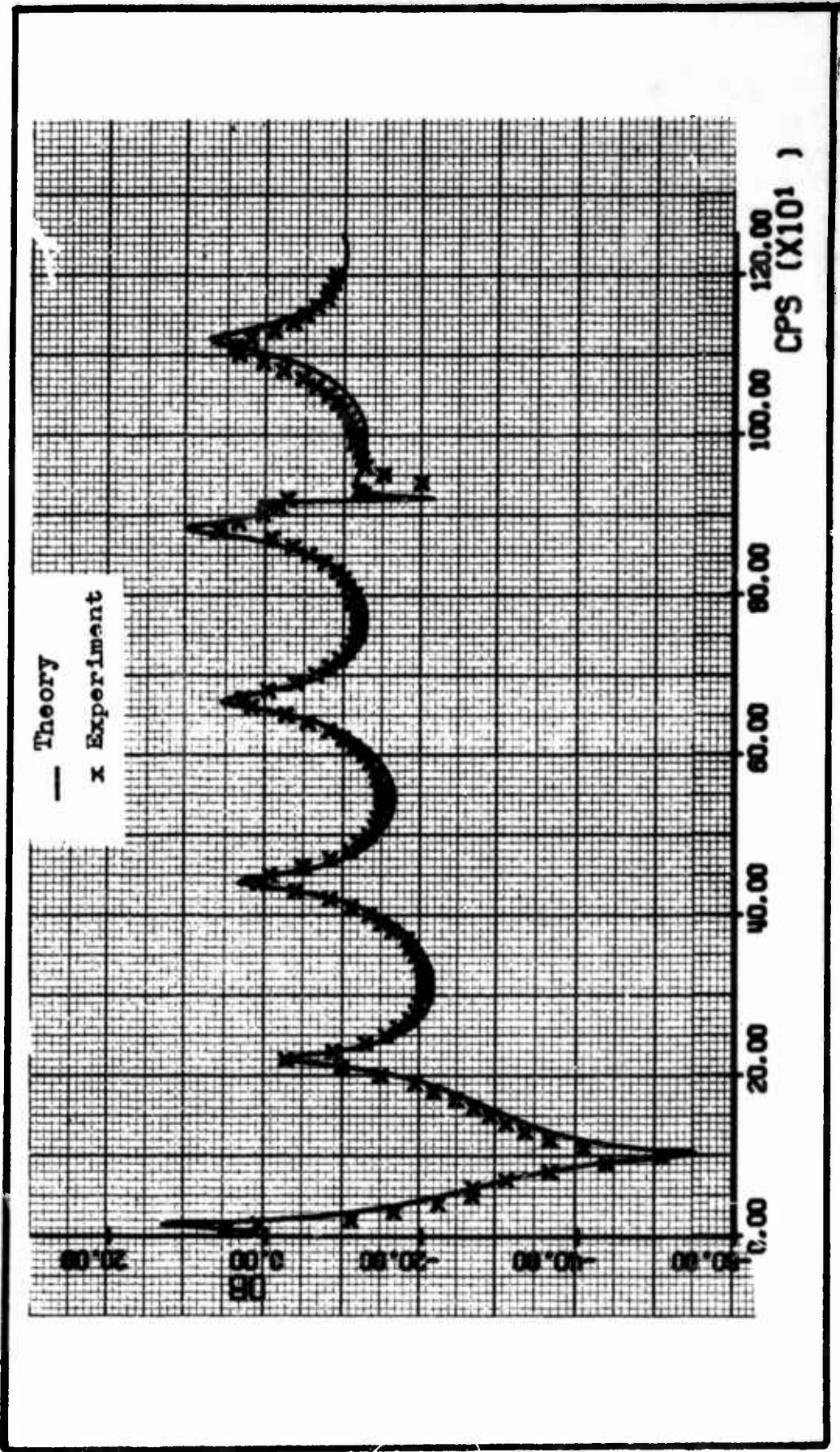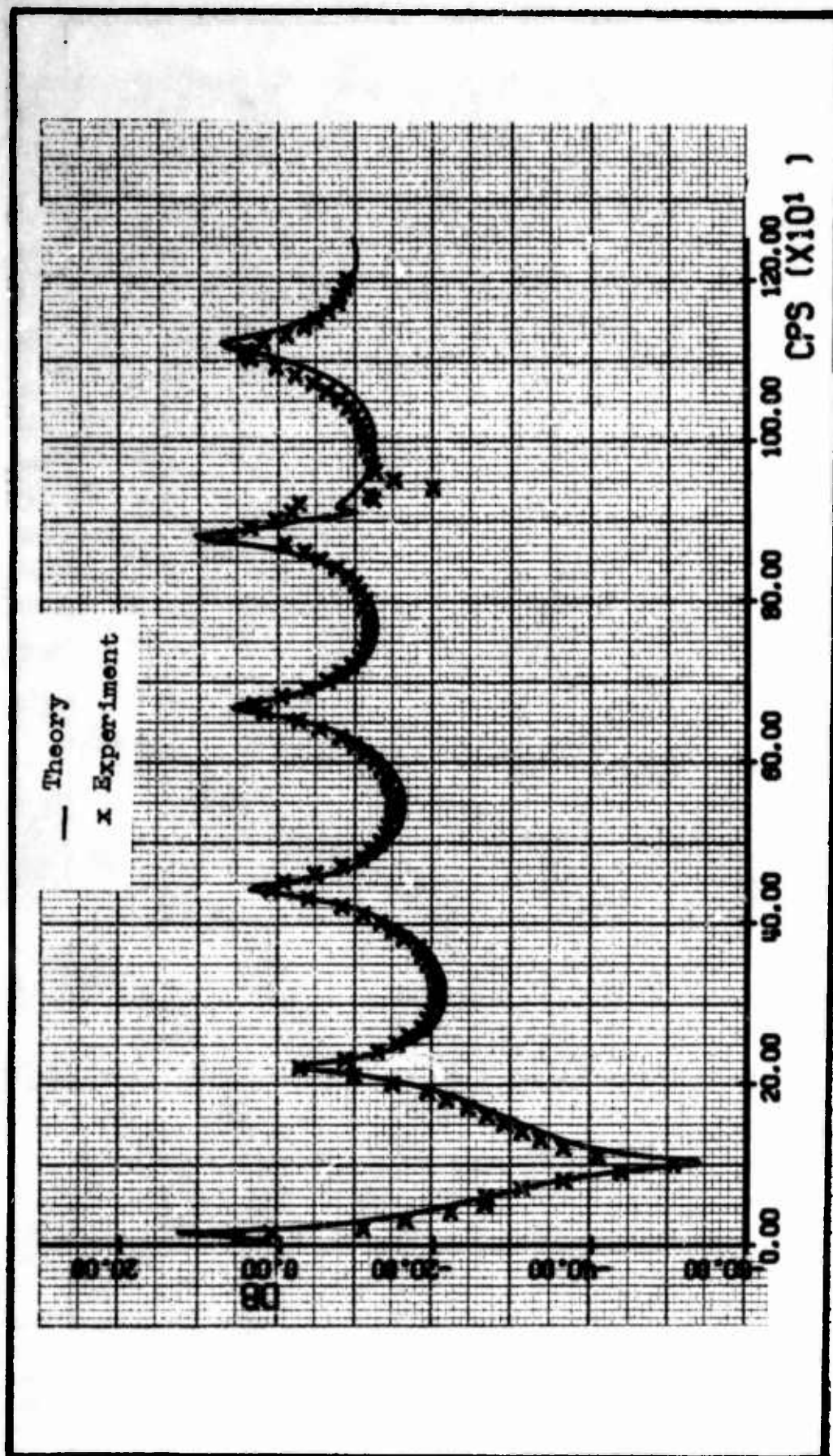
Fig. D-2. Data is the Same as Fig. C-22

Fig. D-3. Data is the Same as Fig. C-22 Except that $\bar{X}_3 = 7.5$ in.

Vita

Charles V. Fada was born ████████████ ███████████████████████████

███████████████████████████ He graduated from ████████████

████████in 1950, attended Red Oak Junior College for one year, and then

transferred to the State University of Iowa where he was awarded the

degree of Bachelor of Science in Electrical Engineering in February of

1956. He was commissioned in USAF Reserve through the ROTC. Before

entering the active service, he was employed by Boeing Aircraft Company

in Wichita, Kansas. He attended Navigators Primary Basic Course at

Ellington AFB, Texas, graduating in October of 1957. From there he was

stationed at Patrick AFB, Florida, as a navigator flying missile re-

entry missions from the Air Force Missile Test Center. He was awarded

a commission in the Regular Air Force in 1959. In 1961 he was assigned

to the Air Force Weapons Laboratory in Kirtland AFB, New Mexico, as an

electrical engineer. In 1966 he was assigned to the Air Force Institute

of Technology.

Permanent address: ████████████
████████████

This thesis was typed by Mrs. Marian M. Whitaker.